FULLERENE AND DENDRIMER BASED NANO-COMPOSITE GAS SEPARATION MEMBRANES

The research described in this thesis was supported by the Dutch Technology Foundation STW, applied science division of NWO.

Fullerene and dendrimer based nano-composite gas separation membranes

D.M. Sterescu, PhD Thesis, University of Twente, The Netherlands

ISBN: 978-90-365-2561-9

Cover
designed by D.M. Sterescu

Printed by Wöhrmann Print Service, Zutphen, The Netherlands.

FULLERENE AND DENDRIMER BASED NANO-COMPOSITE GAS SEPARATION MEMBRANES

DISSERTATION

to obtain
the degree of doctor at the University of Twente,
under the authority of the rector magnificus,
prof. dr. W.H.M. Zijm,
on account of the decision of the graduation committee
to be publicly defended
on Thursday 20th of September 2007 at 13.15

by

Dana Manuela Sterescu

born 14th of June 1974
in Rm. Sarat, Romania

This dissertation has been approved by:

Promotor:	Prof. Dr.-Ing. M. Wessling
Assistant promotor:	Dr. D.F. Stamatialis

... In memoria bunicului meu Mihail, odihneasca-se in pace.

Dedicated to my beloved husband,
Jörg

"Somewhere, over the rainbow, way up high.
There's a land that I heard of Once in a lullaby.
Somewhere, over the rainbow, skies are blue.
And the dreams that you dare to dream
Really do come true.
Someday I'll wish upon a star and wake up where the clouds are far Behind me.
Where troubles melt like lemon drops, Away above the chimney tops.
That's where you'll find me.
Somewhere, over the rainbow, bluebirds fly. Birds fly over the rainbow,
Why then - oh, why can't I?
If happy little bluebirds fly beyond the rainbow,
Why, oh, why can't I?"

Table of contents

Chapter 1: Introduction

1. Gas separation 6

2. Transport in Polymers 6

3. Free volume 8

4. The Permeability-Selectivity Trade-off Rule: A Fundamental Limitation to the Separation of Permanent Gases 9

5. Mixed Matrix membranes 11

6. Transport in Heterogeneous Materials 12

7. Polymers for gas separation 13

7.1 Poly (2, 6-dimethyl-1,4-phenylene oxide) (PPO) 14

7.2 Polyimides 15

8. Nano-scale additives to polymers 16

8.1 Fullerenes (C_{60}) 16

8.2 Dendrimers and hyperbranched polymers 19

9. Scope of this thesis 22

10. Structure of this thesis 23

11. References 25

Chapter 2: Novel gas separation membranes containing covalently bonded fullerenes

1.Introduction 30

2. Experimental part 30

2.1 Materials 30

2.2 Synthesis of PPO-C_{60} 31

2.3 Preparation of membranes 33

2.4. Characterization of membranes 34

3. Results and Discussion 34

4. Conclusions 40

5. References 40

Chapter 3: Fullerene-modified poly (2, 6-dimethyl-1,4-phenylene oxide) gas separation membranes: Why binding is better than dispersing

1. Introduction 44

2. Background 45

2.1 Transport in Polymers 45

2.2 Transport in Heterogeneous Materials 46

3. Experimental 48

3.1 Modification of PPO 48

3.2 Preparation of membranes 48

3.3 Characterization of membranes 49

3.4 WAXS measurements 50

4. Results and discussion 51

4.1 H-NMR 51

4.2 DSC-T_g 51

4.3 WAXS analysis 52

4.4 Gas permeability and gas sorption 58

5. Conclusions 63

6. Appendix 64

7. References 64

Chapter 4: Fullerene-modified Matrimid gas separation membranes

1. Introduction 68

2. Experimental 69

2.1 Materials 69

2.2 Modification of Matrimid 69

2.3 Preparation of membranes 70

2.4 Characterization of membranes 71

3. Results and discussion 73

3.1 Scanning Electron Microscopy (SEM) 73

3.2 DSC and Density measurements 75

3.3 WAXS analysis 75

3.4 Gas permeability and gas sorption 78

3.5 Influence of the polymer structure on the free volume 82

4. Conclusions 83

5. References 83

Chapter 4: Appendix I

I.1 Introduction 87

I.2 Materials 87

I.3 Membrane preparation 87

I.4 Gas permeability and sorption 88

I.5 Conclusions 90

I.6 References 90

Chapter 5: Boltorn-modified poly (2, 6-dimethyl-1,4-phenylene oxide) gas separation membranes

1. Introduction 92

2. Experimental 93

2.1 Materials 93

2.2 Preparation of PPO and PPO–Boltorn membranes 94

2.3 Characterization of membranes 94

3. Results and discussion 98

3.1 Gas permeability 98

3.2 Scanning Electron Microscopy (SEM) 101

3.3 Energy Dispersive X-ray Analysis (EDX) 104
3.4 DSC measurements 106
3.5 Positron Annihilation Lifetime Spectroscopy (PALS) 106
3.6 WAXS analysis 108
3.7 Gas sorption 112
4. Conclusions 114
5. References 115

Chapter 6: Boltorn-modified Matrimid and P84 gas separation membranes

1. Introduction 118
2. Experimental 119
2.1 Materials 119
2.2 Preparation of the membranes 120
2.3 Characterization of membranes 121
3. Results and discussion 123
3.1 Scanning Electron Microscopy (SEM) 123
3.2 DSC measurements 128
3.3 WAXS analysis 129
3.4 Gas permeability and gas sorption 131
4. Conclusions 136
5. References 138

Summary 139

Reflections and Outlook 143

Samenvatting 147

Acknowledgement 151

Chapter 1

Introduction

1. Gas separation

The gas separation by a polymer membrane is interesting, especially from the view-point of energy economy[1]. Some examples of gas separation with polymer membranes are: the recovery of hydrogen from refinery streams for recycling, the removal of carbon dioxide, water and hydrogen sulfide from natural gas, the production of nitrogen and oxygen enriched air, the recovery of methane from mines and landfills, purification of H_2 and the recovery of certain gases and vapors from exhausts and vent gases[2-9]. Future large-scale systems will be devoted to health care, food processing, and biotechnology.

Thus membranes have gone through a tremendous development, having better performance, chemical and mechanical stability, and reduction of production costs. However, the technology needs a breakthrough in the membrane materials not only regarding permeability, but also selectivity, as well as durability. Different strategies towards the construction of more efficient membranes have suggested by Koros and Mahajan[10].

2. Transport in Polymers

The permeation of a gas molecule through a dense membrane is usually governed by a solution-diffusion mechanism. The permeability P of a polymer is given as the product of diffusivity, D (kinetic component), and solubility, S (thermodynamic component):

$$P=D\cdot S \tag{1}$$

The ideal selectivity of a membrane for component A relative to component B, $\alpha_{A/B}$, is defined as the ratio of their permeabilities[11,12], which in terms of equation 1 can be rewritten as:

$$\alpha_{A/B} = \frac{P_A}{P_B} = \left(\frac{S_A}{S_B}\right) \times \left(\frac{D_A}{D_B}\right) \tag{2}$$

The first term on the right-hand side is the solubility selectivity and the second term is the diffusivity selectivity.

Over the past three decades, sorption of gas molecules into glassy polymers has been described and analyzed by the dual-mode sorption model[13]. The fundamental assumption of the dual mode sorption theory is the existence of two distinct populations of gas molecules in a polymer matrix. Rubbery polymers are in a hypothetical thermodynamic equilibrium liquid state and their gas solubility obeys Henry's law. On the other hand, glassy polymers are typically assumed to be in a non-equilibrium state containing two components: a frozen-in solid state of unrelaxed free volume and a hypothetical liquid state being in equilibrium. The model is used to represent the sorbed amount of gas (C) of pure gases in polymers as function of the pressure (p), and is expressed by:

$$C = C_D + C_H = k_D p + \frac{C_H' b p}{1 + b p} \qquad (3)$$

where C_D is the gas concentration based on Henry's law sorption, C_H is the gas concentration based on Langmuir sorption, k_D is the Henry's law coefficient, b and C_H' are the Langmuir hole affinity parameter and the capacity parameter, respectively. The k_D parameter represents the penetrant dissolved in the polymer matrix at equilibrium and b characterizes the sorption affinity for a particular gas-polymer system. These parameters can be determined from the measured sorption data. C_H' is often used to measure the amount of the non-equilibrium excess free volume in the glassy state[14].

The diffusivity and diffusivity selectivity are functions of polymer properties on molecular scale such as resistance to torsional motions, inter-segmental backbone spacing, and free volume. Reductions in the mean inter-chain distance require larger segmental motions of polymer molecules to allow local passage of a gas molecule.

3. Free volume

Molecular diffusion through a dense polymer depends strongly on the amount of free volume of the material. Free volume presents diffusing molecules with a low-resistance path for transport, if static voids created by inefficient chain packing or transient gaps generated by thermally induced chain rearrangement. The larger and more numerous these pathways are, the faster molecules migrate through a polymer and vice versa[12].

A quantity frequently used to compare the amount of free volume in polymers is the fractional free volume (FFV), which is defined as

$$FFV = \frac{V_{sp} - V_0}{V_{sp}} \quad (4)$$

where V_{sp} is the polymer bulk specific volume and V_0 is the volume occupied by polymer chains. The value of V_0 may be calculated from

$$V_0 = 1.3 \cdot V_w \quad (5)$$

where V_w is the Van der Waals volume, which can be estimated from group contribution methods such as the method proposed by Bondi[15].

The free volume approach is very useful for describing and understanding transport of small molecules through polymers. The basic concept is that a molecule can only diffuse from one place to another place if there is sufficient empty space or free volume. The mobility of a given penetrant depends on the probability of it finding a hole of sufficient size that allows its displacement. In the case of non-interacting systems (polymer with inert gases such as helium, hydrogen, oxygen, nitrogen or argon), the polymer morphology is not influenced by the presence of these gases which means that there is no extra contribution towards the free volume[11].

4. The Permeability-Selectivity Trade-off Rule: A Fundamental Limitation to the Separation of Permanent Gases

Gas separation membranes need to be highly permeable to one of the mixture components while significantly rejecting the other components. The vast amounts of polymers that have been investigated, however, show the general trend that highly permeable polymers possess low selectivities. This effect – often referred to as the permeability/ selectivity trade off relationship[16] – is shown in Figure 1, where the O_2/N_2 selectivities of various polymers are plotted versus their O_2 permeabilities[17] expressed in Barrer (1 Barrer = 10^{-10} cm^3(STP)cm/cm^2 s cmHg). Robeson has suggested that the permeability-selectivity trade-off possesses an upper bound[18] (see Figure 1). Subsequent to the publication of Robeson's paper, only a few examples of polymeric membranes have been published which exceed the upper bound[10]. Freeman has suggested a theoretical model to describe the upper bound relationship[16].

Polymeric membranes transport gaseous penetrants according to a solution-diffusion mechanism: the penetrant first dissolves in the membrane at the feed side, next diffuses across the membrane to the permeate side where it finally desorbs, entering the adjacent low-pressure gas phase. Hence, the gas solubility- and diffusion coefficient in the membrane determine its transport rate. Often, rubbery polymers are found to be highly permeable but not very selective, while for glassy polymers the reverse is often found. This typical tradeoff behavior is easily explained. As the thermal fluctuations of the atomic positions in rubbery polymers (e.g. vibrational motions in torsion angle potential wells and torsional transitions) are fairly large on the time scale of penetrant diffusion, similarly sized penetrants (e.g. O_2/N_2) can slip through the matrix with comparable ease. This results in almost equal diffusion coefficients for both penetrants. Contrary to this, the polymer atoms in a glassy matrix are frozen at meta-stable positions, rendering the polymeric matrix to have an increased "molecular sieving" ability, but also rendering the matrix less permeable to both penetrants.

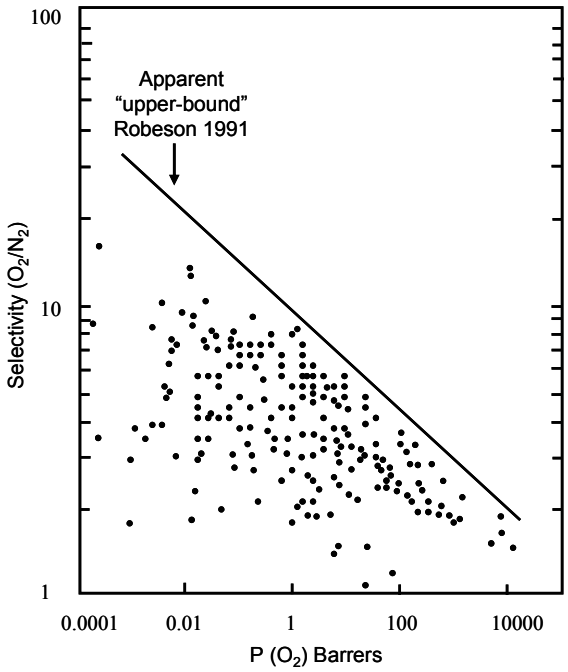

Figure 1: O_2/N_2 upper limit selectivity-permeability trade-off[17] Dots represent various rubbery and glassy polymers investigated. The line represents the boundary to selectivity / permeability pairs. This upper limit has negative slope indicating the general selectivity-permeability trade off for polymeric gas separation membranes.

In the last decades, several promising new membrane concepts have been developed, which have shown performances exceeding the Robeson 1991 upper-bound. Today, researchers concerned with the development of highly permeable and selective gas separation membranes challenge the limitations described above by (1) using the unique properties of molecular sieving materials (pyrolysis of polymeric precursors to develop so-called carbon membranes, development of mixed matrix materials in which the sieving properties of various materials is combined with the film-forming properties of polymers) or (2) developing membranes with a facilitated transport (carrier-mediated transport) function. Koros and Mahajan have suggested that it may be possible to exceed the upper bound significantly by the use of "mixed-matrix membranes"[10]. These polymeric membranes contain a large volume of sub-micro-molecular sieves to combine the processability of membranes with the high performance characteristics of the molecular sieves[19].

5. Mixed matrix membranes

The mixed-matrix membranes are prepared by incorporation of solid particles within a polymer. Generally the presence of particles can have three effects on the permeabilities; they can act as molecular sieves altering the permeabilities, they can disrupt the polymeric structure increasing permeabilities and they can act as barrier reducing permeabilities[19]. In recent studies mixed matrix membranes have demonstrated remarkable separation properties beyond the intrinsic properties of the polymer matrix[20]. In these studies different molecular sieving inserts such as zeolites[21-25] and carbon molecular sieves[21,26,27] were incorporated in several polymer matrices. This concept can also be extended to include microporous media which operate by the "selective surface flow" mechanism[28-30]. Using this mechanism, the larger-pored rigid solids enable the selective adsorption and surface diffusion of the more condensable component in a mixture, while excluding the less condensable component. If the less condensable component is the smaller component of the two penetrants, the selective surface flows offers even a novel way to selectively enhance the permeation of the otherwise slower diffusing penetrant[20].

Generally, the literature has focused on the incorporation of molecular sieves into a polymer matrix. Often these molecular sieves possess superior gas transport properties, but have significant problems with their processability. Aggregation and sedimentation of particles, as well as the formation of spaces between the solid particle and the polymeric material are three potential problems during the formation of effective mixed matrix membranes. Therefore the gases could flow non-selectively around the solid particles[10]. Thompson et al. tried to avoid these problems during the preparation of zeolite containing polymeric mixed matrix membranes by covalent bonding of the zeolite to the polymer matrix[31]. Koros et al. suggested experimental procedures like sonication and decantation of smaller solid particles to increase the viscosity of the casting solution reducing aggregation as well as sedimentation, priming the particles with small amounts of the polymer and / or reducing the evaporation rate of the casting solution to increase solid particle interactions[26]. A number of articles providing an overview of mixed-matrix membranes have been previously published[32,33].

6. Transport in Heterogeneous Materials

Numerous models have been developed to describe transport properties in heterogeneous polymer systems. One of the most known ones is that of Maxwell[12,34,35] used in two forms. The simple form analyzes the steady-state dielectric properties of a dilute suspension of spheres where the permeability of composite, P, made by dispersing of non-porous, impermeable filler in a continuous polymer matrix is expressed as:

$$P = P_p \left(\frac{1 - \varphi_f}{1 + \frac{\varphi_f}{2}} \right) \tag{6}$$

where P_p is the permeability of the pure polymer and φ_f is the volume fraction of filler. Equation 6 suggests that the permeability of the filled polymer is lower than of the pure polymer and decreases with increasing filler concentration. The decreased permeability is caused by reduction in penetrant solubility due to (i) the replacement of polymer through which transport may occur with filler particles and (ii) an increase in the tortuosity[12] of the diffusion path through which the penetrant molecules cross the polymeric film. It is important to note that in the case of clustering of filler particles, and the formation of interstitial voids with no polymer into them, the structure gets more complex by inducing morphological changes in the polymer matrix.

The second generalized form[36] is used to estimate the permeation through a structured biphasic material wherein the additive component is randomly dispersed with sharp interfaces in a continuous matrix of the polymer expressed as:

$$P = P_p \left[1 + \frac{(1+G)\varphi_f}{\left(\frac{P_f/P_p + G}{P_f/P_p - 1} \right) - \varphi_f} \right] \tag{7}$$

where P_f is the permeability of the filler and G is a geometric factor accounting for dispersion shape. If the dispersed phase is oriented in lamellae parallel to the direction of permeation, $G \rightarrow \infty$, and there is minimal resistance to flow. If the dispersed phase is oriented in lamellae perpendicular to the direction of permeation, $G \rightarrow 0$, and maximal impedance of flow occurs due to obstructive layers of the less permeable component. The volume fraction of the filler in the polymer can be estimated using the equation:

$$\varphi_f = \frac{w_f}{w_f + \frac{\rho_f}{\rho_p}(1 - w_f)} \qquad (8)$$

where ρ_p and ρ_f are the density of the pure polymer and the filler, respectively, and w_f is the weight fraction of the filler in the polymer.

Koros and co-workers have compared theoretical permeabilities with experimental derived permeabilities of Matrimid 5218 and Ultem® 1000 mixed with carbon molecular sieves (CMS)[27]. Chung et al. have formed mixed-matrix membranes from Matrimid 5218 and a benzylamine-modified fullerene[36]. The authors suggest that the fullerene is causing rigidification of the polymer matrix, leading to a decrease in the diffusion coefficient and therefore of the permeability. Spontak, Merkel and co-workers have formed mixed-matrix membranes from cross-linked poly(ethylene oxide) and various nanoparticles[37,38].These membranes were examined primarily for their CO_2/H_2 separation performance.

7. Polymers for gas separation

Gas separation membranes can be prepared from various polymers, such as cellulose acetate and poly (sulfone). These polymers are used because of their commercial availability and their processability combined with acceptable gas separation properties. The ideal gas separation membrane however, combines a high selectivity with a high permeability. Rigid aromatic glassy polymers, like for example polycarbonates, polyetherimides, sulphonated polysulfones polyamides, polyamideimides and polyimides are the new generation polymers[39].

7.1 Poly (2, 6-dimethyl-1,4-phenylene oxide) (PPO)

The first and so far the best known representative of the family of polyphenylene ethers – poly 2, 6-dimethyl-1,4-phenylene oxide, commonly called poly (phenylene oxide) or PPO – is also the one most intensively studied with respect to gas separation. The first study of gas permeability through PPO membranes known to the author was published by Yasuda and Rosengren in 1970[40].: the gas permeability through PPO was unexpectedly high. At that time with the exception of natural rubber, PPO was the most permeable polymeric material.[41] Later on, with the appearance of poly [1-(trimethylsylil)-1-propyne], or PTMSP, and polyimides[5], the attention of the researchers shifted towards those materials.

In the search for the gas separation membrane materials of improved permeability and selectivity, various chemical modifications of PPO have been investigated– e.g. carboxylation[42,43], fluorination[44], nitration[45], bromination[46-48] and sulfonation[49]. In this thesis, we focus on investigations of unmodified PPO with the repeat unit represented by Figure 2 and PPO modified with fullerenes (C_{60}) and hyperbranched polymers (HPB) – Boltorn.

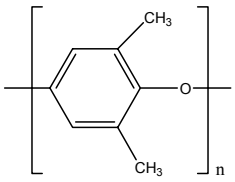

Figure 2: Poly (2, 6-dimethyl-1,4-phenylene oxide) (PPO)

7.2 Polyimides

Polyimides are polymers containing cyclic imide groups in the main macromolecular chain[50]. Dependent on the structure of the radicals attached to the imide group, polyimides can be aliphatic, alicyclic, or aromatic and linear or three dimensional, depending on the chain structure[51]. In this thesis aromatic polyimides are used because of their high thermal stability and carbon yield. Aromatic polyimides are formed in a polycondensation reaction of an aromatic tetracarboxylic acid dianhydride with an aromatic diamine. This reaction can be performed by a

two- or a one-step method, where the two-step process is the most common. In the first step the dianhydride is added to a diamine solution reacting to a polyamic acid (PAA)[39,50].

In the second step the dehydrative cyclisation (imidisation) of the PAA takes place through thermal (thermal imidisation) or chemical (chemical imidisation) induction. The acronyms identifying the polyimides are referring to the dianhydride (first part) and the diamine (second part). Aromatic polyimides containing bulky side groups are soluble.

Aromatic polyimides are one of the most important classes of high performance polymers. They are highly thermally stable, have high glass transition temperatures and relatively low dielectric constants. The various polyimides have become important in many applications, such as semiconductor devices, high temperature adhesives, and high performance composite materials[52,53].

Polyimides are selected as membrane material for gas separations because of their significantly better permselective performance than membranes made of conventional glassy polymers[54]. Matrimid 5218 is a commercial available polyimide manufactured by Ciba Specialty Chemicals Co. It is a soluble solid polyimide and consists of 3,3`-4,4`-benzophenone tetracarboxylic dianhydride (BTDA) and diaminophenylindane (DAPI)[55].

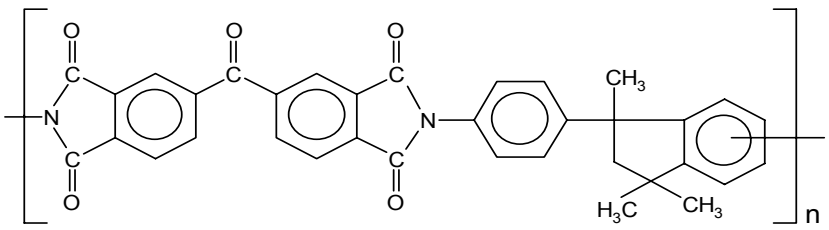

Figure 3: Chemical structure of the Matrimid monomer unit.

The final polyimide is a mixture of the 5-amino and 6-amino isomers of DAPI (Figure 3). During manufacturing the polyimide is fully imidized and is soluble in a variety of common solvents, like N-methylpyrrolidone (NMP), N,N-dimethylformamide (DMF), N,N-dimethyl-acetamide (DMAc), chloroform and methylene chloride[55,56]. Matrimid 5218 exhibits a combination of selectivity and permeability for industrially significant gas pairs superior to that of most other readily available

polymers. Its permeation properties combined with its processability (i.e., solubility in common solvents), chemical resistance and good thermal properties makes it an ideal candidate for gas separation applications[57,58].

8. Nano-scale additives to polymers

One way to enhance the gas separation performance of polymeric membranes is to fill inorganic nanoparticles such as silica, metal oxides, carbon black, carbon nanotubes and zeolites into the polymer to form organic-inorganic hybrid nanocomposite membranes[59,60]. In this thesis the focus will be on one inorganic and one organic additive.

8.1 Fullerenes (C_{60})

Although carbon clusters have been known to exist since 1959[61], it took decades to elucidate the structure and properties of the new carbon allotrope family of fullerenes. This interesting group of molecules opened up a new area of chemistry when Kroto et al[62] described for the first time in 1985 the nature and chemical reactivity of C_{60}. Another breakthrough for synthetic chemists, a method for preparing macroscopic quantities of C_{60}, was suggested by Krätschmer et al[62] in 1990. It is evident that hardly any other molecule has received so much attention in recent times as the new carbon allotrope C_{60}[61]. C_{60} was named buckminsterfullerene after Buck-minster Fuller, an American architect and constructor of the geodesic dome. C_{60} (buckminsterfullerene) and C_{70} (falmarene) are the most accessible members of the family on which extensive studies have been carried out. They have also become of increasing interest to polymer chemists as building blocks for the construction of novel materials with interesting properties[64]. The multifunctionality of fullerene opens the possibility for versatile two-dimensional and three- dimensional exohedral modification, i.e. modification outside the spherical molecule of fullerene. However, their derivatization reactions frequently produce a large number of products, which are difficult to separate and characterize. Each molecule of the fullerene family consists of 12 pentagons, C_{60} is composed of 32 faces, of which 12 are pentagons and 20 are hexagons, and the carbon atoms are arranged at the 60 vertices of a truncated icosahedron. Because the

spherical surface of C_{60} contains 30 reactive [6,6] - double bonds, a huge number of regio-isomeric multiple addition products are possible in principle. However, due to the identical physical environment of each carbon atom on C_{60}, for chemical modification of C_{60} it is not easy to control the attaching sites on the C_{60} cage and the number of the modified functional group, which leads to a huge number of different addition products which are impossible to isolate[65].

Results show that the C_{60} molecule acting as a special functional group can be introduced into the main chain of an organic polymer to form a "pearl necklace" polymer, or into the side chain of a polymer as a pendant group to form a "charm bracelet" polymer. The C_{60} molecule may be introduced into the side chain of a polymer as a pendant group to form "charm bracelet" polymers in two ways: 1) the reaction of C_{60} or a C_{60} derivative with a preformed polymer; and 2) polymerization of a monomer containing fullerene functional groups. In 1994, Hawker[66] reported a simple and versatile method for the synthesis of "charm bracelet" type C_{60} polystyrene copolymers. He found that simple linear polymers containing azide functional groups, such as azidomethyl-substituted polystyrenes, can be used and would be expected to react with C_{60} to give soluble processable polymers.

Addition of fullerenes, increases the T_g of polystyrene [67] because of specific interactions,. Because of this and other interesting features, many possibilities lie open for the use of fullerene in different areas[61]. Fullerenes provide additional sorption sites for CO_2, ethylene, 1- butene and n - butane in the membrane[68,69]. Pure fullerenes can be mixed with polymers[67], the fullerenes can be functionalized first[58,66], and they can be incorporated within the polymer backbone[61,70]. Adding fullerene to a relative low gas permeable, but highly permselective polymer such as polystyrene, contributes to an increase in free volume, and therefore increases the permeability[69]. Adding fullerene to a highly permeable but low permselective polymer such as poly(1-methylsilyl-1-propyne) (PTMSP), decreases the free volume, thereby decreasing the permeability[68]. In the case of adding functionalized fullerenes to a polyimide, the gas permeability decreases upon increasing the fullerene content[36]. The presence of the benzylamine-modified C_{60} seems to serve as impenetrable volumes within the polymer matrix and appears to increase the diffusion pathways of the penetrants[36]. The large permeability reduction may also be due to the

rigidification of the polymer, pulling the matrix together[36]. Upon mixing PPO with fullerene the density increased, i.e., the polymer coils become more compact and the free volume of the fullerene-containing PPO decreased, resulting in lower permeability[71]. For polystyrene (PS) Polotskaya proposed that plastification phenomena take place at compositions 0.5 and 1 wt % C_{60}[72]. The fullerene molecules weaken the inter-chain interaction and reduce polymer glass transition temperature. The C_{60} molecules are capable of strong intermolecular interaction because of many conjugate links in the C_{60} structure. When C_{60} content exceeds 1 wt % the chance of interaction between C_{60} molecules in the PS-C_{60} system may increase and lead to physical linking of PS chains[72].

Covalent attachment of C_{60} to specific polymers may allow combination of the outstanding characteristics of fullerene with those of the polymeric matrix. The chemical and physical properties of these polymers depend largely on the content of fullerene covalently bound to the polymer matrix and on the chain-length of the attached polymer. Polymer-bound C_{60} should be easily processable into thin films by spin-coating or casting. A number of problems arise in the polymeric modification of fullerenes. Some crosslinking has been observed from the reaction of more than one polymer chain with a given fullerene molecule, resulting in crosslinked, intractable and insoluble materials. The key to the development of polymer-modified fullerene is to form selectively soluble fullerenated polymers with interesting specific properties in high yield under very mild conditions.

The addition of dendritic macromolecules[61] to fullerenes significantly improves their solubility and would provide a more compact insulating layer around the clusters than would linear polymers, while maintaining the globular shape of the structures[73].

8.2 Dendrimers and hyperbranched polymers

Dendrimers and hyperbranched polymers have recently be used to prepare permselective membranes. Due to their free volume[74], they might be attractive to control permselectivities for small molecules like gases for gas separation applications.

The first use of dendrimers for gas separation membrane has shown that the dendrimer membranes appear to function as a molecular gate for CO_2 compared to inert gases[75]. This initiated the use of dendrimers in gas separation membranes. Research has indicated that the improvement of diffusion selectivity is due to the space persistency because of the stiff and crowded dendritic structure[76]. Binding the dendrimers to the membranes involved the immersion of the polymeric membrane in a dendrimer containing solution. With immersion time the dendrimer was allowed to diffuse in the polymer film and cross-link with the polymer backbone. With increasing degree of cross-linking, higher selectivity can be achieved because of reduced swelling and chain mobility, however, permeability decreases because of reduced free volume[77]. In crosslinked membranes, big size dendrimers need more time to penetrate into the polymer matrix[78]. As a result, the polymer modification can be non homogenous throughout the film[78]. There appears to be an optimum in cross-linking time[77]. During the cross-linking process the polymer matrix swells by the solvent. The increase of fractional free volume due to swelling and the densification due to the cross-linking effect are interplaying[78,79]. The latter effect is tightening the polymer chains (due to covalent carbon, as well as hydrogen bonding) filling the interchain spaces and rearranging the free volume distributions. Dendrimers of higher generation have denser and more spherical structure, therefore the G1 and G2 polyamidoamine (PAMAM) dendrimers slightly increased the permeability after long immersion times, possibly due to their more open structure, as compared to the G0 dendrimer[78]. For shorter immersion times the relative permeability decreases and follows the order of G1>G2>G3, mainly resulting from cross-linking effects. Comparing the dendrimer cross-linked with the non-crosslinked the relative permeability decreases in the following order CH_4>N_2>CO_2>O_2>H_2>He, except for CO_2 this follows their kinetic diameter[80]. Reasons for this CO_2 deviation can be differing orientations of this anisometric molecule and/or its highly condensable nature. Altogether the permeability-selectivities are above the Robeson's upper-bound[80].

It is well known that linear polyimide membranes show good gas separation performance. Crosslinking modification of these membranes was carried out in order to overcome the problem that most of polyimide membranes suffered severe aging and performance decay due to

densification and/or plasticization[76]. Recently, 6FDA-durene polyimide membrane was crosslinked with polyamidoamine (PAMAM) or polypropyleneimine (DAB-AM) dendrimers[77-79]. The permeability decreased with increasing the crosslinking time but the selectivity increased. The decrease of gas permeability values were attributed to the crosslinking structure, the increased intersegmental interaction among the amide groups with the aid of hydrogen bonds, and the reduced free volume due to the space filling effect by dendrimers.

Hyperbranched polymers have many branched units as same as dendrimers, although the shape-persistency of the hyperbranched polymers is less than that of the dendrimers. Therefore, the hyperbranched polymers may be considered as the polymers linking various generations of dendrimers. Hyperbranched polyimide membranes were prepared via casting the corresponding polyamic acid solution which was synthesized from 1,3,5-tris(4-aminophenoxy)benzene (TAPOB) and 4,4'-(hexafluoroisopropylidene) diphthalic anhydride (6FDA)[81]. Gas permeability of 6FDA-TPER was lower than for 6FDA-TPEQ because of the lower diffusivity of 6FDA-TPER attributed to both the lower FFV and the increased inhibition of the segmental mobility, besides its higher O_2/N_2 selectivity. On the other hand, hyperbranched polyimide 6FDA-TAPOB showed high gas permeability due to the higher FFV and had higher O_2/N_2 permselectivity. This behavior was explained as follows: low segmental mobility and unique size and distribution of free volume holes arising from the characteristic hyperbranched structure of 6FDA-TAPOB provided effective O_2/N_2 selectivity in comparison with 6FDA-TPEQ.

First, the permselectivity of gas permselective membranes using dendrimers was enhanced due to their dendrimers features such as inhibition to the segmental mobility, the control of FFV, and a huge number of interior sites with good affinity to permeate molecules. Since the performance of the dendrimer-membrane separation often depended on the space among dendrimer molecules, in order to clarify the effect of dendrimer-structure on their permselective behavior, it would be necessary to design new dendrimer-membranes which can vanish or decrease the space among dendrimer molecules, or show the negligible permeation through the space among dendrimer molecules. Hence, hyperbranched polymers commercially available as Boltorn® H20, H30, H40 from Perstorp Specialty Chemicals AB, Sweden, attracted

our attention. The hyperbranched polymers studied in this work are aliphatic polyesters using ethoxylated pentaerythritol as central cores and 2,2-bis(methylol)propionic acid (bis-MPA) as dendritic units. Boltorn H20 statistically contains two generations of bis-MPA, while Boltorn H30 and H40 have three and four generations of MPA, respectively. The products are all hydroxyl functional, but differ in molecular weight and hydroxyl functionality.

9. Scope of this thesis

The objective of this thesis is to develop new materials for membrane based gas separation processes. Synthetic membranes for gas separation need to be highly permeable to one of the mixture components while significantly rejecting the other components. The vast amounts of polymers that have been investigated, however, show the general trend that highly permeable polymers possess low selectivities. This effect is often referred to as the permeability/selectivity trade off relationship[16]. Often, rubbery polymers are found to be highly permeable but not very selective, while for glassy polymers the reverse is often found. A very exciting new class of materials consists of super-glassy high free volume polymers. These polymers generally contain a super-rigid backbone structure combined with bulky pendant groups. The combination of chain rigidity and side group bulkyness severely frustrates chain packing in the glassy amorphous state, resulting in extremely large amounts of (nonequilibrium) excess free volume.

In this thesis long-term stable, loosely packed (high free volume) amorphous polymer films were prepared by introducing super-molecular pendant groups, which possess hard-sphere properties to avoid dense molecular scale packing of adjacent polymer chains during membrane preparation resulting in high free volume, super-glassy amorphous structures with high gas permeabilities and selectivities.

In the first part of this thesis we focus on Fullerene-based polymer modification concepts to develop a new branch of polymers for high performance membrane separations. In the second part of this thesis we focus on hyperbranched polymers (HPB) – based polymer modification concepts to develop high free volume polymer films.

10. Structure of this thesis

In **Chapter 2, "Novel gas separation membranes containing covalently bonded fullerenes",** shows superior mass transport properties of polymers prepared by covalent coupling of super-molecular carbon cages (fullerenes, bucky-balls) based on poly (2, 6-dimethyl-1, 4-phenylene oxide) (PPO) polymer. In comparison to the pure PPO, dispersing the bucky-balls into the polymer reduces gas permeability whereas covalent bonding enhances permeability up to 80%. Gas pair selectivity, however, is not compromised and stays constant.

Chapter 3, "Fullerene-modified poly (2, 6-dimethyl-1,4-phenylene oxide) gas separation membranes: Why binding is better than dispersing", characterizes the permeation properties of poly (2, 6-dimethyl-1,4-phenylene oxide) (PPO) dense polymer films containing fullerenes (C_{60}) dispersed or covalently bonded to PPO at various concentrations. The gas permeability of PPO-C_{60} bonded increases up to 80 % with increasing fullerene concentration, while the gas pair selectivity stays constant. This behavior is due to the increase of free volume. The gas permeability through the PPO-C_{60} dispersed decreases in comparison to pure PPO. This reduction is due to C_{60} clustering in the polymer. The clusters seem to induce polymer crystallinity and they are probably aligned along the film plane creating an extra barrier for gas permeation.

In **Chapter 4, "Fullerene-modified Matrimid gas separation membranes",** super molecular carbon cages (e.g., fullerenes, bucky balls) were covalently coupled or dispersed in the commercial BTDA-AAPTMI polyimide (Matrimid 5218). The dispersion of fullerenes (0.25 and 1.0 wt %) and the covalent bonding of 0.25 wt % fullerenes to Matrimid did not affect the permeability and selectivity compared to the pure polymer. The covalent coupling of 1.0 wt % of fullerenes resulted in a tremendous increase in permeability but significant loss in selectivity.

In **Chapter 5, "Boltorn-modified poly (2, 6-dimethyl-1,4-phenylene oxide) gas separation membranes",** the preparation, characterization and the permeation properties of PPO containing aliphatic hyperbranched polyesters, Boltorn (H20, H30 and H40) are described. The Boltorn are

dispersed in PPO at various concentrations. The gas permeability of PPO with 1.0 wt % of Boltorn is 2-3 times higher than the pure polymer. At higher concentration (9.1 wt %) of Boltorn the permeability becomes almost 50 % of the pure polymer. The gas pair selectivity stays constant for all concentrations. The increase in permeability at low concentration of Boltorn is due to the increase of the free volume, probably due to hydrogen bonds between Boltorn and the oxygen of PPO backbone. The decreased permeability of PPO containing higher concentration of Boltorn (9.1 wt %) is due to two reasons: decrease in free volume as determined by PALS as well as phase separation. The hyperbranced polyesters form aggregates that migrate to the top surface of the membrane.

Chapter 6, "Boltorn-modified Matrimid and P84 gas separation membranes", shows the preparation, characterization and the permeation properties of polyimide BTDA-AAPTMI (Matrimid 5218) and co-polyimide BTDA-TDI/MDI (P84) dense polymer films containing aliphatic hyperbranched polyesters, Boltorn (H40). The Boltorn are dispersed in Matrimid and P84, respectively at various concentrations. For Matrimid-Boltorn 1.0 wt % the nitrogen permeability increases with significant loss in selectivity, while at higher concentrations (5.0 and 10.0 wt %) of Boltorn the permeability becomes lower than of the pure polymer while the selectivity generally stays constant. The dispersion of various concentration of Boltorn (1.0, 5.0 and 10.0 wt %) in P84 decreases the permeability for all concentrations used in comparison to P84 pure. The selectivity generally stays constant.

11. References

[1] Haggin, J. *Chem. Eng. News* **1988**, *6*, 7.

[2] Baker, R.W. *Ind. Eng. Chem. Res.* **2002**, *41*, 1393.

[3] Koros, W.J. *Macromol. Symp.* **2002**, *188*, 13.

[4] Maier, G. *Angew. Chem. Int. Ed.* **1998**, *37*, 2960.

[5] Stern, S.A., *J. Membrane Sci.* **1994**, *94*, 1.

[6] Paul, D.R.; Yampol'skii, Y.P. Polymeric Gas Separation Membranes, CRC Press, Boca Raton, **1994**.

[7] Koros, W.J.; Fleming, G.K. *J. Membrane Sci.* **1993**, *83*, 1.

[8] Freeman, B.D.; Pinnau, I. *ACS Symp. Series* **1999**, *733*, 1.

[9] Langsam, M. *Plastics Eng*. **1996***, 36*, 997.

[10] Koros, W.J.; Mahajan, R. *J. Membrane Sci.* **2000**, *175*, 181.

[11] Mulder, M. Basic Principles of Membrane Technology, Kluwer Academic, London, **1992**.

[12] Merkel, T.C.; Freeman, B.D.; Spontak, R.J.; He, Z.; Pinnau, I.; Meakin, P.; Hill, A.J. *Chem. Mater*. **2003**, *15*, 109-123.

[13] Kanehashi, S.; Nagai, K. *Journal of Membrane Science* **2005**, *253 (1-2),* 117-138.

[14] Story, B.J.; Koros, W.J. *J. Polym. Sci. Part B: Polym. Phys.* **1989**, *27*, 1927-1948.

[15] Bondi, A. *J. Phys. Chem.* **1964**, *68*, 441.

[16] Freeman, B.D. *Macromolecules* **1999**, *32*, 375.

[17] Singh, A.; Koros, W.J. *Ind. Eng. Chem. Res.* **1996**, *35*, 1231.

[18] Robeson, L. *J. Membrane Sci.* **1991**, *62*, 165.

[19] Powell, C.E.; Qiao, G.G. *J. Membrane Sci.* **2006**, *279*, 1.

[20] Moore, T.T.; Mahajan, R.; Vu, D.Q.; Koros, W.J. *Separations* **2004**, 50, 311.

[21] Duval, J.M.; Folkers, B.; Mulder, M.H.V.; Desgrandchamps, G.; Smolders, C.A. *J. Membrane Sci.* **1993**, *80*, 189.

[22] Jia, M.; Peinemann, K.V.; Behling, R.D. *J. Membrane Sci.* **1991**, *57*, 289.

[23] Mahajan, R.; Koros, W.J. *Ind. Eng. Chem. Res.* **2000**, *39*, 2692.

[24] Mahajan, R.; Koros, W.J. *Polym. Eng. And Sci.* **2002**, *42*, 1420.

[25] Mahajan, R.; Koros, W.J. *Polym. Eng. And Sci.* **2002**, *42*, 1432.

[26] Vu, D.Q.; Koros, W.J. ; Miller, S.J. *J. Membrane Sci.* **2003**, *211*, 311.

[27] Vu, D.Q.; Koros, W.J. ; Miller, S.J. *J. Membrane Sci.* **2003**, *211*, 335.

[28] Anand, M.; Langsam, M.; Rao, M.B.; Sircar, S. *J. Membrane Sci.* **1997**, *123*, 17.

[29] Nicholson, D. *J. Membrane Sci.* **1997**, *129*, 209.

[30] Sircar, S.; Rao, M.B.; Thaeron, C.M.A. *Sep. Sci. and Tech.* **1999**, *34*, 2081.

[31] Thomson, R.W; Libby, B.E.; Berry, M.B.; Rose, K.; Haas, K.-H. US Patent 6,248,682 B1 **2001**.

[32] Zimmerman, C.M.; Singh, A.; Koros, W.J. *J. Membrane Sci.* **1997**, *137*, 145.

[33] Mahajan, R.; Zimmerman, C.M.; Koros, W.J. *ACS Symp. Series* **1999**, *733,* 277.

[34] Merkel, T.C.; Freeman, B.D.; Spontak, R.J.; He, Z.; Pinnau, I.; Meakin, P.; Hill, A.J. *Science*, **2002**, *296*, 519.

[35] Arnold, M.E.; Nagai, K.; Freeman, B.D.; Spontak, R.J.; Betts, D.E.; DeSimone, J.M.; Pinnau, I. *Macromolecules* **2001**, *34*, 5611-5619.

[36] Chung, T. S.; Chan, S. S.; Wang, R.; Lu, Z. H. and He, C. B. *Journal of Membrane Science* **2003**, *211(1)*, 91.

[37] Patel, N.; Miller, A.C.; Spontak, R.J. *Adv. Mater.* **2003,** *15*, 729.

[38] Patel, N.; Miller, A.C.; Spontak, R.J. *Adv. Funct. Mater.* **2004,** *14*, 699.

[39] Bos, A. *"High pressure CO2/CH4 separation with glassy polymer membranes – Aspects of CO2-induced plasticization",* PhD Thesis, University of Twente, Enschede **1996**.

[40] Yasuda, H.; Rosengren, K. *J. Appl. Polym. Sci.* **1970**, *14*, 2839.

[41] Paul, D.R., Ber. Bunsenges, *Phys. Chem.* **1979**, *83*, 294.

[42] Koros, W.J.; Story, B.J.; Jordan, S.M.; O'Brien, K.C.; Husk, G.R. *Polym. Eng. Sci.* **1987**, *27*, 603.

[43] Story, B.J.; Koros, W.J. *J. Appl. Polym. Sci.* **1991**, *42*, 2613.

[44] LeRoux, J.D.; Paul, D.R.; Kampa, J.; Lagow, R.J. *J. Membrane Sci.* **1994**, *90*, 21.

[45] Ghosal, K.; Chern, R.T. *J. Membrane Sci.* **1992**, *72*, 91.

[46] Chern, R.T.; Sheu, F.R.; Jia, L.; Stanet, V.T.; Hopfenberg, H.B. *J. Membrane Sci.* **1987**, *35*, 103.

[47] Chern, R.T.; Jia, L.; Shimoda, S.; Hopfenberg, H.B. *J. Membrane Sci.* **1990**, *48*, 333.

[48] Story, B.J.; Koros, W.J. *J. Membrane Sci.* **1992**, *67*, 191.

[49] Laverty, B.W.; Vujosevic, R.; Deng, Sh.; Yao, B.; Matsuura, T.; Chowdhury, G. UK Patent Appliction 2 334 526, **1999**.

[50] Bessonov, M.I.; Koton, M.M.; Kudryavtsev, V.V.; Laius, L.A. Polyimides – Thermally Stable Polymers, Consultants Bureau, New York **1987**.

[51] Encyclopedia of Polymers, Sovetskaya Entsiklopediya, Moscow, Vol. 1 **1972**; Vol. 2 **1974**, *288*, 831.

[52] Kawakami, H.; Mikawa, M.; Nagaoka, S. *J. Membr. Sci.* **1996**, *118*, 223.

[53] Kawakami, H.; Mikawa, M.; Nagaoka, S. *J. App. Polym. Sci.* **1996***, 62,* 965.

[54] Koros, W.J.; Walker, D.R.B. *Polymer J.* **1991**, *23*, 481.

[55] Bateman, J.; Gordon, D.A. Soluble polyimides derived from phenylindane diamines and dianhydrides, US Patent 3.856.752.**1974.**

[56] Shusen, W.; Meyun, Z.; Zhizhong, W. *J. Mem. Sci.* **1996**, *109*, 267.

[57] Clausi, D.T.; Koros, W.J. *J. Membr. Sci.* **2000**, *167,* 79.

[58] Guiver, M.D.; Robertson, G.P.; Dai, Y.; Bilodeau, F.; Kang, Y.S.; Lee, K.J.; JHO, J.Y.; Won, J. *J. Polymer Sci.* **2002**, *40*, 4193.

[59] Cong, H.; Hu, X.; Radosz, M.; Shen, Y. *Ind. Eng. Chem. Res.* **2007**, *46*, 2567.

[60] Cong, H.; Zhang, J.; Radosz, M.; Shen, Y. *J. Mem. Sci.* **2007**, *294*, 178.

[61] Geckeler, K.E.; Samal, S. *Polym. Int.* **1999**, *48*, 743.

[62] Kroto, H.W.; Heath, J.R.; O'Brien, S.C.; Curl, R.F.; Smalley, R.F. *Nature* **1985**, *318*, 162.

[63] Krätschmer, W.; Lamb, L.D.; Fostiropoulos, K.; Huffman, D.R. *Nature* **1990**, *347*, 354.

[64] Geckeler, K.E. *Trends Polym. Sci.* **1994**, *2*, 355.

[65] Chen, Y.; Huang, Z.E.; Cai, R.F. and Yu, B.C. *Eur. Polym. J.* **1998**, *34 (2),* 137.

[66] Hawker, C.J., *Macromolecules* **1994**, *27*, 4836.

[67] Weng, D.; Lee, H. K.; Levon, K.; Mao, J.; Scrivens, W. A.; Stephens, E. B. and Tour, J. M. *European Polymer Journal* **1999**, *35(5)*, 867.

[68] Higuchi, A.; Yoshida, T.; Imizu, T.; Mizoguchi, K.; He, Z. J.; Pinnau, I.; Nagai, K. and Freeman, B. D. *Journal of Polymer Science Part B-Polymer Physics* **2000**, *38(13)*, 1749.

[69] Higuchi, A.; Agatsuma, T.; Uemiya, S.; Kojima, T.; Mizoguchi, K.; Pinnau, I.; Nagai, K. and Freeman, B. D. *Journal Of Applied Polymer Science* **2000,** *77(3)*, 529.

[70] Ball, Z. T.; Sivula, K. and Frechet, J. M. J. *Macromolecules* **2006**, *39(1)*, 70.

[71] Polotskaya, G. A.; Andreeva, D. V. and El'yashevich, G. K. *Technical Physics Letters* **1999**, *25(7)*, 555.

[72] Polotskaya, G. A.; Gladchenko, S. V. and Zgonnik, V. N. *Journal of Applied Polymer Science* **2002**, *85(14)*, 2946.

[73] Wooley, K.L.; Hawker, C.J.; Frechet, J.M.J. *J. Am. Chem. Soc.* **1993**, *115*, 9836.

[74] Rittinge, R. *Bachelor thesis*, "Free Volume Characterization of Hyperbranched Polymers", Lunds University, Sweden, **2002**.

[75] Kovvali, A. S.; Chen, H. and Sirkar, K. K. *Journal of the American Chemical Society* **2000**, *122(31),* 7594.

[76] Aoki, T. and Kaneko, T. *Polymer Journal* **2005**, *37(10)*, 717.

[77] Chung, T. S.; Chng, M. L.; Pramoda, K. P. and Xiao, Y. C. *Langmuir* **2004**, *20(7),* 2966.

[78] Xiao, Y. C.; Chung, T. S. and Chng, M. L. *Langmuir* **2004**, *20(19)*, 8230.

[79] Shao, L.; Chung, T. S.; Goh, S. H. and Pramoda, K. P. *Journal of Membrane Science* **2004**, *238(1-2)*, 153.

[80] Shao, L.; Chung, T. S.; Wensley, G.; Goh, S. H. and Pramoda, K. P. *Journal of Membrane Science* **2004**, *244(1-2)*, 77.

[81] Suzuki, T.; Yamada, Y.; Tsujita, Y. *Polymer* **2004**, *45*, 7167.

Chapter 2

Novel gas separation membranes containing covalently bonded fullerenes

Dana M. Sterescu, Lydia Bolhuis -Versteeg, Nico F. A. van der Vegt, Dimitrios F. Stamatialis, Matthias Wessling

Abstract

In this work, we report superior mass transport properties of polymers prepared by covalent coupling of super-molecular carbon cages (fullerenes, bucky-balls) based on poly (2, 6-dimethyl-1, 4-phenylene oxide) (PPO) polymer. Dispersing the bucky-balls into the polymer reduces gas permeability whereas covalent bonding enhances permeability up to 80 % in comparison to the pure PPO. Gas pair selectivity, however, is not compromised and stays constant.

Sterescu D.M. et al. *Macromol. Rapid Commun.* **2004**, *25*, 1674

1. Introduction

Gas separation based on polymeric membranes has become a major industrial application over the last years. Synthetic membranes for gas separation need to be highly permeable to one of the gas mixture components while significantly reject the other. The vast amount of polymers that have been investigated, however, show the general trend that highly permeable polymer possess low selectivity. This often referred to as the permeability / selectivity trade off relationship[1].

In recent years, considerable interest has been shown in the structure, properties and chemical reactivity of super-molecular carbon cages (fullerene, bucky balls, C_{60}) owing to their potential applications[2,3]. Fullerenes are potentially interesting materials for the preparation of membranes. Their hard-sphere properties may inhibit molecular polymer chain packing possibly resulting in high free volume. We hypothesize that covalent binding (rather than dispersing) is required to make the polymers highly permeable.

In the past, others have tried to disperse C_{60} in poly (1 - trimethylsilyl – 1- propyne) (PTMSP)[4], Matrimid[5] and poly (2, 6-dimethyl-1, 4-phenylene oxide) (PPO)[6]. The obtained membranes showed lower gas permeability than the initial material. In this work, we covalently couple the C_{60} at various weight percentages on PPO following the procedure described elsewhere[7]. This chapter presents the first successful increase of gas permeabilities based on covalent bonding of C_{60} and characterizes thoroughly the effect of each of the chemical modifications.

2. Experimental part

2.1 Materials

For the polymer synthesis the following materials were used: Poly (2,6-dimethyl-1, 4-phenylene oxide) (PPO) (Parker Filtration and Separation, MW = 150000 measured by GPC), 1,1,2,2-Tetra chloroethane (TCLE, 95 %, Fluka), bromine (Br_2, 99.5 %, Fluka), ethanol (Merck), chloroform (Merck), toluene (99.7 %, Fluka), dimethyl sulfoxide (DMSO, 99.5 %, Fluka), sodium

azide (NaN_3, 99 %, Fluka), methanol (Fluka), C_{60} (99.5 %, SES Research Company), chlorobenzene (99.5 %, Fluka), hexane (Fluka).

2.2 Synthesis of PPO-C_{60}

The PPO-C_{60} was synthesized following a three-step process (shown schematically in Figure 1).

Step 1: PPO bromination

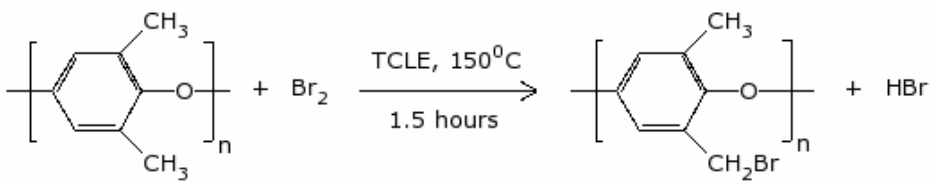

Step 2: Conversion to PPO-N_3

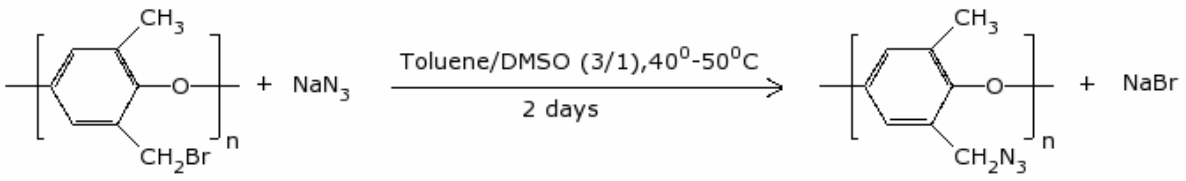

Step 3: Conversion to PPO-C_{60}

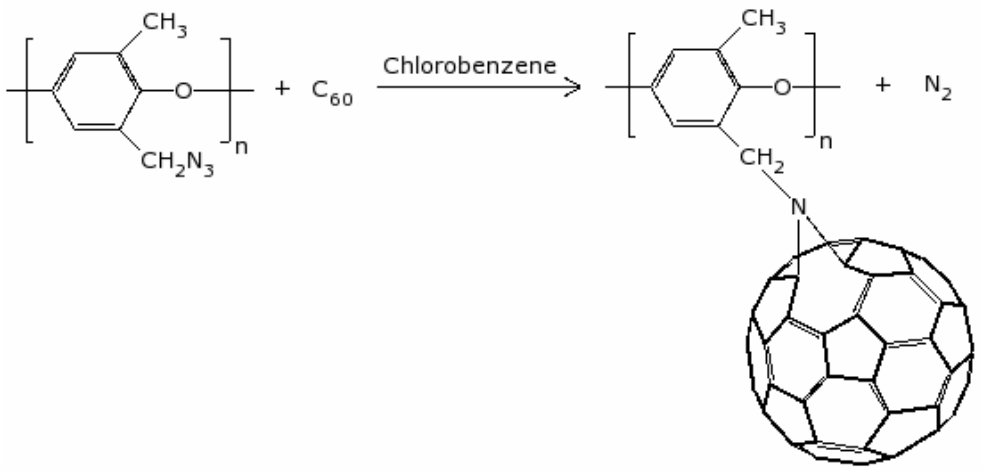

Figure 1:. Schematic presentation of the three step synthesis of PPO-C_{60}.

Step 1: PPO bromination (PPO-Br). For the PPO bromination, a mixture of PPO (24.50 g), TCLE (681 ml) and bromine (0.58 g) was allowed to reflux for 1.5 hours, under nitrogen stream, at 150 °C. Under these conditions, side group bromination without ring substitution is obtained[8]. This was also confirmed by ^{1}H-NMR spectroscopy (results not shown here). The bromine solution was added drop by drop when all the PPO was dissolved and the solution was boiling. The solution was then washed with a small amount of ultra pure water in a separatory funnel. The PPO-Br was obtained by precipitation using excess of ethanol (2 liters) under stirring. The polymer was purified by several dissolution/precipitation cycles using chloroform as solvent and ethanol as non-solvent. The reaction product was filtered and dried under nitrogen stream first at room temperature for 2 days and afterwards at 60 °C for 4 days. Elemental analysis showed that the PPO-Br contained 0.93 wt % Br, corresponding to 1.4 mol. % brominated PPO unit. Similarly, by using other suitable amounts of PPO and bromine, we prepared three more polymers, which contained 0.44, 1.64 and 2.03 wt % Br, respectively.

Step 2: PPO-Br conversion to PPO-N_3. The PPO-Br (18 g) was allowed to react with NaN_3 (0.6 g) in 1080 ml of a mixture of toluene/dimethyl sulfoxide (3/1) at 40 - 50 °C for 2 days. The NaN_3 was added when the polymer was completely dissolved in the mixture of solvents. The PPO-N_3 was obtained by precipitation using excess of methanol and purified by several dissolution / precipitation cycles using chloroform as solvent and methanol as non-solvent. The product was filtered and dried under nitrogen stream, first at room temperature for 4 days and afterwards at 40 - 50 °C for 4 more days. Elemental analysis showed that the PPO-N_3 contained 0.62 wt % of nitrogen, corresponding to 1.78 mol. % PPO-N_3 indicating that all bromine of PPO-Br has been quantitatively converted to azide. Similarly, by using other suitable amounts of PPO-Br and NaN_3, we prepared three more polymers which contained 0.32, 1.08 and 1.15 wt % of nitrogen, respectively.

Step 3: PPO-N_3 conversion to PPO-C_{60} [9]. The PPO-N_3 (5.0 g) and C_{60} (0.68 g, 1.3 times the molar amount of azide groups) were dissolved separately in 300 ml of chlorobenzene. After

complete dissolution of both, the two solutions were mixed. The mixture was refluxed under nitrogen for 41 hours till the strong IR band of the azide group had completely disappeared[7], proving complete conversion of PPO-N_3 to PPO-C_{60}. The chlorobenzene was removed by rotary evaporation and the solution was precipitated in n-hexane. To remove the unreacted C_{60} the precipitate was washed repeatedly with n-hexane until the n-hexane layer became colorless.

2.3 Preparation of membranes

For the preparation of pure PPO membranes, the polymer was dissolved in chloroform (10 wt %). The PPO solution was cast on a glass plate and dried initially under nitrogen atmosphere at room temperature (20 - 25 °C) for 3 days and then in a vacuum oven at 50 °C under nitrogen atmosphere for 2 days. For the preparation of PPO-C_{60} covalently bonded membranes, the polymer containing various percentages of C_{60} was dissolved in chlorobenzene (solution 1 wt %). The PPO-C_{60} solution was poured on flat Petri dishes and the membranes were formed by drying the solution, following initially the protocol used for pure PPO and after in a vacuum oven at 150 °C for 48 hours. The PPO-C_{60} films of 60-100 μm thickness were then peeled off the flat Petri dishes and kept under vacuum at 30 °C for 1 week[10].

For comparison, the PPO-Br and PPO-N_3 membranes were also prepared following similar procedure as for the PPO-C_{60} bonded membranes using a 6 wt % polymer solution.

For the preparation of PPO membranes with C_{60} dispersed, the PPO and C_{60} were dissolved separately in chlorobenzene (6 wt % PPO). After complete dissolution, they were mixed at various percentages together and stirred until the solution became homogeneous and allowed to stand for at least 24 h. The membranes were prepared using the same method like for PPO-C_{60} covalently bonded membranes.

2.4. Characterization of membranes

Infrared spectra of the pure PPO and PPO-C_{60} membranes were performed (using a Bio-Rad FTS-60 instrument) in order to prove the existence of C_{60} in the membrane structure.

The density measurements of PPO and PPO-C_{60} membranes were performed using an AccuPyc 1330 Pycnometer with a 0.1 cm^3 sample insert. The pressures observed upon filling the sample chamber with the gas and then discharging it into a second empty chamber allows computation of the density of the sample.

The permeation of pure nitrogen (N_2), oxygen (O_2) and carbon dioxide (CO_2) through the pure PPO, PPO-Br, PPO-N_3 and PPO-C_{60} (dispersed and covalently bonded) was investigated, using the set up described elsewhere[11]. All the gas permeation tests were performed at 35 °C. Values and error bars reported in the Tables and Figures are based on two different membrane samples.

3. Results and Discussion

Figure 2 (a) shows typical IR spectra of the PPO and PPO-C_{60} bonded polymers. The spectrum of PPO-C_{60} exhibits an absorption band at 525 cm^{-1}, corresponding to C_{60}[10] while such band does not exist at the spectrum of PPO. Figure 2 (b) shows that the intensity of this band increases with the amount of C_{60} in the polymer.

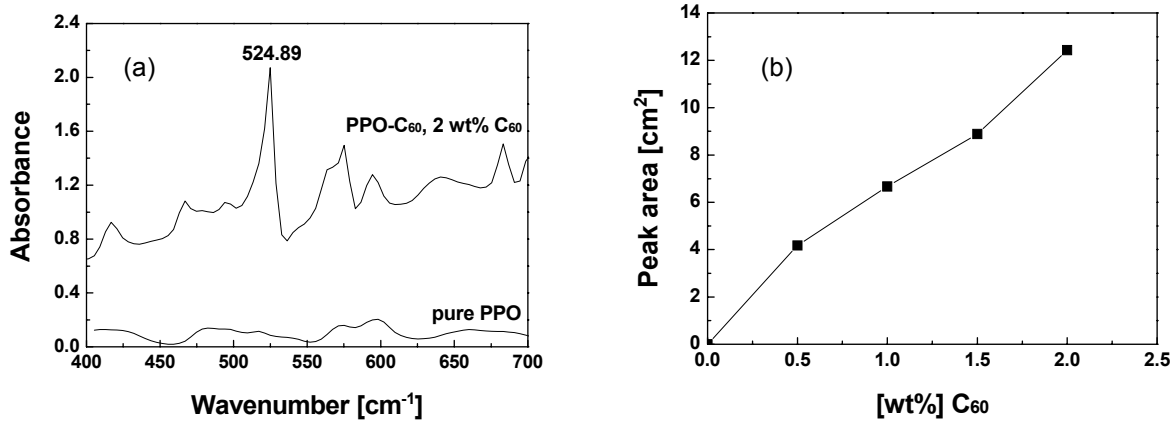

Figure 2:. (a) Infrared spectra of the PPO and PPO-C_{60} bonded containing 2.0 wt % C_{60}.
(b) The peak area at 525 cm^{-1} for various wt % of C_{60} in the PPO-C_{60} bonded.

The density for PPO and PPO-C_{60} bonded at 0.5 wt %, 1.0 wt%, 1.5 wt % and 2.0 wt % C_{60} is 1.13, 1.17, 1.18, 1.21 and 1.21 g/cm^3, respectively. However, the density of the PPO-C_{60} dispersed reported in the literature increases with the wt % of C_{60}, too[6]. In both cases, the increased density is probably due to the high density of C_{60} (~1.72 g/cm^3, larger than that of PPO) and cannot give us insight about the membrane structure (free volume, chain packing etc). The detailed structure of the new polymers will be further investigated by ^{1}H-NMR, TGA, DSC, PALS-free volume measurements and will be the topic of a subsequent paper.

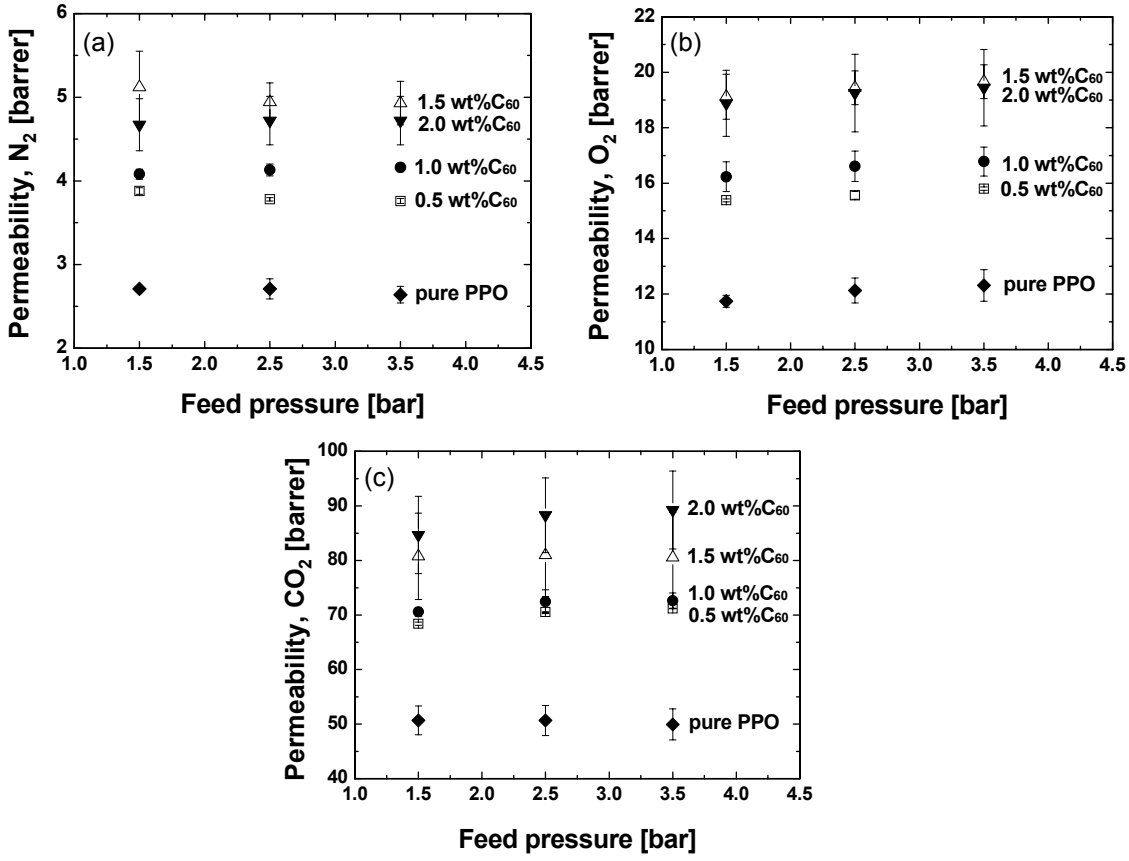

Figure 3: Permeability of (a) N_2, (b) O_2 and (c) CO_2 versus feed pressure for pure PPO (◆) and PPO-C_{60} bonded membranes containing: 0.5 wt % C_{60} (□), 1.0 wt % C_{60} (●), 1.5 wt % C_{60} (△) and 2.0 wt % C_{60} (▼).

The gas transport through the membranes at various feed pressures was characterized using the gas permeability coefficient, P[11]. Figure 3 shows the results of the permeability versus feed pressure for N_2, O_2 and CO_2 for PPO membranes with different content of C_{60} covalently

bonded. The gas permeability is constant at different feed pressures and increases significantly with increasing of C_{60} content. Figure 4 shows the ratio of gas permeability of PPO-C_{60} bonded over the pure PPO. The permeability coefficient significantly increases with increasing C_{60} content for all three gases. It seems, however, that above 1.5 wt % C_{60} the permeability of PPO-C_{60} reaches a plateau. Apparently, the N_2 permeability increases the strongest but we have no explanation for it at present. Any attempts to explain this before obtaining data on the free volume of the polymer and on the diffusion and solubility constants, would be largely speculative.

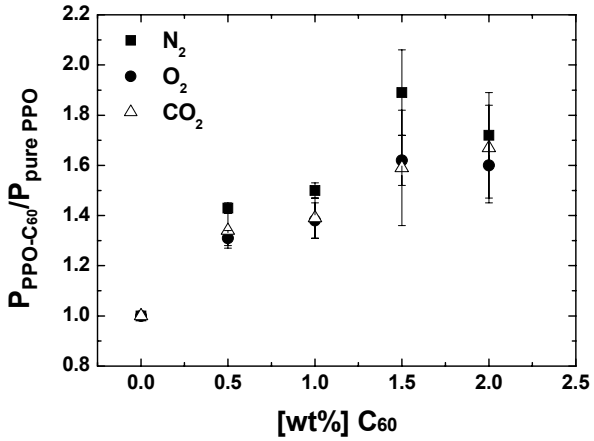

Figure 4: Permeability of PPO-C_{60} bonded normalized with the permeability of pure PPO versus the wt % C_{60}. Gases: N_2 (■), O_2 (●) and CO_2 (△).

In contrast to the significant increase of the gas permeability of the PPO-C_{60} bonded membranes in comparison to pure PPO, the selectivity coefficients seem to be independent of C_{60} content. Table 1 presents typical results at feed pressure 1.5 bar. Similar results, however, are found at feed pressures 2.5 and 3.5 bar.

Table 2 compares the permeability of the PPO-C_{60} bonded membranes with those of PPO-Br and PPO-N_3 and PPO-C_{60} dispersed membranes for all three gases. The PPO-Br and PPO-N_3 have almost the same permeability with the pure PPO membranes indicating that the addition of Br and N_3 groups does not contribute to the increase of polymer permeability. The PPO-C_{60} dispersed membranes, however, exhibit lower gas permeability than the pure PPO in

agreement with other studies[6,12]. Moreover, the selectivity of these membranes is not significantly different than that of pure PPO and PPO-C_{60} bonded (see Table 1).

Table 1: Ideal gas selectivity of PPO-C_{60} bonded and dispersed, (Feed pressure: 1.5 bar, T = 35 °C).

	Ideal Selectivity		
wt% C_{60}	**P_{O2}/P_{N2}**	**P_{CO2}/P_{N2}**	**P_{CO2}/P_{O2}**
0	4.3 ± 0.1	18.7 ± 1.1	4.3 ± 0.3
bonded			
0.5	4.0 ± 0.1	17.6 ± 0.3	4.4 ± 0.1
1.0	4.0 ± 0.2	17.3 ± 0.5	4.3 ± 0.2
1.5	3.7 ± 0.5	15.7 ± 2.9	4.2 ± 0.6
2.0	4.0 ± 0.5	18.1 ± 2.7	4.5 ± 0.6
dispersed			
1.0	3.5 ± 1.0	14.6 ± 4.6	4.2 ± 1.9

In general, physical aging results in a decrease in gas permeability over time due to polymer densification[13-15]. In order to get some insight into the aging of these membranes, we stored samples in vacuum oven at 30 °C and at 100 °C for a year. Then, the gas permeability of N_2, O_2 and CO_2 through PPO pure and PPO-C_{60} bonded with 1 and 2 wt % of C_{60} was measured again (see Table 3 and Figure 5).

Table 2: Permeability of PPO, PPO-Br, PPO-N_3, PPO-C_{60} bonded and PPO with C_{60} dispersed, (Feed pressure: 1.5 bar, T = 35 °C)

	Permeability, [barrer]				
	PPO	PPO-Br	PPO-N_3	PPO with C_{60} dispersed 1 wt % C_{60}	PPO-C_{60} bonded 1 wt % C_{60}
N_2	2.7 ± 0.1	2.9 ± 0.1	3.1 ± 0.1	2.6 ± 0.2	4.1 ± 0.1
O_2	11.7 ± 0.2	11.9 ± 0.4	10.0 ± 0.4	9.0 ± 1.9	16.2 ± 0.5
CO_2	50.7 ± 2.6	50.6 ± 1.4	42.9 ± 8.9	37.8 ± 8.9	70.6 ± 0.8

The permeability of pure PPO aged at 30 °C and 100 °C decreases ~ 5 % and 8 % respectively in comparison to the original sample, for all three gases. The N_2 permeability of PPO-C_{60} 1.0 wt % bonded, kept at 30 °C and 100 °C decreases 10 % and 41 % respectively in comparison to the original sample. Similar trend was found for O_2 and CO_2 (Table 3).

Table 3: Comparison between gas permeability and selectivity of fresh and aged films stored under vacuum at 30 °C and 100 °C, for a year.

Feed pressure: 3.5 bar, T = 35 °C

wt % C_{60} bonded to PPO	Treatment	Permeability, [barrer]			Selectivity		
		N_2	O_2	CO_2	P_{O2}/P_{N2}	P_{CO2}/P_{N2}	P_{CO2}/P_{O2}
0	no	2.6 ± 0.1	12.3 ± 0.6	50.0 ± 2.8	4.6 ± 0.4	18.9 ± 1.8	4.1 ± 0.4
	30 °C	2.5 ± 0.2	11.8 ± 0.8	47.4 ± 3.5	4.8 ± 0.7	19.1 ± 2.7	4.0 ± 0.6
	100 °C	2.4 ± 0.1	11.6 ± 0.1	45.9 ± 0.1	4.9 ± 0.1	19.3 ± 0.1	4.0 ± 0.1
1.0	no	4.2 ± 0.1	16.8 ± 0.5	72.7 ± 1.4	4.0 ± 0.2	17.5 ± 0.6	4.3 ± 0.2
	30 °C	3.8 ± 0.1	13.3 ± 1.7	61.8 ± 5.5	3.5 ± 0.5	16.3 ± 1.5	4.7 ± 1.0
	100 °C	2.5 ± 0.1	10.0 ± 1.4	43.1 ± 0.6	4.0 ± 0.8	17.2 ± 1.3	4.3 ± 0.7
2.0	no	4.7 ± 0.3	19.5 ± 1.4	89.3 ± 7.2	4.1 ± 0.5	18.9 ± 2.7	4.6 ± 0.7
	30 °C	4.4 ± 0.1	18.5 ± 0.7	81.9 ± 5.0	4.2 ± 0.3	18.5 ± 1.7	4.4 ± 0.4
	100 °C	3.0 ± 0.1	13.4 ± 0.2	54.2 ± 0.3	4.5 ± 0.1	18.2 ± 0.1	4.1 ± 0.1

The N_2 permeability of PPO-C_{60} bonded with 2.0 wt % C_{60} decreases only 6 % at 30 ^{0}C and 36 % at 100 °C. Similar trends were found also for the O_2 and CO_2 permeability. The decrease in permeability of the aged PPO-C_{60} bonded membranes can be due to two factors. First, the polymer stored in time and under temperature has the tendency to organize itself in a more ordered structure resulting in higher crystalline fraction regarded as impermeable. Thus, the gas permeability of crystalline films is substantially lower than in a more amorphous membrane[16] due to the reduced space available for diffusion and the tortuous path around the crystallites. Second,

the densification of the polymer can occur, due to the relaxation of nonequilibrium chain conformations[13,14] resulting in a decrease of gas permeability.

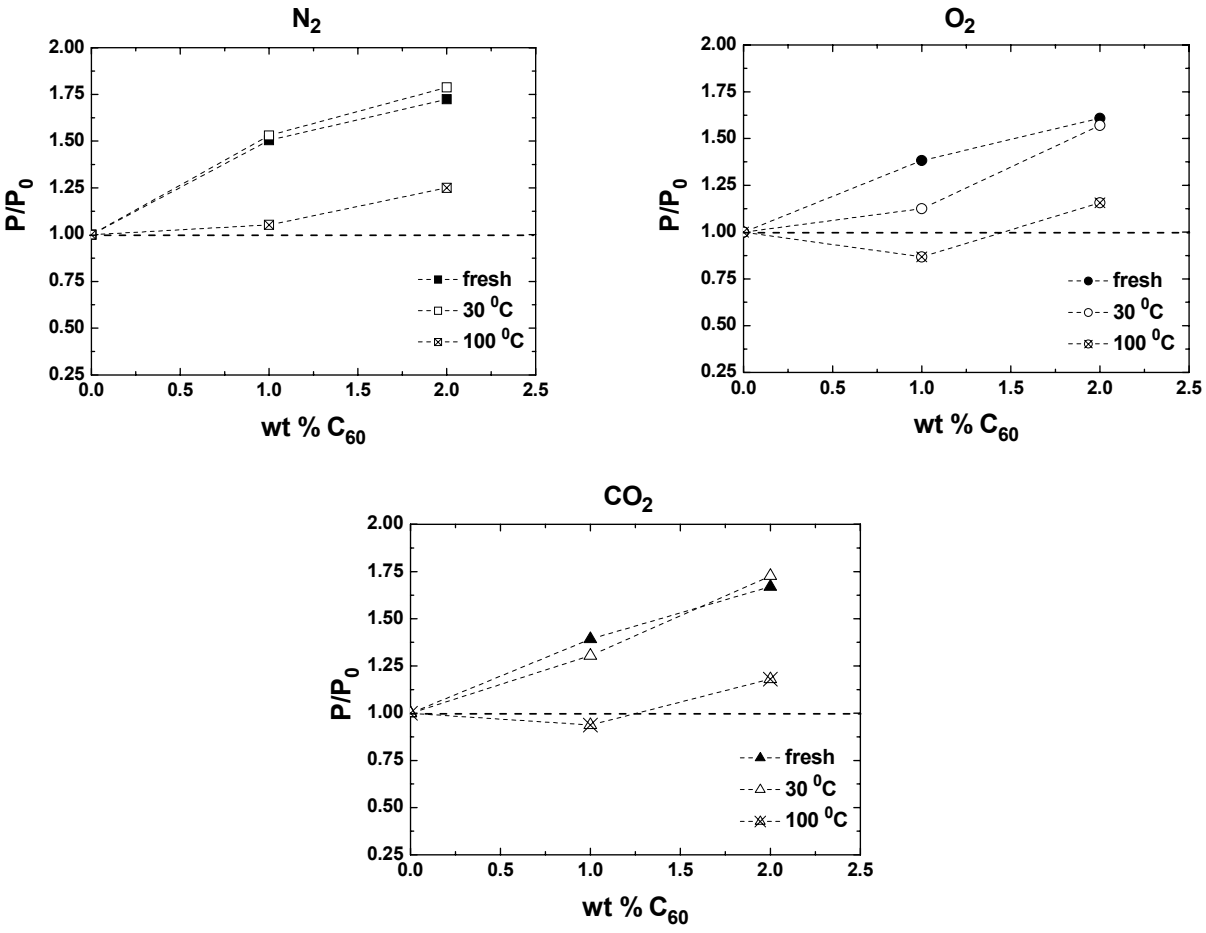

Figure 5: Gas permeability through PPO-C_{60} bonded with 1 wt % and 2 wt % C_{60} normalized with the permeability of pure PPO versus the wt % C_{60} for N_2, O_2 and CO_2 to fresh membranes, aged membranes at 30 °C and aged membranes at 100 °C.

The decrease of permeability of N_2, O_2 and CO_2 of PPO-C_{60} bonded with 2.0 wt % C_{60} is less than the PPO-C_{60} bonded with 1.0 wt % C_{60} (Figure 5). Probably for the PPO-C_{60} 2 wt % the polymer has less mobility, less space to move for polymer segments and also hindrance of the rotational movements. The more C_{60} bonded to PPO the more hindrance of the rotational movements of PPO takes place, lowering the packing density of the polymer.

In conclusion, for the PPO-C_{60} bonded membranes at the same wt % C_{60} the gas separation properties of the membranes kept at 30 °C are close to the properties of the original samples. However, the membranes kept at 100 °C show ~ 30 - 40 % lower gas permeabilities than the original samples (Figure 5). Besides, the membranes containing 2.0 wt % of C_{60} seem to be more resistant to aging at 100 °C.

Table 3 shows the ideal selectivity calculated at 3.5 bar feed pressure and 35 °C (similar results were found at feed pressures of 1.5 and 2.5 bar). In contrast to the remain gas permeability of the aged membranes the ideal selectivity seems to keep constant.

4. Conclusions

This work presents the preparation of novel membranes by covalent coupling of C_{60} to PPO. The PPO-C_{60} bonded membranes exhibit significantly higher gas permeability (up to 80%) in comparison to pure PPO without compromise in selectivity. The PPO-C_{60} bonded membranes stored at 30 °C have the same high permeation properties as the freshly prepared ones. However, the membranes stored at 100 °C show 30 to 40 % lower gas permeability than the fresh samples due to polymer aging.

These preliminary results represent a first step in analyzing the relationship between the C_{60} bonded on the polymer chain and the gas transport properties. Our future work (see Chapter 3) will include systematic analysis of their structure using ^{1}H-NMR, WAXS, DSC, PALS - free volume. In addition, gas sorption measurements will be performed to identify the reason behind the significant increase of the gas permeability through the PPO-C_{60} bonded membranes.

5. References

[1] Freeman, B.D. *Macromolecules* **1999**, *32*, 375.

[2] Chen, Y.; Huang, Z.E.; Cai, R.F. and Yu, B.C. *European Polymer J.* **1998**, *34(2)*, 137.

[3] Geckeler, K.E.; Samal, S. *Polym. International* **1999**, *48*, 743.

[4] Higuchi, A.; Yoshida, T.; Imizu, T.; Mizoguchi, K.; He, Z.; Pinnau, I.; Nagai, K.; Freeman, B.D. *J. Polymer Science, Part B: Polymer Physic,* **2000**, *38*, 1729.

[5] Chung, T.-S.; Chan, S.S.; Wang, R.; Lu, Z. and He, C. *J. Membrane Science* **2003**, *211*, 91.

[6] Polotskaya, G.A.; Andreevna, D.V. and El'yashevich, G.K. *Technical Phys. Lett.* **1999**, *25 (7)*, 555.

[7] Goh, S.H.; Zheng, J.W. and Lee, S.Y. *Polymer* **2000**, *41*, 8721.

[8] Cabasso, I.; Jagur-Grodzinski, J. and Vofsi, D.*J. Applied Polymer Science* **1974**, *18,* 1969.

[9] Hawker, C.J. *Macromolecules* **1994**, *27*, 4836.

[10] Higuchi, A.; Agatsuma, T.; Uemiya, S.; Kojima, T.; Mizoguchi, K.; Pinnau, I.; Naga, K. and Freeman, B.D. *J. Applied Polymer Science* **2000**, *77*, 529.

[11] Barsema, J.N.; Kapantaidakis, G.C.; van der Vegt, N.F.A.; Koops, G.H. and Wessling, M. *J. Membrane Science* **2003**, *216*, 195.

[12] Polotskaya, G.A.; Gladchenko, S.V. and Zgonnik, V.N. *J. Applied Polymer Science* **2002**, *85*, 2946.

[13] Merkel, T.C.; Freeman, B.D.; Spontak, R.J.; He, Z.; Pinnau, I.; Meakin, P.; Hill, A.J. *Chem. Mater*. **2003**, *15*, 109.

[14] Nagai, K.; Nakagawa, T. *Journal of Membrane Science* **1995**, *105*, 261.

[15] Morisato, A.; He, Z.; Pinnau, *I. In Polymer Membranes for Gas and Vapor Separation: Chemistry and Materials Science*; Freeman, ; B.D.; Pinnau, I. Eds.; American Chemical Society: Washington, D.C., 1999, p. 56.

[16] Khulbe, K.C.; Matsuura, T. *Journal of Membrane Science* **2000**, *171*, 273.

Chapter 3

Fullerene-modified poly (2, 6-dimethyl-1,4-phenylene oxide) gas separation membranes: Why binding is better than dispersing

Dana M. Sterescu, Dimitrios F. Stamatialis, Eduardo Mendes, Michael Wübbenhorst, Matthias Wessling

Abstract

This paper describes the preparation, characterization and the permeation properties of poly (2, 6-dimethyl-1,4-phenylene oxide) (PPO) dense polymer films containing fullerenes (C_{60}). The C_{60} are either dispersed or covalently bonded to PPO at various concentrations. The gas permeability results are very different between covalently bonded and dispersed PPO-C_{60}.

The gas permeability of PPO-C_{60} bonded increases up to 80 % with increasing fullerene concentration. The gas pair selectivity, however, stays constant. This behavior is probably due to stiffening of the polymer structure and increase of free volume. The gas permeability through the PPO-C_{60} dispersed decreases in comparison to pure PPO. This reduction is due to C_{60} clustering in the polymer. The clusters seem to induce polymer crystallinity and they are probably aligned along the film plane creating an extra barrier for gas permeation.

Sterescu D.M. *et al. Macromolecules* **2006**, *39*, 9234

1. Introduction

The control of gas permeability and selectivity for polymer membranes separating molecular mixtures of gases has become a subject of intense research in both the industrial and academic fields[1]. Special attention has been concentrated on the relationship between the polymer structure and gas separation properties. Most of the polymers that have been investigated, however, show the general trend that highly permeable polymers possess rather low selectivity. This often referred to as the permeability / selectivity trade off relationship[2].

The permeation properties of a polymer depend primarily on the packing density, the polymer chain mobility and the free volume of the polymer structure, which can be increased by the introduction of bulky substituents. For this, a considerable interest has been shown in super-molecular carbon cages (fullerene, bucky balls, C_{60}) containing polymers[3-7]. The hard-sphere properties of C_{60} may inhibit molecular polymer chain packing possibly resulting in high free volume and improved permeation properties.

Only very few polymers are actually used for the industrial production of gas separation membranes; poly (2, 6-dimethyl-1,4-phenylene oxide) (PPO) is one of them[8]. PPO is particularly interesting for the production of nitrogen-enriched air due to its high permeability and acceptable selectivity. It is highly desirable to identify methods to modify PPO chemically in order to increase permeability without compromising selectivity. In our earlier study[3], we have shown that the coupling of the bulky C_{60} groups to PPO backbone can increase the gas permeability (up to 80 %) without compromise to selectivity. In this paper, we study the permeation properties of PPO-C_{60} dispersed, too. Small amount of C_{60} dispersed into PPO seems to cause significant reduction of membrane permeability. A systematic analysis of both PPO-C_{60} bonded and dispersed is performed using differential scanning calorimetry (DSC), Wide Angle X-ray Scattering (WAXS) measurements and gas sorption experiments in order to investigate the reasons of the difference in the permeation performance between the bonded and dispersed C_{60}.

2. Background

2.1 Transport in Polymers

The permeation of a gas molecule through a dense membrane is usually governed by a solution-diffusion mechanism. The permeability P of a polymer is given as the product of diffusivity, D (kinetic component), and solubility, S (thermodynamic component):

$$P=D\cdot S \tag{1}$$

The ideal selectivity of a membrane for component A relative to component B, $\alpha_{A/B}$, is defined as the ratio of their permeabilities[9,10], which in terms of equation 1 can be rewritten as:

$$\alpha_{A/B} = \frac{P_A}{P_B} = \left(\frac{S_A}{S_B}\right) \times \left(\frac{D_A}{D_B}\right) \tag{2}$$

The first term on the right-hand side is the solubility selectivity and the second term is the diffusivity selectivity.

Over the past three decades, sorption of gas molecules into glassy polymers has been described and analyzed by the dual-mode sorption model[11]. The fundamental assumption of the dual mode sorption theory is the existence of two distinct populations of gas molecules in a polymer matrix. Rubbery polymers are in a hypothetical thermodynamic equilibrium liquid state and their gas solubility obeys Henry's law. On the other hand, glassy polymers are typically assumed to be in a non-equilibrium state containing two components: a frozen-in solid state of unrelaxed free volume and a hypothetical liquid state being in equilibrium. The model is used to represent the sorbed amount of gas (C) of pure gases in polymers as function of the pressure (p), and is expressed by:

$$C = C_D + C_H = k_D p + \frac{C_H' b p}{1 + b p} \quad (3)$$

where C_D is the gas concentration based on Henry's law sorption, C_H is the gas concentration based on Langmuir sorption, k_D is the Henry's law coefficient, b and C_H' are the Langmuir hole affinity parameter and the capacity parameter, respectively. The k_D parameter represents the penetrant dissolved in the polymer matrix at equilibrium and b characterizes the sorption affinity for a particular gas-polymer system. These parameters can be determined from the measured sorption data. C_H' is often used to measure the amount of the non-equilibrium excess free volume in the glassy state[12].

The diffusivity and diffusivity selectivity are functions of polymer properties on molecular scale such as resistance to torsional motions, inter-segmental backbone spacing, and free volume. Reductions in the mean inter-chain distance require larger segmental motions of polymer molecules to allow local passage of a gas molecule.

2.2 Transport in Heterogeneous Materials

Numerous models have been developed to describe transport properties in heterogeneous polymer systems. One of the most known ones is that of Maxwell[10,13,14] used in two forms. The simple form analyzes the steady-state dielectric properties of a dilute suspension of spheres where the permeability of a composite, P, made by dispersing of non-porous, impermeable filler (as C_{60}) in a continuous polymer matrix is expressed as:

$$P = P_p \left(\frac{1 - \varphi_f}{1 + \frac{\varphi_f}{2}} \right) \quad (4)$$

where P_p is the permeability of the pure polymer and φ_f is the volume fraction of filler. Equation 4 suggests that the permeability of the filled polymer is lower than of the pure polymer and decreases with increasing of the filler concentration. The decreased permeability is the result of a reduction in penetrant solubility due to (i) the replacement of polymer through which transport may occur with filler particles and (ii) an increase in the tortuosity[10] of the diffusion path through which the penetrant molecules cross the polymeric film. It is important to note that in the case of clustering of filler particles, and the formation of interstitial voids with no polymer into them, the structure gets more complex by inducing morphological changes in the polymer matrix.

The second generalized form[14] is used to estimate the permeation through a structured biphasic material wherein the additive component is randomly dispersed with sharp interfaces in a continuous matrix of the polymer expressed as:

$$P = P_p \left[1 + \frac{(1+G)\varphi_f}{\left(\frac{P_f/P_p + G}{P_f/P_p - 1} \right) - \varphi_f} \right] \qquad (5)$$

where P_f is the permeability of the C_{60}, G is a geometric factor accounting for dispersion shape. If the dispersed phase is oriented in lamellae parallel to the direction of permeation, $G \rightarrow \infty$, and there is minimum resistance to flow. If the disperse phase is oriented in lamellae perpendicular to the direction of permeation, $G \rightarrow 0$, and maximum impedance of flow occurs due to obstructive layers of the less permeable component. In this work, the C_{60} volume fraction in PPO has been estimated using the equation:

$$\varphi_f = \frac{w_f}{w_f + \frac{\rho_f}{\rho_p}(1 - w_f)} \qquad (6)$$

where ρ_p and ρ_f is the density of the pure polymer and C_{60}, respectively, and w_f is the C_{60} weight fraction in the polymer.

3. Experimental

3.1 Modification of PPO

The preparation of PPO-C_{60} bonded polymer was performed in three steps[3]: a) PPO bromination (PPO-Br); b) PPO-Br conversion into PPO-N_3 and c) PPO-N_3 conversion into PPO-C_{60} bonded. The bromination of PPO is a selective reaction that can introduce bromine into the phenylene rings or into the benzyl position[15-17]. In our work, free radical bromination of PPO was carried out to provide PPO containing bromo-methyl groups and, it was subsequently used for the preparation of PPO-N_3[17]. The bromo-methylation of PPO was confirmed by ^{1}H-NMR spectroscopy (using a Varian Unity INOVA 300 MHz spectrometer).

3.2 Preparation of membranes

Membranes of PPO pure, PPO-C_{60} bonded and dispersed at various concentrations (0.5 – 2.0 wt %) were prepared using the method described elsewhere[3]. There is a limit in the preparation of PPO-C_{60} bonded membrane. Above 2.0 wt % C_{60}, the polymer becomes insoluble, intractable and not processable. In contrary, for PPO-C_{60} dispersed membrane there is no such limit regarding the C_{60} concentration. Besides, C_{60} undergoes aggregation in polar aromatic solvents like, benzonitrile (BZN) and benzyl alcohol (BZA), but not in relatively non-polar solvents like, benzene (BZ), toluene (TL), chlorobenzene (CBZ)[18]. Therefore, to avoid the C_{60} aggregation we have used chlorobenzene as a solvent for the preparation of the PPO-C_{60} membranes. Since the membrane structure depends on the casting solvent[19], PPO pure membranes were prepared in chlorobenzene and chloroform for comparison. The thickness of all membranes was in the range of 50 – 100 μm. After the preparation, the samples were mainly stored in vacuum oven at 30 °C. Some samples have also been stored at 100 °C to study the membrane aging.

3.3 Characterization of membranes

The thermal properties of pure PPO, PPO-C_{60} bonded and dispersed were measured using a Perkin Elmer DSC-7 (Differential Scanning Calorimeter) in nitrogen atmosphere. The samples were initially heated from 50 °C until 350 °C, cooled with liquid nitrogen, held for 5 minutes, and reheated two more times following the same steps, under nitrogen atmosphere. The heating rate was 10 °C/min and the cooling rate was 20 °C/min. The glass transition temperature, T_g of the polymer was obtained from the third scan.

The permeation of pure nitrogen (N_2), oxygen (O_2) and carbon dioxide (CO_2) through the PPO and PPO-C_{60} (dispersed and covalently bonded) was investigated, using the set up described elsewhere[20]. Pure gas permeability coefficients were calculated from the steady state pressure increase in time in a calibrated volume at the permeate side by using the equation:

$$\frac{P}{l} = \frac{V \times 273.15 \times (p_{pt} - p_{p0})}{A \times T \times \frac{(p_{ft} + p_{f0})}{2} \times 76 \times t} \times 10^6 \qquad (7)$$

where the ideal gas law is assumed to be valid, p_{pt} , p_{ft} [bar] is the pressure at the permeate and feed side at time t, p_{p0} p_{f0} is the permeate and feed pressure at t=0, T [K] is the temperature, V [cm^3] is the calibrated permeate volume, and A [cm^2] the membrane area. The gas permeance (P/l) is expressed in GPU, i.e. 10^{-6} cm^3cm^{-2} s^{-1} $cmHg^{-1}$. Multiplying the gas permeance with the thickness of dense membranes, l [µm], gives the permeability coefficient in Barrer. All the gas permeation experiments were performed at 35 °C. Values and error bars reported in the tables and figures are based on measurements of two different membrane samples.

The gas sorption isotherms of N_2, O_2 and CO_2 in dense PPO pure and PPO-C_{60} bonded and dispersed (1.5 wt %) films were measured at 35 °C, using a magnetic suspension balance[21] (MSB, Rubotherm). The experimental procedure was divided into five steps: a) evacuation of pressure vessel and sample for at least 24 hours; b) increase of gas pressure to desired value; c) wait until equilibrium in mass change is reached; d) record equilibrium mass, temperature and pressure; e) repeat steps b and c or if the maximum pressure is reached: evacuate sample (step

a) and start measurement with new gas or new sample. The equilibrium mass increase was corrected for buoyancy by subtracting the weight at zero sorption at a certain pressure from the vacuum weight of the sample. Using the equilibrium weight increase and the density of the polymer, the concentration (in cm^3 STP) inside the polymer (cm^3 polymer) was calculated[21].

3.4 WAXS measurements

Knowledge of crystalline morphology is of great importance in understanding the permeation properties of the polymeric membranes. In general, the crystalline phase may be regarded as impermeable. For this reason the gas permeability in a semi-crystalline polymer membrane is substantially lower than in the more amorphous membrane because of the reduced space available for diffusion and the tortuous path around the crystallites. Permeation sites may be of either amorphous material or interstices between crystallites[19].

The most generally applicable technique that provides information about the crystalline structure is the X-Ray diffraction (XRD). In this study, Wide Angle X-ray Scattering (WAXS) experiments were performed using a Bruker-Nonius D8-Discover equipped with 2D detector.

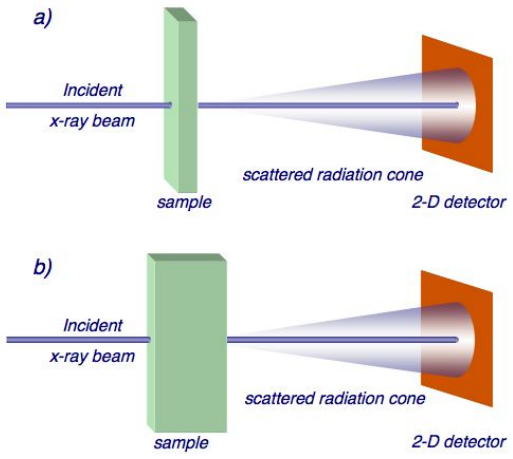

Figure 1: Sample geometry used in the WAXS experiments incident x-ray beam: a) perpendicular to the film plane; b) on the side of the film.

Standard background (air and sample holder) subtraction measured at the same time and conditions were applied to all data. The sample-detector (S-D) distance was set at 10 cm and the incident beam wavelength was 1.54Å (Cu-Kα). Measurements were performed both perpendicular and in the plane of the membrane (see Figure 1). In the first case, the sample thickness as seen by the incident beam was always less than 0.5 mm.

4. Results and discussion

4.1 H-NMR

The ^{1}H-NMR chemical shift values (300 MHz) are reported as δ in [ppm] using the residual solvent signal as an internal standard ($CDCl_3$ δ = 7.29). ^{1}H-NMR spectra in $CDCl_3$ were performed for PPO pure and PPO-Br 2 wt %. The spectrum of the pure compound shows two singlets, one at 2.11 ppm for the methyl protons and one at 6.49 ppm for the aromatic protons. The spectrum of the 2 % brominated compound shows, besides the two singlets, an extra peak at 4.36 ppm specific for the CH_2Br protons[15]. This confirms that the bromination has taken place on the methyl group and the further modification by coupling of C_{60} took place on the methyl group of PPO, too.

4.2 DSC-T_g

Figure 2 shows that the T_g of PPO-C_{60} bonded increases with the increase of the C_{60} concentration, from 214 °C for the pure PPO to 235 °C for the PPO-C_{60} 2wt %. This indicates that the PPO-C_{60} bonded polymer becomes more stiffened and probably there is suppressed inter-chain packing due to hindering the torsional motion of the phenyl ring around the ether linkage as well as some possible conformational changes in the backbone. Perhaps, as a consequence an extra interstitial chain space is created and the free volume of the membrane increases, too. In contrast, for the PPO-C_{60} dispersed membranes the T_g decreases in comparison to pure PPO indicating a more compact polymer structure in agreement with literature[22]. More detailed investigation of the PPO-C_{60} structure (bonded and dispersed) using Positron Annihilation

Lifetime Spectroscopy (PALS) and dielectric relaxation spectroscopy is currently under investigation and will be the subject of a future submission.

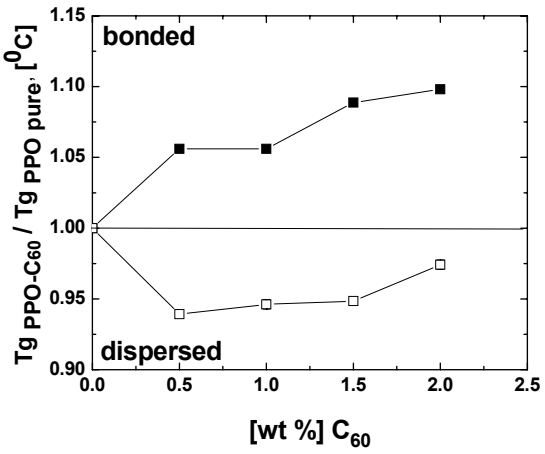

Figure 2: The T_g of PPO-C_{60} bonded and dispersed over T_g of pure PPO membranes versus the wt % C_{60} content.

4.3 WAXS analysis

It is well known that the C_{60} show anomalous behavior due to the formation of aggregates[23,24]. Figure 3 shows the results recorded in a 2-D detector for PPO-C_{60} bonded and dispersed with 2.0 wt % C_{60}. The scattering from the pure C_{60} powder and pure PPO are also shown for comparison. For PPO-C_{60} the incident beam geometry corresponds to Figure 1a, incident beam perpendicular to the film plane. The scattering pattern of C_{60} powder (see Figure 3a) exhibits typical crystalline structure. The peak positions are displayed in Figure 5a as a function of the scattering angle and are indexed following the convention used in the literature[25]. The scattering of the pure PPO film is also displayed (Figure 5b), and it is in agreement with previously published data[19]. Some of the scattering peaks in C_{60}, namely (111) and (220), are used as references in the interpretation of the scattering from bonded and dispersed films. They correspond to d-spacings of 14.17 Å, the crystalline face centred cubic (fcc) lattice constant and 7.53 Å, the C_{60} diameter (Figure 5a).

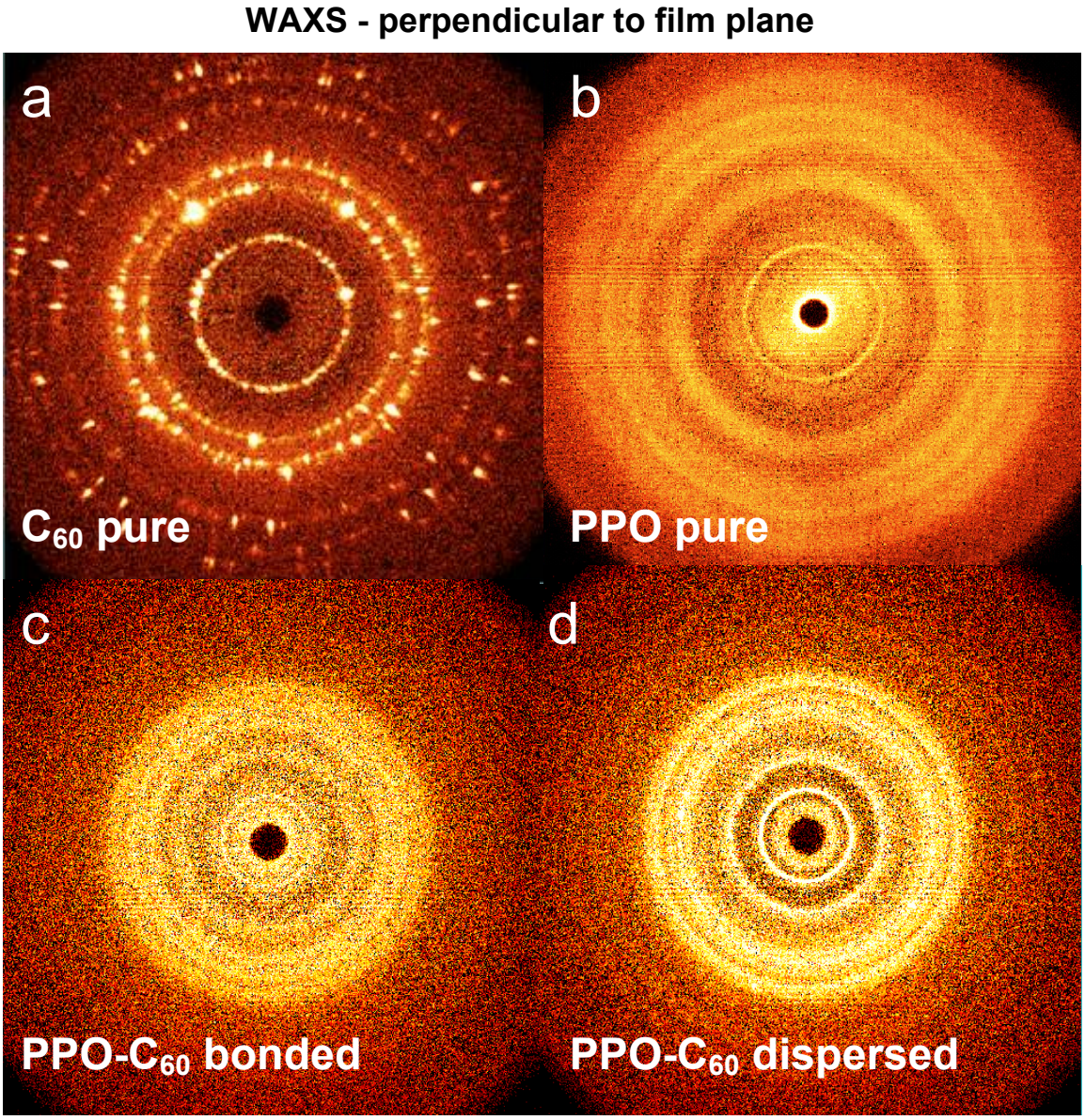

Figure 3: Scattering data recorded on a 2-D detector for the two basic components of the samples, a) pure C_{60} powder; b) pure PPO c) PPO-C_{60} 2.0 wt % bonded and d) PPO-C_{60} 2.0 wt % dispersed.

The scattering peaks from C_{60} (Figure 3a), as well as those of the pure PPO films (Figure 3b), are also present in the scattering patterns of the bonded and dispersed films, (see Figures 3c and 3d, respectively). Despite the fact that both samples contain the same amount of fullerene (2 wt %), the scattering fullerene peaks, (111) and (220) are far more intense in the PPO-C_{60}

dispersed. This intensity scattering difference in bonded and dispersed samples as a function of the scattering angle, 2θ can be easily observed in Figures 5b and 5c.

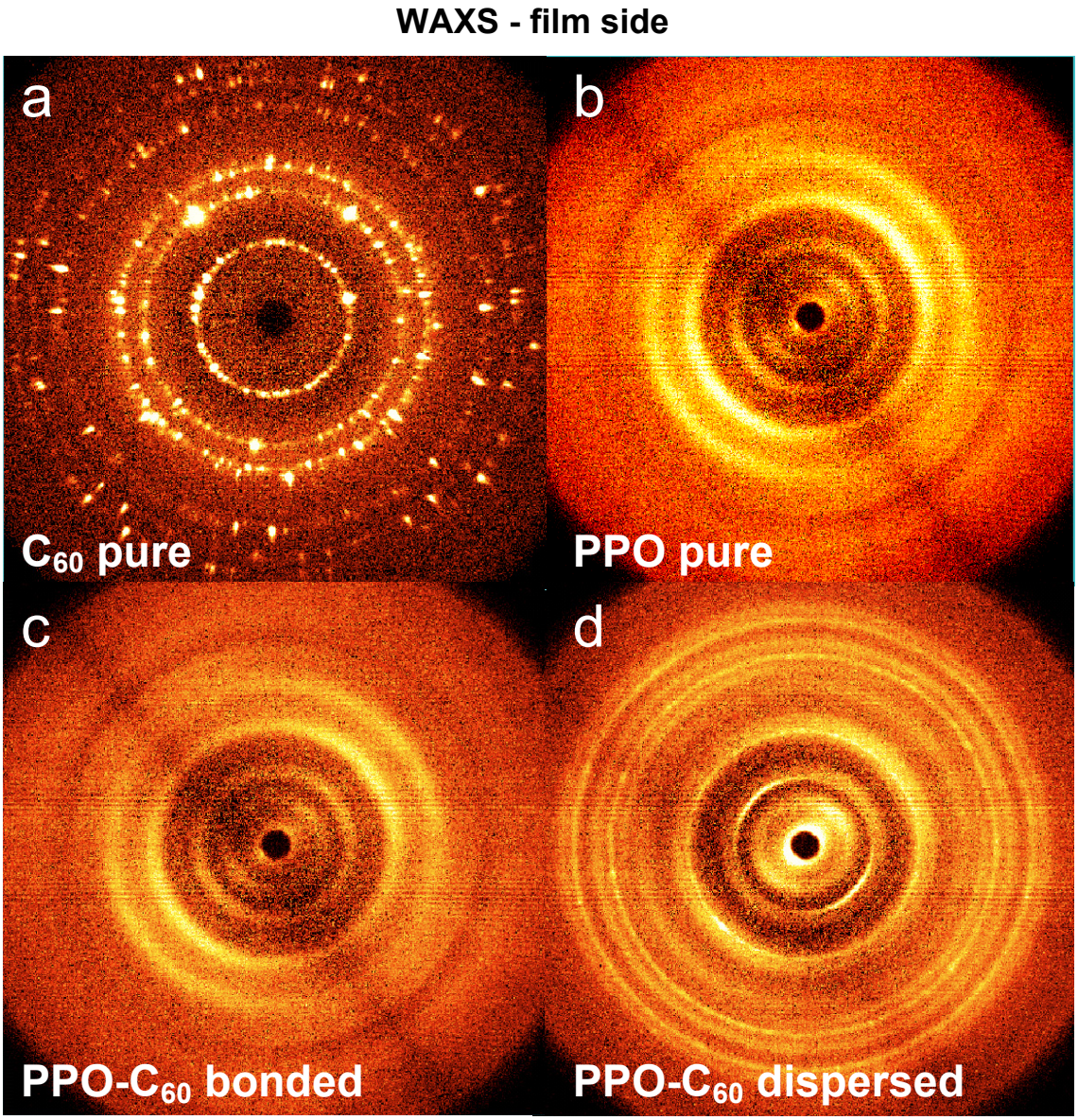

Figure 4: Scattering data recorded on a 2-D detector for the two basic components of the samples, a) pure C_{60} powder; b) pure PPO, c) PPO-C_{60} 2.0 wt % bonded and d) PPO-C_{60} 2.0 wt % dispersed.

We assume that the peak (∗) comes from the PPO since it is present in all PPO-C_{60} bonded and dispersed samples and in the pure polymer (see Figure 5c and 5d) and absent in the pure C_{60} (Figure 5a). The intensity changes in the (∗) peak area of PPO-C_{60} dispersed (Figure 5d) results from the influence of the presence of C_{60} that may aggregate and simultaneously inducing more short-range order in the polymer. In the PPO-C_{60} bonded, the (∗) peak has low intensity, probably because the crystallization is less due to the hindrance of the rotational movements of the polymer segments by the presence of the C_{60}.

The peak around the (111) fullerene position seems much more distinct in the dispersed than in the bonded sample strongly indicating clustering of fullerene in the dispersed system. Note, however, that the pure polymer also exhibits a peak about the same position (Figure 5b). This could contribute to the scattering in the dispersed case, especially, if the degree of fullerene clustering is large enough to provide the polymer more freedom to crystallize than that in the bonded system. This picture is also supported by the scattering of the PPO-C_{60} bonded film where no peak at that position is observed, indicating absence of strong fullerene clustering in the bonded film. It also suggests partial suppression of crystallinity in the film containing bonded fullerene.

More evidence for fullerene clustering in the dispersed sample can be found in Figure 5d, where the scattering from samples containing different amounts of fullerene are displayed. The peaks indicating clustering of fullerene increase strongly with fullerene concentration in the dispersed films (Figure 5d) while it practically does not change in the case of bonded films (Figure 5c). Comparing both sets of diffraction patterns, it seems that clustering is the major factor of difference. The variation of polymer scattering peaks is more prominent in the dispersed case.

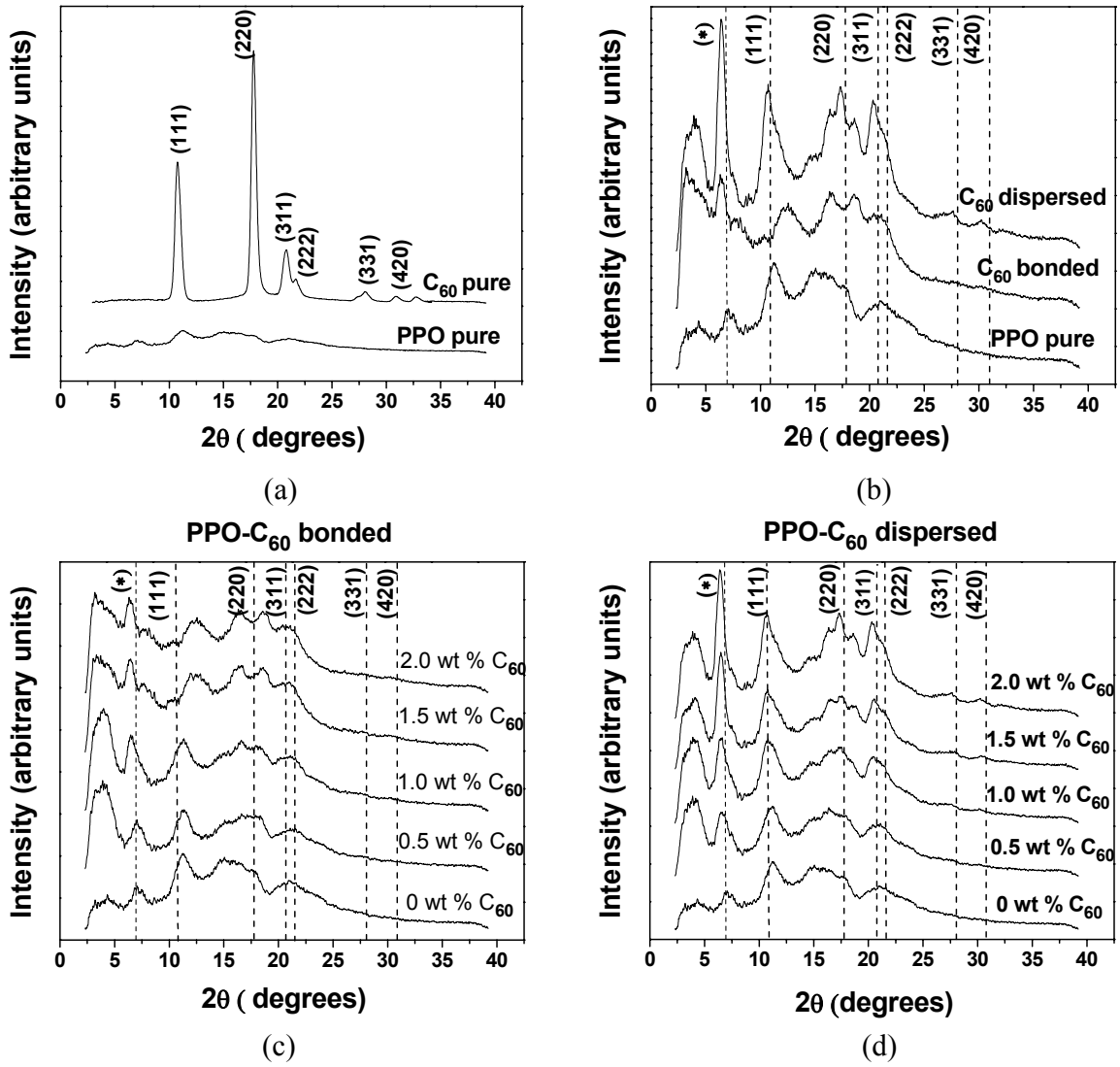

Figure 5: Scattering intensity as function of the scattering angle for:
(a) Pure C_{60} powder and pure PPO film cast with the same procedure as samples.
(b) Pure PPO, PPO-C_{60} 2 wt % bonded and PPO-C_{60} 2 wt % C_{60} dispersed. The scattering peaks of pure C_{60} are also represented (dashed lines).
(c) Samples containing different amounts of bonded C_{60}.
(d) Samples containing different amounts of dispersed C_{60}.

Enhancement of gas permeability is known to be partially driven by the amount of interface between the polymer and the filler particles, fullerenes in the present case. In the case of the dispersed samples, clustering of fullerenes diminishes the amount of interface between the two species and, therefore, it should in principle decrease the membrane permeability. Clustering of fullerene may, however, also decrease the membrane permeability by creating an extra barrier for gas transport. Not only the size and shape of the clusters are of importance but also their orientation in the sample may constitute the most important feature. Figure 4 shows the scattering of the two samples of bonded and dispersed films containing 2 wt % of fullerenes. In this case, the scattering geometry used is incident X-ray beam on the film side. Figure 4d clearly shows that the scattering peaks of the fullerenes in the dispersed case are very anisotropic. For instance, the (111) reflection corresponding to the fcc lattice distance of the fullerene clusters are croissant-shaped. They are also aligned along the film direction. Such a scattering clearly indicates that fcc unit cells are aligned along the film plane. A perfect alignment of an fcc monolayer would lead to a very bright delta-function scattering also aligned in the same direction. It is more reasonable to consider the observed scattering as the result of sheet-like fullerene aggregates that are aligned along the film plane. Variation of thickness and fluctuations on the alignment of such clusters certainly lead to such a croissant-like scattering patterns. Since the density of the fullerene molecules is far larger than that of the polymer, it is very probable that during the drying process segregation of the fullerenes occurs preferentially to the face of the film in contact with the glass plate. Figure 4c shows that this phenomenon is practically absent in the case of bonded samples and if present, it concerns only a very small amount of the fullerene molecules that would search contact with the substrate.

In conclusion, the WAXS results indicate some significant changes in the polymer structure due to introduction of the fullerenes: For the PPO-C_{60} bonded membranes; the crystallization is probably partially suppressed in comparison to PPO-C_{60} dispersed. For the PPO-C_{60} dispersed membranes, significant clustering of C_{60} occurs. The clusters seem to align parallel to the film plane.

4.4 Gas permeability and gas sorption

The gas permeability and selectivity of PPO prepared in the chloroform and chlorobenzene are the same within the experimental error of the gas permeability set-up (see Appendix). Therefore, it is reasonable to conclude that these casting solvents have no significant influence on PPO structure. In this work, the permeability of pure PPO prepared in chloroform will be compared with the permeability of PPO-C_{60} bonded and dispersed.

The PPO-C_{60} bonded and dispersed membranes were prepared using chlorobenzene solvent at various C_{60} concentrations, 0.5, 1.0, 1.5 and 2.0 wt %. The color of the films becomes darker with the increase of C_{60} content in both bonded and dispersed membranes. The type of interaction between the fullerene and PPO, and also the influence of both components on structural and kinetic parameters of the PPO-C_{60} system determines the physical properties of the polymer material. The PPO-C_{60} bonded membranes are transparent, flexible, and mechanically stable. However, the PPO-C_{60} dispersed membranes are not transparent and rather brittle. Their fragility increases with increasing of C_{60} content.

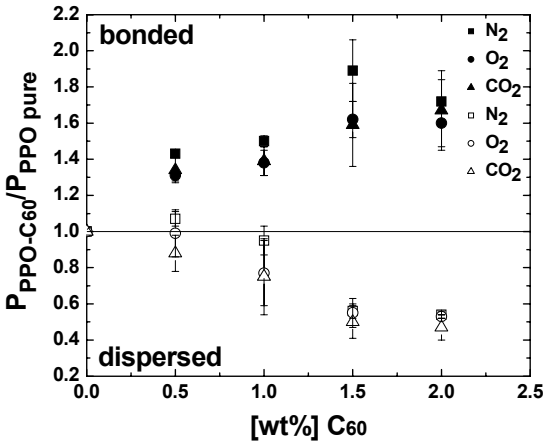

Figure 6: Permeability of PPO-C_{60} normalized with the permeability of pure PPO versus the wt % C_{60} content bonded for gases N_2 (■), O_2 (●) and CO_2 (▲) and for dispersed N_2 (□), O_2 (○) and CO_2 (△), at 1.5 bar feed pressure and 35 °C.

Figure 6 and Table 1 show the comparison of the gas permeability of PPO-C_{60} bonded and dispersed with the pure PPO membranes. The permeability coefficient significantly increases

with the C_{60} content for PPO-C_{60} bonded. In contrary, it decreases for the PPO-C_{60} dispersed. Besides, the gas permeability through pure PPO membranes and PPO-C_{60} bonded and dispersed is constant at different feed pressure for all three gases measured N_2, O_2 and CO_2[3].

Table 1: Gas permeability, solubility and apparent diffusivity of PPO films.

Membrane	N_2			O_2			CO_2		
	P	S	D	P	S	D	P	S	D
PPO pure	2.7	8.4	3.2	11.7	11.0	10.7	50.7	78.3	6.5
PPO-C_{60} bonded 1.5 wt %	5.1	8.9	5.8	19.1	15.3	12.5	80.8	90.2	9.0
PPO-C_{60} dispersed 1.5 wt %	1.5	10.3	1.5	6.5	12.8	5.1	25.5	79.9	3.2
Change % bonded	89	5	80	63	39	17	59	15	38
Change % dispersed	-44	22	-54	-45	16	-53	-50	2	-51

Feed pressure: 1.5 bar, T = 35 °C
P (barrer), S (10^{-3}, cm^3 (STP)/cm^3cm Hg, D (10^{-8}, cm^2/sec).

Table 2 presents the ideal gas selectivity at a feed pressure of 1.5 bar corresponding to the average of two different membrane samples. The average value might differ but if one takes in to account the standard deviation statistically they do not differ.

The DSC and WAXS results give an insight into the thermal and morphological parameters. In the PPO-C_{60} bonded systems, the stiffness of the chain probably increases (see Tg, in Figure 2) and the forced increase of interface between polymer and carbon cage enhances the free volume and the mobility of gas molecules at molecular scales and, therefore, permeability increases.

In the PPO-C_{60} dispersed systems, the clustering of fullerenes (see WAXS results) probably decreases the interface between polymer and fillers resulting in a decrease in free volume and mobility of gas molecules. This same segregation mechanism probably forms lamellae-like clusters parallel to the film plane. The combination of these two mechanisms and

the more compact structure (indicated by the lowering of T_g) contribute to the decrease in gas permeability as a function of fullerene concentration. In addition, for the PPO-C_{60} dispersed probably there is a much higher crystalline gas impermeable fraction (due to the clustering) than in pure PPO or PPO-C_{60} bonded. This can also contribute to decrease of gas permeability.

Table 2: Ideal gas selectivity of PPO films.

	Ideal Selectivity		
wt % C_{60} in PPO	**P_{O2}/P_{N2}**	**P_{CO2}/P_{N2}**	**P_{CO2}/P_{O2}**
0	4.3 ± 0.1	18.7 ± 1.1	4.3 ± 0.3
wt % C_{60} bonded			
0.5	4.0 ± 0.1	17.6 ± 0.3	4.4 ± 0.1
1.0	4.0 ± 0.2	17.3 ± 0.5	4.3 ± 0.2
1.5	3.7 ± 0.5	15.8 ± 2.9	4.2 ± 0.6
2.0	4.0 ± 0.5	18.1 ± 2.7	4.5 ± 0.7
wt % C_{60} dispersed			
0.5	4.0 ± 0.6	15.3 ± 1.4	3.8 ± 0.7
1.0	3.5 ± 1.0	14.6 ± 4.6	4.2 ± 1.9
1.5	4.2 ± 0.8	16.7 ± 3.2	3.9 ± 1.0
2.0	4.3 ± 0.1	16.2 ± 1.8	3.8 ± 0.4

Feed pressure: 1.5 bar, T = 35 °C

For the PPO-C_{60} dispersed membranes, the Maxwell model (see, eq. 4 and 5) has been used for the simulation of the experimental results. For all gases (N_2, O_2 and CO_2), the simple Maxwell model (eq 4) cannot represent the decrease of the permeability. The experimental results are always much lower than the predictions (see Fig. 7 dotted lines). The generalized Maxwell model (eq 5), however, gives much better predictions (see Figure 7, full lines). For all cases, the estimated G parameter is low (G_{N2} = 0.02, G_{O2} = 0.02, G_{CO2} = 0.01). These results suggest that the structure of the PPO-C_{60} dispersed membranes contains lamellae C_{60} clusters

oriented perpendicular to the direction of permeation, consistent with the WAXS results. The C_{60} clusters impede the gas diffusion through the material resulting in reduced gas permeability.

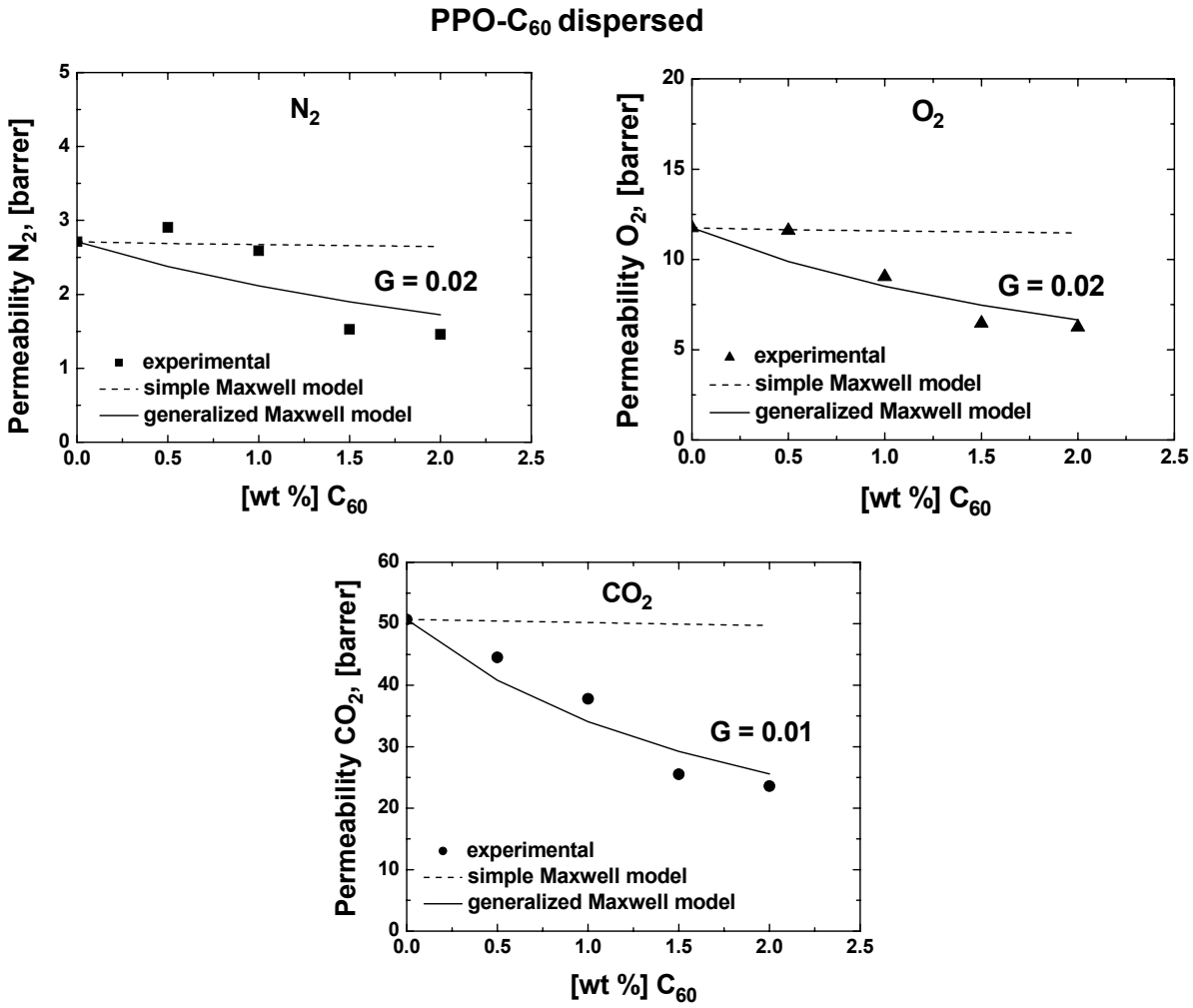

Figure 7: The gas permeability through PPO-C_{60} dispersed versus the wt % C_{60} content. The dotted line represents the prediction of simple Maxwell model. The solid line represents the prediction of generalized Maxwell model. The symbols represent the experimental results: (a) N_2 (■), (b) O_2 (▲) and (c) CO_2 (●).

Figure 8 presents the sorption isotherms of CO_2, N_2 and O_2 through PPO pure and PPO-C_{60} bonded and dispersed at 35 °C. The sorption isotherms are fitted by the dual mode sorption model (see equation 3) and the obtained parameters are shown in Table 3. For N_2 the difference in sorption between the polymers is not significant. However, for CO_2 and O_2 the sorption is

higher for PPO-C_{60} bonded probably due to a lower crystallinity (as indicated by WAXS) and to the increase of free volume (as indicated by WAXS and DSC).

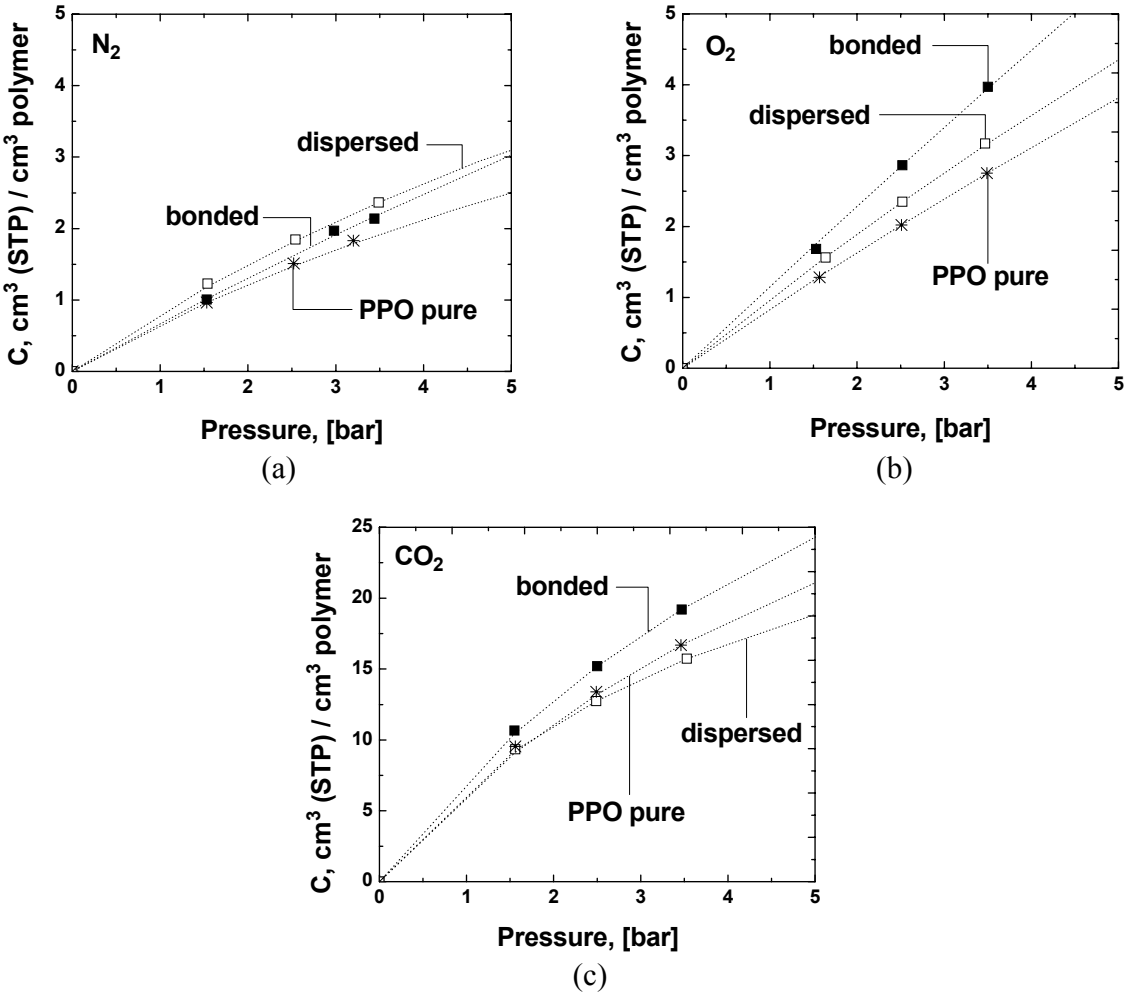

Figure 8: Sorption isotherms of (a) N_2, (b) O_2, and (c) CO_2 for of PPO-C_{60} with 1.5 wt % C_{60} content bonded (■) and dispersed (□) in comparison with pure PPO (✳). The dotted lines are model lines, which are fitted according to the dual mode sorption model. T = 35 °C

The sorption isotherms are necessary to de-convolute the permeability into its solubility and diffusivity contributions. Table 1 reports the permeability, solubility and apparent diffusivity coefficients of N_2, O_2 and CO_2 gases in PPO, PPO-C_{60} 1.5 wt % bonded and dispersed, at 35 °C and 1.5 bar feed pressure. The solubility coefficient S was estimated from the gas sorption measurements and the apparent diffusion coefficient D was calculated from the P/S ratio.

Table 3: Dual mode sorption parameters for N_2, O_2 and CO_2 in PPO pure, PPO-C_{60} bonded and dispersed films with 1.5 wt % C_{60}, k_D expressed in cm^3 (STP)/cm^3bar, C'_H expressed in cm^3(STP)/cm^3, and b expressed in bar^{-1}. Pressure = 1.5/2.5/3.5 bar, T = 35 °C

	N_2			O_2			CO_2		
Membrane	k_D	C'_H	b	k_D	C'_H	b	k_D	C'_H	b
PPO pure	0.13	5.13	0.116	0.28	18.5	0.03	0.59	41.19	0.159
PPO-C_{60} bonded 1.5 wt %	0.19	14.6	0.033	0.78	11.78	0.032	0.78	45.29	0.165
PPO-C_{60} dispersed 1.5 wt %	0.27	4.12	0.158	0.45	11.4	0.047	0.67	26.4	0.29

The N_2 solubility coefficients are about equal for PPO-C_{60} and PPO pure membranes. Then, the increase of N_2 permeability for the bonded membranes should be mostly attributed to increase of D. For O_2 and CO_2 however, the increase of permeability through the PPO-C_{60} bonded in comparison to PPO pure membranes could be attributed to both increase of S and D. Interestingly, the increase of O_2 permeability seems to be mostly due to increase of S (39 %) and of CO_2 mostly due to increase of D (38 %) (Table 1). For the PPO-C_{60} dispersed, the decrease of gas permeability in comparison to PPO pure should be mostly attributed to decrease of D (Table 1). This fits well with the results obtained with WAXS suggesting significant clustering and increase of crystallinity. Interestingly, the solubility of N_2 and O_2 to the PPO-C_{60} dispersed membranes increases somewhat in comparison to pure PPO but of the CO_2 remains unchanged.

5. Conclusions

The permeability of PPO-C_{60} bonded increases with increasing of C_{60} concentration. This is probably due to the stiffening of the polymer chain by the introduction of C_{60} leading to increase of the polymer free volume. The free volume increase was proven by Kruse J. et al.[26] using positron annihilation lifetime spectroscopy (PALS).

The permeability of PPO-C_{60} dispersed decreases with increasing of C_{60} concentration. This is probably due to the clustering of the dispersed fullerene and the higher crystalline gas

impermeable fraction (due to the clustering) than in pure PPO or PPO-C_{60} bonded. The clusters seem to form lamellas oriented parallel to the membrane plane.

6. Appendix

Pure PPO membranes were prepared using two different casting solvents; chloroform and chlorobenzene. The table presents the gas permeability and ideal selectivity of these membranes at 1.5 bar gas feed pressure and at 35 °C.

Casting solvent	Permeability [barrer]			Ideal Selectivity		
	N_2	O_2	CO_2	P_{O2}/P_{N2}	P_{CO2}/P_{N2}	P_{CO2}/P_{O2}
chloroform	2.7 ± 0.1	11.7 ± 0.2	50.7 ± 2.6	4.3 ± 0.1	18.7 ± 1.1	4.3 ± 0.3
chlorobenzene	3.3 ± 0.3	11.8 ± 0.2	47.0 ± 7.2	3.6 ± 0.3	14.2 ± 3.2	4.0 ± 0.7

7. References

[1] Wang, Y.-C.; Huang, S.-H.; Hu, C.-C.; Li, C.-L.; Lee, K.-R.; Liaw, D.-J.; Lai, J.-Y. *Journal Membrane Science* **2004**, *248*, 15-25.

[2] Freeman, B.D. *Macromolecules* **1999**, *32*, 375.

[3] Sterescu, D.M.; Bolhuis-Versteeg, L.; van der Vegt, N.F.A.; Stamatialis, D.F.; Wessling, M. *Macromolecular Rapid Communications* **2004**, *25*, 1674-1678.

[4] Chen, Y.; Huang, Z.E.; Cai, R.F. and Yu, B.C. *Eur. Polym. J*. **1998**, *34 (2),* 137.

[5] Dai, L.; *Polym. Adv. Technol.* **1999,** *10*, 357.

[6] Geckler, K.E.; Samal, S. *Polym. Int.* **1999**, *48*, 743.

[7] Goh, S.H.; Zheng J.W. and Lee, S.Y. *Polymer* **2000**, *41*, 8721.

[8] Albers, J.H.M.; Smid, J.; Kusters, A.P.M. *US Patent 5.129.920*, "Gas separation apparatus and also method for separating gases by means of such an apparatus", **1992**.

[9] Mulder, M. Basic Principles of Membrane Technology, Kluwer Academic, London, **1992**.

[10] Merkel, T.C.; Freeman, B.D.; Spontak, R.J.; He, Z.; Pinnau, I.; Meakin, P.; Hill, A.J. *Chem. Mater*. **2003**, *15*, 109-123.

[11] Kanehashi, S.; Nagai, K. *Journal of Membrane Science* **2005**, *253 (1-2),* 117-138.

[12] Story, B.J.; Koros, W.J. *J. Polym. Sci. Part B: Polym. Phys.* **1989**, *27*, 1927-1948.

[13] Merkel, T.C.; Freeman, B.D.; Spontak, R.J.; He, Z.; Pinnau, I.; Meakin, P.; Hill, A.J. *Science*, **2002**, *296*, 519.

[14] Arnold, M.E.; Nagai, K.; Freeman, B.D.; Spontak, R.J.; Betts, D.E.; DeSimone, J.M.; Pinnau, I. *Macromolecules* **2001**, *34*, 5611-5619.

[15] Cabasso, I.; Grodzinski, J.J.; Vofsi, D. *J. of Applied Polymer Science* **1974**, *18*, 1969.

[16] Verdet, L.; Stille, J.K. *Organometallics* **1982**, *1*, 380.

[17] Percec, V.; Auman, B.C. *Makromol. Chem.* **1984**, *185,* 2319-2336.

[18] Nath, S.; Pal, H.; Sapre, A. V. *Chemical Physics Letters* **2002**, *360*, 422-428.

[19] Khulbe, K.C.; Matsuura, T.; Lamarche, G.; Lamarche, A.-M. *Journal of Membrane Science* **2000**, 170, 81-89.

[20] Barsema, J.N.; Kapantaidakis, G.C.; van der Vegt, N.F.A.; Koops, G.H.; Wessling, M. *Journal of Membrane Science* **2003**, *216*, 195.

[21] Visser, T.; Koops, G.H.; Wessling, M. *Journal of Membrane Science* **2005**, *252*, 265-277.

[22] Polotskaya, G.A.; Gladchenko, S.V.; Pen'kova, A.V.; Kuznetsov, V.M. and Toikka, A.M. *Russian Journal of Applied Chemistry* **2005**, *78*, 9, 1468-1473.

[23] Polotskaya, G.A.; Gladchenko, S.V.; Zgonnik, V.N. *J. of Applied Polymer Science* **2002**, *85*, 2946-2951.

[24] Higuchi, A.; Agatsuma, T.; Uemiya, S.; Kojima, T.; Mizoguchi, K.; Pinnau, I.; Nagai, K. and Freeman, B.D. *J. App. Polym. Science* **2000,** *77*, 529.

[25] Weng, D.; Lee, H.K.; Levon, K.; Mao, J.; Scrivens, W.A.; Stephens, E.B.; Tour, J.M. *European Polymer Journal* **1999**, *35,* 867-878.

[26] Kruse, J.; Rätzke, K.; Faupel, F.; Sterescu, D.M.; Stamatialis, D.F.; Wessling, M., „Free volume in C_{60} modified PPO polymer membranes by positron annihilation lifetime spectroscopy", to be submitted.

Chapter 4

Fullerene-modified Matrimid gas separation membranes

Dana M. Sterescu, Dimitrios F. Stamatialis, Matthias Wessling

Abstract

In this chapter, the commercial polyimide Matrimid was modified to improve its membrane-transport properties as a gas-separation material. Therefore super molecular carbon cages (e.g., fullerenes, bucky balls) were covalently coupled or dispersed in the polymer. The dispersion of fullerenes (0.25 and 1.0 wt %) and the covalent bonding of 0.25 wt % fullerenes to Matrimid did not affect the permeability and selectivity compared to the pure polymer. The covalent coupling of 1.0 wt % of fullerenes resulted in a tremendous increase in permeability but significant loss in selectivity.

1. Introduction

In the last few years gas separation has become a major industrial application. Gas separation membranes have to be highly permeable to one of the gas mixture components while significantly reject the other[1]. The application area of existing gas separation membranes is limited by commercially available polymers. The separation performance of these polymers is not sufficient for effective separation processes[2]. The vast amount of polymers that have been investigated, show the general trend that highly permeable polymer possess low selectivity. This often referred to as the permeability/selectivity trade off relationship[1].

Polyimides show excellent intrinsic gas separation properties and robust mechanical properties to withstand high-pressure gas feeds[3]. Matrimid has attracted a lot of attention in the last decade as material for gas separation membranes[4]. It exhibits some of the most attractive gas-transport properties of any commercially available polymer due to the combination of relatively high gas permeability coefficients and separation factors coupled with excellent mechanical properties[4,5]. In combination with its solubility in common solvents, it is an good candidate for gas separation membranes, especially for O_2/N_2 separation, because of its high selectivity[5]. However, compared to other polymers, e. g. poly(2,6-dimethyl-1,4-phenylene oxide) (PPO), the permeability of Matrimid is rather low[4,6]. Therefore, using fullerenes to increase also the gas permeability of Matrimid without compromising the selectivity became an interesting idea.

The permeation properties of a polymer depend primarily on the packing density, the polymer chain mobility and the free volume of the polymer structure, which can be increased by the introduction of bulky substituents. Therefore considerable interest has been shown in the structure, properties and chemical reactivity of super-molecular carbon cages (fullerene, bucky balls, C_{60}) owing to their potential applications[7,8]. Fullerenes are potentially interesting materials for the preparation of membranes. Their hard-sphere properties may inhibit molecular polymer chain packing possibly resulting in high free volume. In the past, others have tried to disperse C_{60} in poly (1-trimethylsilyl-1-propyne) (PTMSP)[9], Matrimid[10] and poly(2,6-dimethyl-1,4-phenylene oxide) (PPO)[6,11]. The obtained membranes showed lower gas permeability than the initial

material. Only the covalent binding of C_{60} to the polymer backbone of PPO[6,12] resulted in an increased permeability without compromising selectivity.

In this work, we dispersed and covalently coupled the C_{60} on Matrimid at various weight percentages following similar procedure as Goh S.H. et al.[13] for PPO. The influence of the addition of C_{60} on the membrane properties is investigated and compared with the results obtained in Chapters 2 and 3.

2. Experimental

2.1 Materials

As membrane material, a BTDA-AAPTMI polyimide (Matrimid 5218, Ciba Specialty Chemicals Corp., MW = 74240 measured by gel permeation chromatography (GPC)), was used. The chemical structure is shown in Figure 1. Other chemicals used: 1,1,2,2-Tetra chloroethane (TCLE, 95%, Fluka), bromine (Br_2, 99.5%, Fluka), ethanol (Merck), chloroform (Merck), dimethyl sulfoxide (DMSO, 99.5%, Fluka), sodium azide (NaN_3, 99%, Fluka), methanol (Fluka), C_{60} (99.5%, SES Research Company), hexane (Fluka).

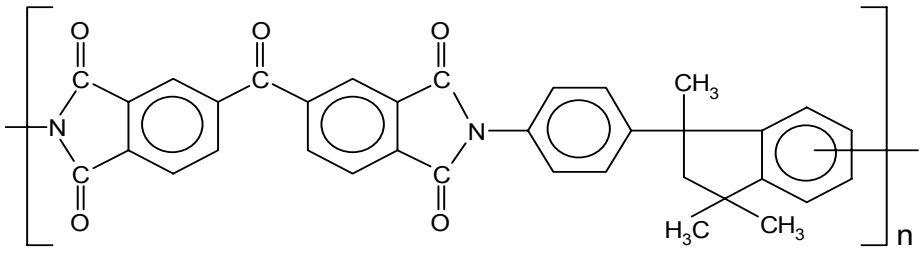

Figure 1: Chemical structure of Matrimid 5218 polyimide.

2.2 Modification of Matrimid

The preparation of Matrimid-C_{60} bonded polymer was performed in three steps following a similar procedure as for PPO[13], described in chapter 2: a) Matrimid bromination (Matrimid-Br); b) Matrimid-Br conversion into Matrimid-N_3 using dimethyl sulfoxide as solvent and c) Matrimid-N_3 conversion into Matrimid-C_{60} bonded using TCLE as solvent. The bromination of

Matrimid is a selective reaction that can introduce bromine into the phenylene rings[5] or into the benzyl position. In our work, free radical bromination of Matrimid was carried out to provide Matrimid containing bromo-methyl groups and, it was subsequently used for the preparation of Matrimid-N_3. We prepared Matrimid-Br containing 0.25 and 1.09 wt % Br confirmed by elemental analysis. The bromo-methylation of Matrimid was also confirmed by ^{1}H-NMR spectroscopy (using a Varian Unity INOVA 300 MHz spectrometer). The ^{1}H-NMR chemical shift values (300 MHz) are reported as δ in [ppm] using the residual solvent signal as an internal standard ($CDCl_3$ δ = 7.29). ^{1}H-NMR spectra in $CDCl_3$ were performed for Matrimid pure and Matrimid-Br 1 wt %. The ^{1}H-NMR spectrum of Matrimid pure is in good agreement with the literature[5]. For Matrimid-Br 1 wt % the chemical shifts of the signals appeared in the aliphatic region suggest that they are the result of bromination occurring on the methyl group corresponding especially to proton signal H27[5] of the indane cyclopentane (results not shown here). This confirms that the bromination has taken place on the methyl group and the further modification by coupling of C_{60} took place on the methyl group of Matrimid, too.

2.3 Preparation of membranes

For the preparation of pure Matrimid membranes, the polymer was dissolved in TCLE (10 wt %). The Matrimid solution was cast on a glass plate and dried initially under nitrogen atmosphere at room temperature (20 - 25 °C) for 3 days, then in a vacuum oven at 50 °C under nitrogen atmosphere for 3 days and after in a vacuum oven at 150 °C for 48 hours. Membrane samples of 50-80 μm thickness were prepared.

For the preparation of Matrimid-C_{60} covalently bonded membranes, the polymer containing various percentages of C_{60} was also dissolved in TCLE (solution 10 wt %). The Matrimid-C_{60} solution was poured on flat Petri dishes and the membranes were formed by drying the solution, following the protocol used for pure Matrimid. The Matrimid-C_{60} films of 50-80 μm thickness were then peeled off the flat Petri dishes and kept under vacuum at 30 °C for 1 week.

For comparison, the Matrimid-Br and Matrimid-N_3 membranes were also prepared following similar procedure as for the Matrimid-C_{60} bonded membranes using a 10 wt % polymer solution.

For the preparation of Matrimid membranes with C_{60} dispersed, the C_{60} and Matrimid were dissolved separately in TCLE (10 wt % Matrimid). After complete dissolution, they were mixed at various percentages, stirred until the solution became homogeneous and allowed to stand for at least 24 h. The membranes were prepared using the same method like for Matrimid-C_{60} covalently bonded membranes.

2.4 Characterization of membranes

Density measurements

The density measurements of Matrimid and Matrimid-C_{60} membranes were performed using an AccuPyc 1330 Pycnometer with a 0.1 cm^3 sample insert. The pressures observed upon filling the sample chamber with the gas and then discharging it into a second empty chamber allow computation of the density of the sample[12].

DSC measurements

The thermal properties of pure Matrimid, Matrimid-C_{60} bonded and dispersed were measured using a Perkin Elmer DSC-7 (Differential Scanning Calorimeter) in nitrogen atmosphere. The samples were initially heated from 50 °C until 430 °C, cooled with liquid nitrogen, held for 5 minutes, and reheated two more times following the same steps, under nitrogen atmosphere. The heating rate was 10 °C/min and the cooling rate was 20 °C/min. The glass transition temperature, T_g of the polymer was obtained from the third scan.

Scanning Electron Microscopy (SEM)

The geometrical characteristics and the morphology of the developed Matrimid-C_{60} membranes were determined by using a Jeol JSM-5600 LV Scanning Electron Microscope. The

membrane samples were freeze fractured using liquid nitrogen and sputtered with a thin layer of gold using a Balzers Union SCD 040 sputtering apparatus.

Gas permeability and Sorption

The permeation of pure nitrogen (N_2), oxygen (O_2) and carbon dioxide (CO_2) through the Matrimid and Matrimid-C_{60} (dispersed and covalently bonded) was investigated, using the set up described elsewhere[14]. Pure gas permeability coefficients were calculated from the steady state pressure increase in time in a calibrated volume at the permeate side by using the equation:

$$\frac{P}{l} = \frac{V \times 273.15 \times (p_{pt} - p_{p0})}{A \times T \times \frac{(p_{ft} + p_{f0})}{2} \times 76 \times t} \times 10^6 \qquad (1)$$

where the ideal gas law is assumed to be valid, p_{pt} , p_{ft} [bar] is the pressure at the permeate and feed side at time t, p_{p0} p_{f0} is the permeate and feed pressure at t=0, T [K] is the temperature, V [cm^3] is the calibrated permeate volume, and A [cm^2] the membrane area. The gas permeance (P/l) is expressed in GPU, i.e. 10^{-6} cm^3cm^{-2} s^{-1} $cmHg^{-1}$. Multiplying the gas permeance with the thickness of dense membranes, l [cm], gives the permeability coefficient in Barrer. All the gas permeation experiments were performed at 35 °C. Values and error bars reported in the tables and figures are based on measurements of two different membrane samples.

The gas sorption isotherms of N_2, O_2 and CO_2 in dense Matrimid pure and Matrimid-C_{60} bonded and dispersed (0.25 and 1.0 wt %) films were measured at 35 °C, using a magnetic suspension balance[15] (MSB, Rubotherm). The experimental procedure was described elsewhere[6]. The equilibrium mass increase was corrected for buoyancy by subtracting the weight at zero sorption at a certain pressure from the vacuum weight of the sample. Using the equilibrium weight increase and the density of the polymer, the concentration (in cm^3 STP) inside the polymer (cm^3 polymer) was calculated[15].

Crank[16] shows that the sorption of a penetrant in a polymer matrix is proportional to the square root of time, assuming a constant diffusion coefficient. This behavior is called ideal Fickian sorption and the mass uptake (g) in time (M(t)) can be described with the following equation:

$$\frac{M(t)}{M_\infty} = 1 - \frac{8}{\pi^2}\sum_{m=0}^{\infty}\frac{1}{(2m+1)^2}\exp\left\{-\frac{D(2m+1)^2\pi^2 t}{L^2}\right\} \quad (2)$$

where M_∞ is the amount of mass (g) sorbed by Fickian sorption at infinite time, D is the diffusion coefficient (m^2/s), t is the time (s), and L is the sample thickness (m). Fitting of the sorption data into this equation leads to the diffusion coefficients[17].

WAXS measurements

Wide Angle X-ray Scattering (WAXS) experiments were performed using a Bruker-Nonius D8-Discover equipped with 2D detector. Standard background (air and sample holder) subtraction measured at the same time and conditions were applied to all data. The sample-detector (S-D) distance was set at 10 cm and the incident beam wavelength was 1.54 Å (Cu-Kα). Measurements were performed both perpendicular and in the plane of the membrane[6]. In the first case, the sample thickness as seen by the incident beam was always less than 0.5 mm.

3. Results and discussion

3.1 Scanning Electron Microscopy (SEM)

To investigate the distribution of C_{60} in the Matrimid structure, Scanning Electron Microscopy (SEM) was used. The Matrimid-pure, Matrimid-C_{60} bonded and dispersed with 0.25 wt % and 1.0 wt % content membranes were analyzed. The micrographs were obtained using a Jeol JSM-5600 LV Scanning Electron Microscope with magnification of 1000x and 5000x.

Figure 2 shows the cross sections of Matrimid pure in comparison to Matrimid–C_{60} bonded and dispersed with two different C_{60} concentrations (0.25 and 1 wt %). The cross-sections of the Matrimid-C_{60} dispersed with 0.25 wt % C_{60} and 1 wt % C_{60} show dense homogeneous and compact structure comparable to pure Matrimid, whereas the Matrimid-C_{60} 1.0 wt % bonded show some differences. The cross-section of Matrimid-C_{60} bonded 0.25 wt % looks very similar to the pure Matrimid, while Matrimid-C_{60} bonded 1.0 wt % shows more heterogeneous defective structure.

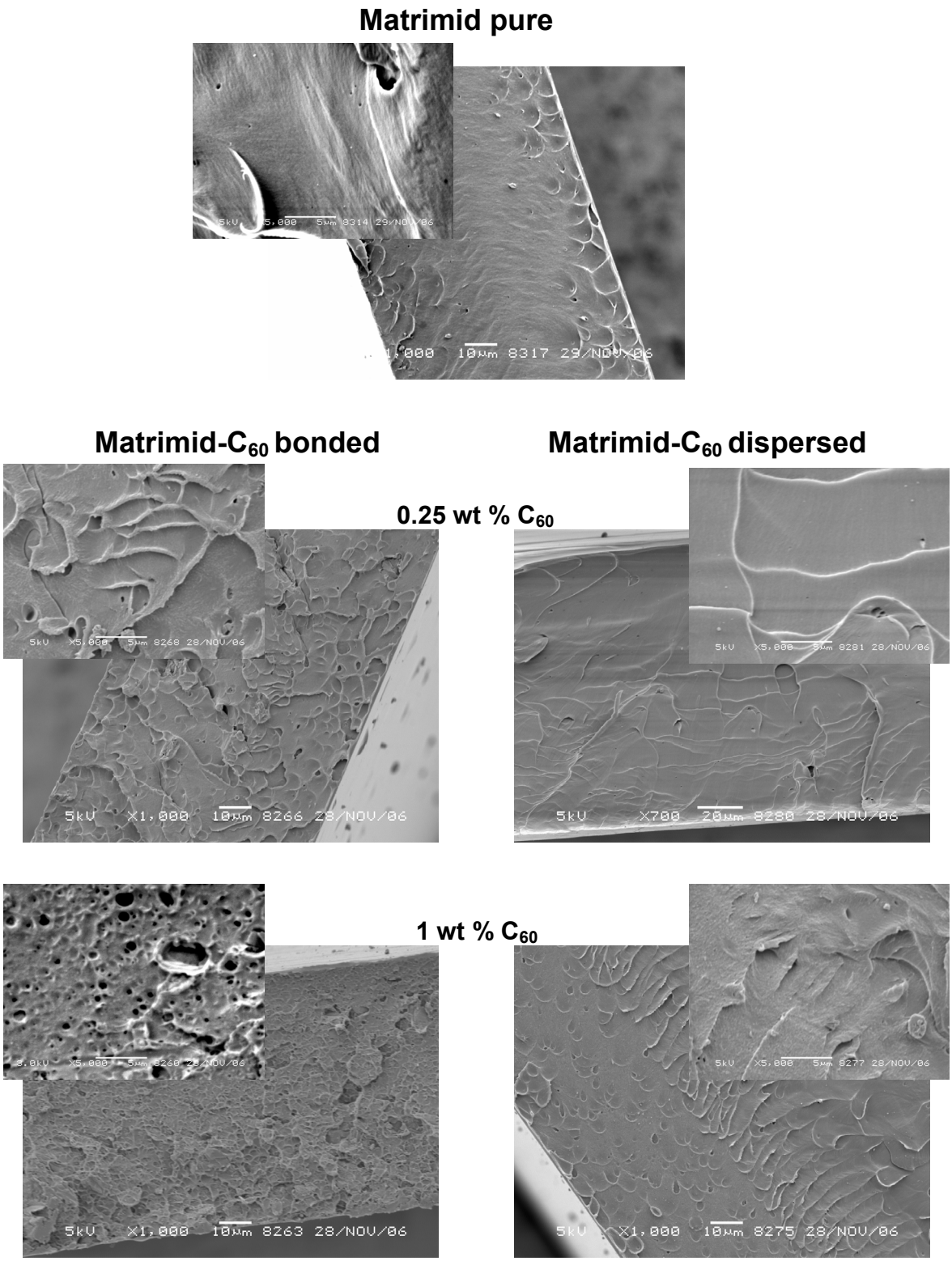

Figure 2: SEM micrographs of Matrimid pure, Matrimid-C_{60} 0.25 wt % and 1.0 wt % bonded and dispersed membranes cross-section (that includes a zoom of the top surface, 5000x).

3.2 DSC and Density measurements

Table 1 shows that the T_g of Matrimid-C_{60} 1.0 wt % bonded increases to 347 °C in comparison to pure Matrimid (T_g = 333 °C). This indicates that the Matrimid polymer chain bonded with 1.0 wt % C_{60} becomes more stiffened and probably there is suppressed inter-chain packing as well as some possible conformational changes in the backbone. Perhaps, as a consequence an extra interstitial chain space is created and the free volume of the membrane might increase, too. Additionally, the density of Matrimid-C_{60} 1.0 wt % bonded decreases to 1.21 g/cm^3 in comparison to pure polymer (ρ = 1.32 g/cm^3) , suggesting more open structure. For the Matrimid-C_{60} 0.25 wt % bonded no significant change in T_g and density was found in comparison to pure Matrimid. For Matrimid-C_{60} 0.25 and 1.0 wt % dispersed the T_g value is not significant different compared to pure Matrimid. The density of Matrimid-C_{60} dispersed is also comparable to pure polymer.

Table 1: DSC and density results of Matrimid, Matrimid-C_{60} bonded and dispersed samples.

wt % C_{60} in Matrimid	T_g, [^{0}C]	Density, [g/cm^3]
0	333	1.32
bonded		
0.25	335	1.33
1.0	347	1.21
dispersed		
0.25	330	1.34
1.0	328	1.36

3.3 WAXS analysis

The Matrimid and Matrimid–C_{60} polymer films were investigated by wide-angle x-ray diffraction with two different incident beam configurations, perpendicular to the film plane and parallel to it. The scattering pattern of C_{60} powder (see Figure 3a) exhibits typical crystalline structure. The peak positions are displayed as a function of the scattering angle and are indexed following the convention used in the literature[18]. Some of the scattering peaks in C_{60}, namely (111) and (220), are used as references in the interpretation of the scattering from bonded and dispersed films. They correspond to d-spacings of 14.17 Å, the crystalline face centred cubic (fcc)

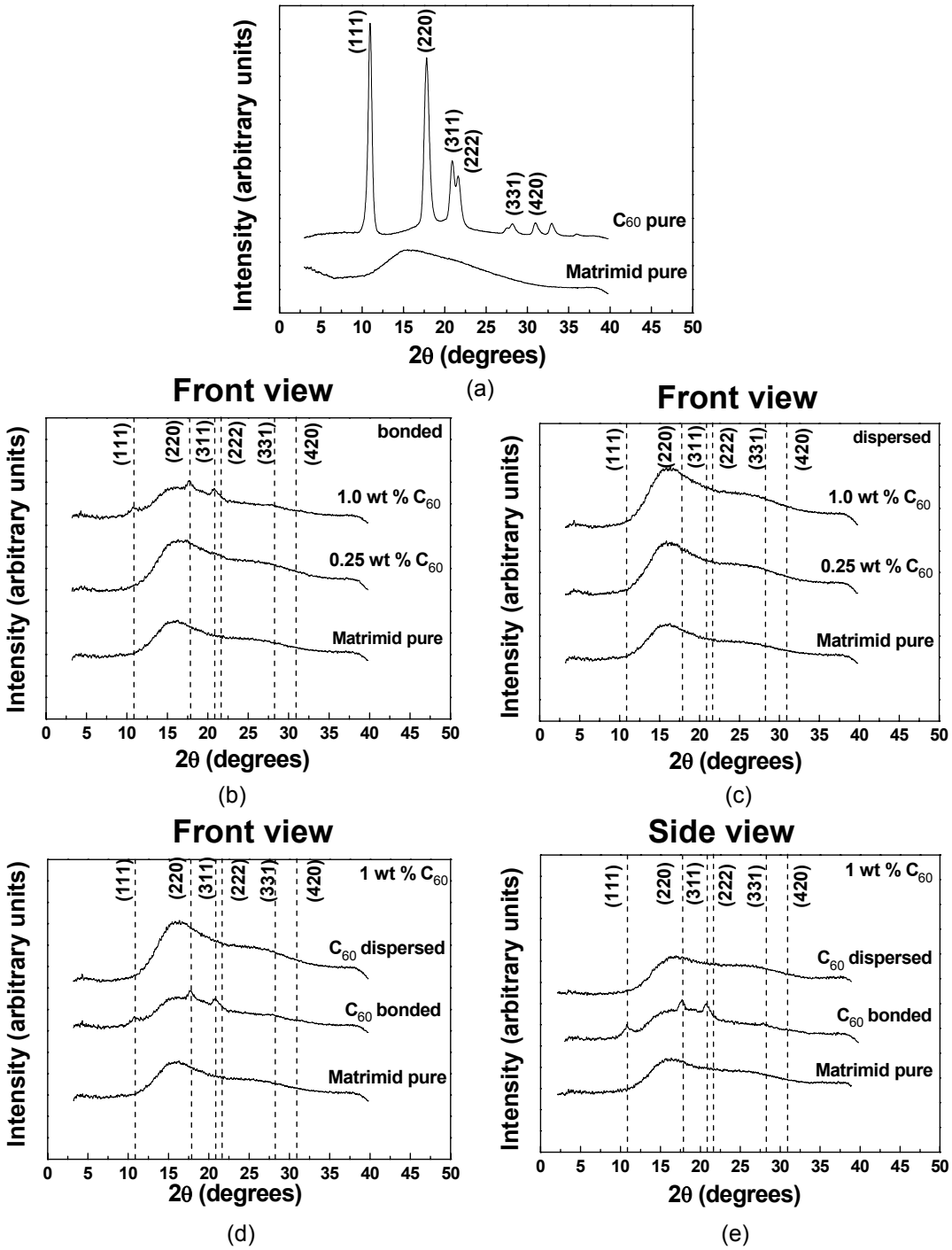

Figure 3: Scattering intensity as function of the scattering angle for: (a) pure C_{60} powder and pure Matrimid film, (b) pure Matrimid, Matrimid-C_{60} 0.25 and 1.0 wt % bonded – front view, (c) pure Matrimid, Matrimid-C_{60} 0.25 and 1.0 wt % dispersed – front view, (d) pure Matrimid, Matrimid-C_{60} 1.0 wt % bonded and dispersed – front view, (e) pure Matrimid, Matrimid-C_{60} 1.0 wt % bonded and dispersed – side view. The scattering peaks of pure C_{60} are also represented (dashed lines).

lattice constant and 7.53 Å, the C_{60} diameter (Figure 3a). The scattering of the pure Matrimid film is also displayed (Figure 3a), resembling the amorphous structure of the polymer. Figures 3b,c,d display spectra of Matrimid-C_{60} bonded and dispersed where the incident beam is perpendicular to the film. Figure 3e displays results from the measurement were the incident beam is parallel to the film (side view). It is well known that the C_{60} show anomalous behavior due to the formation of aggregates[19,20]. The scattering profile of pure Matrimid film is present in the scattering patterns of the bonded and dispersed films, (see Figures 3b and 3c, respectively), whereas some scattering peaks of the C_{60} (Figure 3a) are present only in the scattering pattern of Matrimid-C_{60} 1.0 wt % bonded (Figure 3b).

Comparison of the scattering of the pure Matrimid with that of the Matrimid-C_{60} 0.25 wt % (bonded and dispersed) shown in Figures 3b and 3c, clearly indicates strong similarity: peak position and relative intensity are very similar in all three Matrimid containing samples. These curves suggest that the presence of C_{60} does not introduce significant changes in Matrimid amorphous structure at 0.25 wt % C_{60} concentration bonded or dispersed. In contrary to the dispersed C_{60} in PPO in the chapter 3, no indication of fullerene clustering was observed.

Further increase of the C_{60} concentration to 1.0 wt %, sample Matrimid-C_{60} 1.0 wt % (bonded and dispersed), leads to similar results as displayed in Figures 3d and 3e, front and side view, respectively. The scattering of the Matrimid-C_{60} 1.0 wt % dispersed is very similar to the pure Matrimid film (peak position and relative intensity), from front and side view. Despite the fact that both samples contain the same amount of fullerene (1 wt %), the scattering fullerene peaks, (111), (220) and (311) are present in the Matrimid-C_{60} bonded, but not in the dispersed film as can easily be observed in Figures 3d and 3e. However, the intensity of the peaks is much lower for Matrimid-C_{60} 1.0 wt % bonded than the pure C_{60} indicating absence of clustering of C_{60}. This can be due to the low concentration of fullerene used in Matrimid. The similarity of the peaks (peak position and relative intensity) observed from front and also from side view in Figure 3e suggests no alignment along the film plane.

In conclusion, the WAXS results indicate a strong similarity of Matrimid-C_{60} bonded and dispersed to pure Matrimid membranes, indicating that no relevant changes in polymer

amorphous structure was induced by the low concentration of C_{60} in contrast to the changes induced in PPO[6]. For the Matrimid-C_{60} membranes no indication of clustering or alignment along the film plane of fullerene was found in comparison to pure Matrimid, in contrast to PPO[6].

3.4 Gas permeability and gas sorption

According with the literature[21] it is common that the casting solvent has an influence on membrane properties. Therefore, gas permeability and sorption of pure Matrimid membranes prepared in three different casting solvents as chloroform ($CHCl_3$), 1,1,2,2-Tetra chloroethane (TCLE) and 1-Methyl-2-pyrrolidinone (NMP) were measured and the results are presented in Appendix I.

Table 2 shows the comparison of the gas permeability of Matrimid-C_{60} bonded and dispersed with the pure Matrimid membranes measured at 35 °C and 3.5 bar feed pressure. Only the permeability coefficient of Matrimid-C_{60} 1 wt % bonded increases significantly compared to the pure polymer. Mainly the N_2 permeability increases considerably (more than 10 times) in comparison to pure Matrimid (Table 2), whereas the permeability increases less for O_2 and CO_2.

Table 2: Permeability results and ideal gas selectivities of Matrimid and Matrimid-C_{60} bonded and dispersed films. (Feed pressure: 3.5 bar, T = 35 °C)

wt % C_{60} in Matrimid	Permeability [barrer]			Ideal Selectivity		
	N_2	O_2	CO_2	P_{O2}/P_{N2}	P_{CO2}/P_{N2}	P_{CO2}/P_{O2}
0	0.20 ± 0.03	1.13 ± 0.07	5.23 ± 0.40	5.8 ± 1.3	26.8 ± 6.2	4.6 ± 0.6
bonded						
0.25	0.18 ± 0.01	1.07 ± 0.02	5.27 ± 0.20	6.0 ± 0.4	29.5 ± 2.8	4.9 ± 0.3
1.0	2.15 ± 0.50	2.88 ± 0.31	6.44 ± 0.14	1.3 ± 0.5	3.0 ± 0.8	2.2 ± 0.6
dispersed						
0.25	0.20 ± 0.01	1.09 ± 0.01	5.45 ± 0.10	5.5 ± 0.3	27.4 ± 1.9	5.0 ± 0.1
1.0	0.18 ± 0.01	1.10 ± 0.01	5.26 ± 0.05	6.2 ± 0.4	29.5 ± 1.9	4.8 ± 0.1

Table 2 presents also the ideal gas selectivity at a feed pressure of 3.5 bar corresponding to the average of two different membrane samples. For Matrimid-C_{60} 1.0 wt % bonded membranes, it decreases significantly in comparison to pure Matrimid, whereas the selectivity of

Matrimid-C_{60} 0.25 wt % bonded and dispersed and Matrimid-C_{60} 1.0 wt % dispersed stay constant.

Table 3 shows that Matrimid-Br and Matrimid-N_3 have almost the same permeability as the pure Matrimid membranes indicating that the addition of Br and N_3 groups does not contribute to the increase of polymer permeability[12]. Moreover, the ideal selectivity of these membranes is not significantly different than that of pure Matrimid (Table 3). Therefore, the change in permeability of Matrimid-C_{60} 1.0 wt % bonded membrane compared to the pure Matrimid is due to the bonding of 1.0 wt % C_{60} to the polymer chain.

Table 3: Permeability results and ideal gas selectivities of pure Matrimid, Matrimid-Br, and Matrimid-N_3. (Feed pressure: 3.5 bar, T = 35 °C)

	Permeability, [barrer]			**Ideal Selectivity**		
Gases	**Matrimid**	**Matrimid-Br**	**Matrimid-N_3**	**Matrimid**	**Matrimid-Br**	**Matrimid-N_3**
N_2	0.20 ± 0.03	0.18 ± 0.02	0.18 ± 0.02	5.8 ± 1.3	5.5 ± 0.8	5.9 ± 0.6
O_2	1.13 ± 0.07	0.97 ± 0.03	1.07 ± 0.01	26.8 ± 6.2	26.2 ± 4.1	25.5 ± 2.5
CO_2	5.23 ± 0.40	4.72 ± 0.21	4.68 ± 0.20	4.6 ± 0.6	4.9 ± 0.4	4.3 ± 0.1

The DSC, density and SEM results give an insight into the thermal and morphological parameters for the Matrimid-C_{60} bonded 1 wt % membrane. The T_g is higher than the pure Matrimid. This suggest that probably the stiffness of the chain increases suppressing inter-chain packing and the forced increase of interface between polymer and carbon cage enhances the free volume and the mobility of gas molecules and, therefore, permeability increases. Because the permeability of N_2, the biggest gas molecule diameter from the tested gases, increases strongly, it can be assumed that the free volume introduced in the polymer by coupling the fullerene to the Matrimid chain is rather big and therefore leads to loss in selectivity. The density measurements of the Matrimid-C_{60} resemble this hypothesis, the bonding of 1.0 wt% C_{60} results in a lower density compared to the pure polymer.

There is a strong similarity between Matrimid-C_{60} 0.25 wt % (bonded and dispersed) and Matrimid-C_{60} 1.0 wt % dispersed with pure Matrimid membranes suggested by WAXS, SEM and DSC (see T_g). This means that no relevant change in the amorphous polymer structure was induced by the low concentration of C_{60}. Therefore the permeability of these membranes stays the same as in pure Matrimid.

Figure 4 presents the sorption isotherms of N_2, O_2 and CO_2 through Matrimid pure and Matrimid-C_{60} bonded and dispersed at 35 °C. The sorption isotherms are fitted by the dual mode sorption model[6]. For all three gasses (N_2, O_2 and CO_2) the difference in sorption between the polymers is not significant.

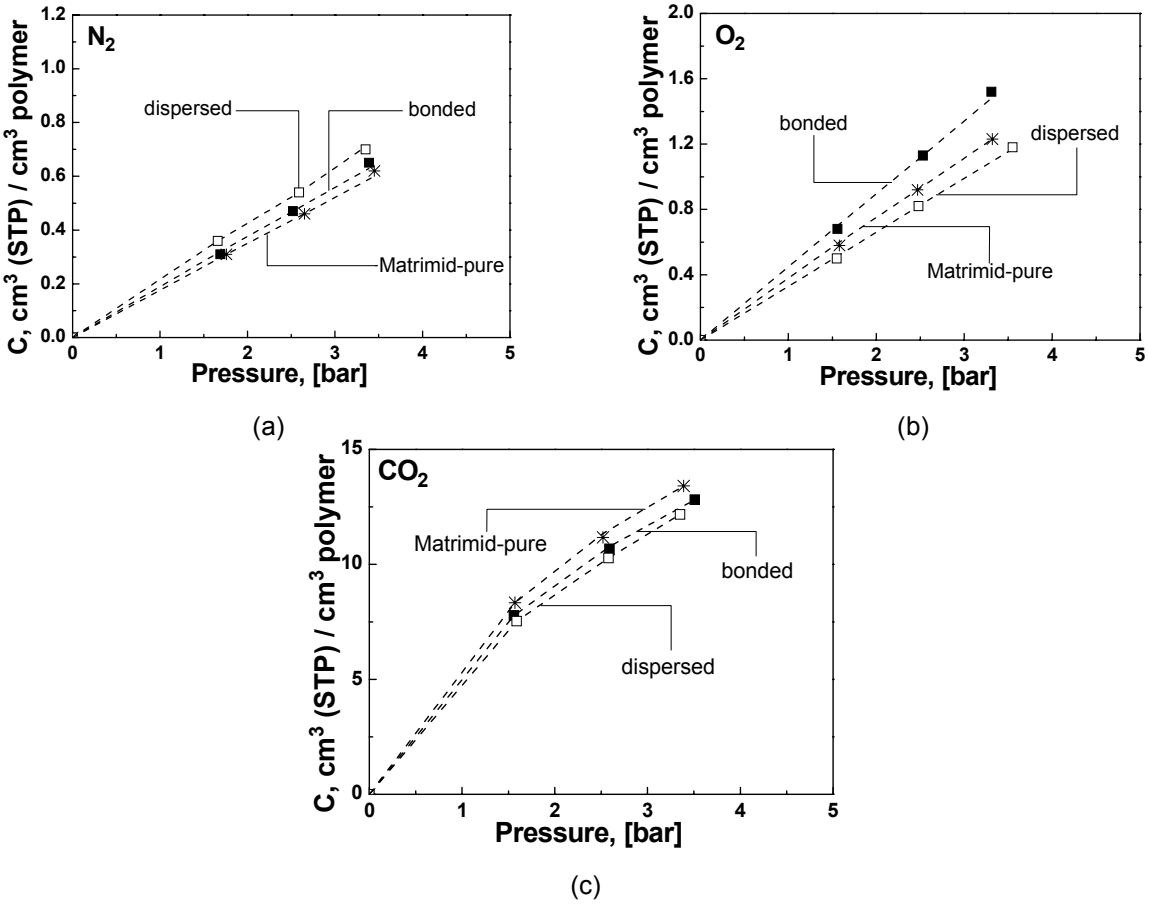

Figure 4: Sorption isotherms for (a) N_2, (b) O_2, and (c) CO_2 of Matrimid-C_{60} with 1.0 wt % C_{60} content bonded (■) and dispersed (□) in comparison with pure Matrimid (✳). The dotted lines are model lines, which are fitted according to the dual mode sorption model. T = 35 °C.

The sorption isotherms are necessary to deconvolute the permeability into its solubility and diffusivity contributions. Table 4 reports the permeability, solubility and diffusivity coefficients of N_2, O_2 and CO_2 gases in Matrimid, Matrimid-C_{60} bonded and dispersed, at 35 °C and 3.5 bar feed pressure. The solubility coefficient S was estimated from the gas sorption measurements and the diffusion coefficient D was calculated from the P/S ratio. To confirm the validity of this calculation the diffusion coefficient D, for all three gases, was also calculated from the sorption kinetics using similar method as in literature[17]. The values of D found by both methods are generally in good agreement (see Table 4).

Table 4: Gas permeability, solubility, and diffusivity of Matrimid and Matrimid-C_{60} bonded and dispersed films.

	N_2				**O_2**				**CO_2**			
wt % C_{60} in Matrimid	P	S	$D^{1)}$	$D^{2)}$	P	S	$D^{1)}$	$D^{2)}$	P	S	$D^{1)}$	$D^{2)}$
0	0.2	2.3	0.8	1.0	1.1	4.9	2.3	2.0	5.2	51.8	1.0	1.2
bonded												
0.25	0.2	2.3	0.8	1.1	1.1	4.5	2.4	2.1	5.3	48.6	1.1	1.5
1.0	2.2	2.5	8.7	8.4	2.9	6.0	4.8	4.5	6.4	50.9	1.3	1.9
dispersed												
0.25	0.2	2.6	0.8	1.2	1.1	4.2	2.6	2.1	5.5	45.4	1.2	1.6
1.0	0.2	2.7	0.7	1.0	1.1	4.4	2.5	1.9	5.3	47.6	1.1	1.7

1) The diffusion coefficient D calculated from the P/S ratio.
2) The diffusion coefficient D calculated from the sorption kinetics.

Feed pressure: 3.5 bar, T = 35 °C
P = [barrer], S = 10^{-3}, cm^3 (STP)/cm^3cm Hg, D = 10^{-8}, cm^2/sec

For Matrimid-C_{60} 0.25 wt % bonded, the gas permeability is comparable to pure Matrimid. The S and D values for N_2, O_2 and CO_2 are very similar to the pure Matrimid, so that the permeability remains unchanged (Table 4). For Matrimid-C_{60} 1 wt % bonded the increase of N_2 permeability is solely attributed to increase of D, while the N_2 solubility coefficients are about equal to pure Matrimid. The increase of diffusion coefficient D can be a result of suppressed inter-chain packing (see DSC) associated with a lower polymer density leading probably to higher free volume. For O_2 and CO_2, however, the solubility slightly differs from the pure polymer, but the increase of permeability is also attributed to the increase of D (Table 4).

For the Matrimid-C_{60} dispersed, the gas permeability is constant in comparison to Matrimid pure. For all three gasses (N_2, O_2 and CO_2) the S and D values are very similar to the pure Matrimid, so that the permeability remains unchanged (Table 4). These results suggest that no relevant changes in polymer structure were induced by the low concentration of C_{60}, in contradiction to the changes induced in PPO[6].

3.5 Influence of the polymer structure on the free volume

Based on WAXS results the Matrimid has an amorphous structure, whereas PPO is a semi-crystalline polymer[22]. This seems to play a role in the behavior of the fullerenes coupled or dispersed in to the polymer matrix. Whereas the permeability of PPO-C_{60} 1.0 wt % bonded for N_2, O_2 and CO_2 increases between 40 – 50 % compared to the pure PPO[6], the permeability of N_2 (the largest gas molecule diameter tested) for Matrimid-C_{60} 1.0 wt % bonded increases more than 10 times compared to the pure Matrimid. This indicates that, in comparison to PPO, the size of the free volume created by the bonding of fullerene to Matrimid is higher than in PPO leading to a tremendous loss in selectivity. The coupling of the bulky C_{60} groups to the Matrimid polymer chain, known as more rigid and containing larger polymer units than the PPO, leads probably to a higher suppression of interchain packing as well as some possible conformational changes in the backbone compared to PPO. This can result in the inhibition of intrachain motion around the flexible hinge points that might create so called defects in the polymer structure. This effect might provide an extra interstitial chain space, and the free volume of the membrane highly increases therefore the selectivity of the polymer decreases. The less increase in permeability and especially of diffusivity coefficient for O_2 and CO_2 compared to N_2 indicates strongly the creation of unselective free volume. In this case the free volume of the polymer is so high that it only affects the diffusivity of the gas molecules with the largest diameter, while the diffusivity of the small gases is affected less.

Guiver et al.[5] have shown that the bromination of Matrimid increases the free volume of the polymer and therefore the permeability increases (60 – 70 %) in comparison to pure polymer. However, the bromine groups bonded to the Matrimid polymer chain increase the d-spacing only

with 0.5 Å compared to the pure polymer, resulting already in slight decrease in selectivity (as a result of lower increase in permeability of the smaller gas molecules). Therefore, the introduction of C_{60}, which has a diameter of 7 Å, might lead to much higher increase of free volume, reducing the ideal gas selectivity tremendously.

4. Conclusions

The permeability of Matrimid increases by coupling of 1.0 wt % C_{60} to the polymer chain. Matrimid is an amorphous polymer with more rigid polymer chain in comparison to PPO, which is known to be a semi-crystalline polymer. Therefore a good packing of the polymer chains around the C_{60} coupled to Matrimid is not possible. Due to the higher suppression of interchain packing by the introduction of bulky C_{60} group to very rigid Matrimid polymer chain, as well as some possible conformational changes in the backbone the intrachain motion around the flexible hinge points can be inhibited creating so called “defects” in the polymer packing that might lead to an higher increase of the polymer free volume compared to the increase of free volume created by the bonding of C_{60} to PPO (see Chapter 2 and 3). Therefore the permeability increases but the ideal gas selectivity decreases in comparison to pure Matrimid. However, this phenomenon seems to be suppressed for Matrimid-C_{60} 0.25 wt % probably due to the low amount of C_{60} used, leading to a similar permeability and selectivity as for pure Matrimid.

The permeability of Matrimid-C_{60} 0.25 and 1.0 wt % dispersed is similar to pure Matrimid. It seems that there are no significant changes in the polymer structure induced by the dispersion of C_{60}, supported by DSC, WAXS and SEM, therefore the permeability and selectivity stay constant.

5. References

[1] Freeman, B.D. *Macromolecules* **1999**, *32*, 375.

[2] Syrtsova, D.A.; Kharitonov, A.P.; Teplyakov, V.V.; Koops, G.-H. *Desalination* **2004**, *163*, 273.

[3] Wind, J.D.; Paul, D.R.; Koros, W.J. *J. Membrane Science* **2004**, *228*, 227.

[4] Shishatskiy, S.; Nistor, C.; Popa, M.; Nunes, S.P.; Peinemann, K.V. *Adv. Eng. Mat.* **2006**, *8*, 390.

[5] Guiver, M.D.; Robertson, G.P.; Dai, Y.; Bilodeau, F.; Kang, Y.S.; Lee, K.J.; Jho, J.Y.; Won, J. *J. Polymer Science, Part A: Polymer Chemistry* **2002**, *40*, 4193.

[6] Sterescu, D.M.; Stamatialis, D.F.; Mendes, E.; Wübbenhorst, M.; Wessling, M. *Macromolecules* **2006**, *39*, 9234.

[7] Chen, Y.; Huang, Z.E.; Cai, R.F.; Yu, B.C. *European Polymer J.* **1998**, *34(2)*, 137.

[8] Geckeler, K.E.; Samal, S. *Polym. International* **1999**, *48*, 743.

[9] Higuchi, A.; Yoshida, T.; Imizu, T.; Mizoguchi, K.; He, Z.; Pinnau, I.; Nagai, K.; Freeman, B.D. *J. Polymer Science, Part B: Polymer Physics* **2000**, *38*, 1749.

[10] Chung, T.-S.; Chan, S.S.; Wang, R.; Lu, Z.; He, C. *J. Membrane Science* **2003**, *211*, 91.

[11] Polotskaya, G.A.; Andreevna, D.V.; El'yashevich, G.K. *Technical Phys. Lett.* **1999**, *25 (7)*, 555.

[12] Sterescu, D.M.; Bolthuis-Versteeg, L.; van der Vegt, N.F.A.; Stamatialis, D.F.; Wessling, M. *Macromol. Rapid Commun.* **2004**, *25*, 1674.

[13] Goh, S.H.; Zheng, J.W.; Lee, S.Y. *Polymer* **2000**, *41*, 8721.

[14] Barsema, J.N.; Kapantaidakis, G.C.; van der Vegt, N.F.A.; Koops, G.H.; Wessling, M. *Journal of Membrane Science* **2003**, *216*, 195.

[15] Visser, T.; Koops, G.H.; Wessling, M. *Journal of Membrane Science* **2005**, *252*, 265-277.

[16] Crank, J., The mathematics of diffusion, 2nd ed., Oxford: Clarendon Press **1975**.

[17] Visser, T., *Ph-D thesis*, "Mixed gas plasticization phenomena in asymmetric membranes" **2006**.

[18] Weng, D.; Lee, H.K.; Levon, K.; Mao, J.; Scrivens, W.A.; Stephens, E.B.; Tour, J.M. *European Polymer Journal* **1999**, *35,* 867-878.

[19] Polotskaya, G.A.; Gladchenko, S.V.; Zgonnik, V.N. *J. of Applied Polymer Science* **2002**, *85*, 2946-2951.

[20] Higuchi, A.; Agatsuma, T.; Uemiya, S.; Kojima, T.; Mizoguchi, K.; Pinnau, I.; Nagai, K. and Freeman, B.D. *J. App. Polym. Science* **2000,** *77*, 529.

[21] Xiao, Y.; Chung, T.-S.; Chng, M.L. *Langmuir* **2004**, *20*, 8230.

[22] Chowdhury, G.; Kruczek, B.; Matsuura, T., Polyphenylene Oxide and Modified Polyphenylene Oxide Membranes Gas, Vapor and Liquid Separation, Kluwer Academic Publishers, USA, **2001**.

Chapter 4

Appendix I

Influence of the casting solvent on pure Matrimid membranes for gas separation

I.1 Introduction

The selection of a polymer for gas separation membrane applications is essentially based on a number of intrinsic properties that control the performance characteristics of the separation system. These properties are the gas permeation properties, the permselectivity, the mechanical properties, and the cost. But, also the properties of solvents used in preparation of membrane casting solutions are a very important factor affecting membrane morphology and performance[1-3]. In this work pure Matrimid membranes were prepared in three different casting solvents as chloroform ($CHCl_3$), 1,1,2,2-Tetra chloroethane (TCLE) and 1-Methyl-2-pyrrolidinone (NMP) and gas permeability and sorption were performed.

I.2 Materials

BTDA-AAPTMI polyimide (known as Matrimid 5218, from Ciba Specialty Chemicals Corp.), 1-Methyl-2-pyrrolidinone (NMP, 99 %, Acros Organics), chloroform (Merck), 1,1,2,2-Tetra chloroethane (TCLE, 95%, Fluka).

I.3 Membrane preparation

For the preparation of pure Matrimid membranes, the polymer was dissolved in various solvents as NMP, $CHCl_3$ and TCLE (10 wt % polymer solution). The solution was cast on a glass plate and dried first under nitrogen atmosphere at room temperature (20 -25 °C) for 7 days, then in a vacuum oven at 80 °C under nitrogen atmosphere for 7 days, and then in a vacuum oven at 100 °C under nitrogen atmosphere for 7 days. Membranes samples of 40 – 80 μm thickness were prepared.

I.4 Gas permeability and sorption

According with the literature[4] it is common that the properties of the casting solvent used in preparation of the membranes can be an important factor affecting membrane morphology and performance[1-3]. Solvents with high dipole moment and boiling point have been found to induce higher interchain packing of the polymer systems, while solvents with lower dipole moment induce low polymer packing density. From literature[5] it is known that PPO prepared in $CHCl_3$ has homogeneous and amorphous structure, whereas for the PPO membranes prepared in ClC_6H_5 more compact packing was found. Thus, the films prepared from more volatile solvents will have more random structures, greater free volume, and greater permeability for gases than those prepared from the less volatile solvents[6].

Pure Matrimid membranes were prepared in three different casting solvents as chloroform ($CHCl_3$), 1,1,2,2-Tetra chloroethane (TCLE) and 1-Methyl-2-pyrrolidinone (NMP), respectively. During the preparation of our membranes the evaporation temperature was constant (room temperature ~ 23 – 25 °C).

Tables 1 presents the gas permeability and ideal gas selectivity measured at 3.5 bar feed pressure and 35 °C. The permeability values for N_2, O_2 and CO_2 of pure Matrimid prepared in NMP are in agreement with the literature[7]. The permeability coefficient of Matrimid membranes increases with decreasing of the boiling point of the casting solvent (BP_{NMP} = 202 °C, BP_{TCLE} = 146 °C, BP_{CHCl3} = 61 °C). Thus the highest permeability coefficient of all was found for Matrimid prepared in $CHCl_3$ as casting solvent, while the lowest permeability coefficient was found for Matrimid pure prepared in NMP (Table 1). The ideal gas selectivity of Matrimid pure membranes generally stays constant with decreasing of the boiling point of the casting solvent.

Table 1: Permeability results and ideal gas selectivities of pure Matrimid films in various casting solvents. (Feed pressure: 3.5 bar, T = 35 °C)

		Permeability, [barrer]			Ideal Selectivity		
Solvent	**Boiling point [°C]**	**N_2**	**O_2**	**CO_2**	**P_{O2}/P_{N2}**	**P_{CO2}/P_{N2}**	**P_{CO2}/P_{O2}**
NMP	202	0.15 ± 0.03	1.02 ± 0.09	5.20 ± 0.40	6.8 ± 2.0	34.7 ± 9.6	5.1 ± 0.8
TCLE	146	0.20 ± 0.03	1.13 ± 0.07	5.23 ± 0.40	5.8 ± 1.3	26.8 ± 6.2	4.6 ± 0.6
$CHCl_3$	61	0.29 ± 0.03	1.90 ± 0.10	8.45 ± 0.30	6.6 ± 1.0	29.1 ± 4.0	4.4 ± 0.4

It is known from literature[8] that the gas sorption is promoted by the presence of free volume in the polymer matrix – where free volume refers to the amount of interchain polymer volume available to the polymer chains for random molecular motions. The gas uptake of polymers containing large fractions of free volume is generally greater than polymers with a highly packed structure. Table 2 reports the permeability, solubility and diffusivity coefficients of N_2, O_2 and CO_2 gases in Matrimid pure prepared in NMP, TCLE and $CHCl_3$, respectively as casting solvents at 35 °C and 3.5 bar feed pressure. The solubility coefficient S was estimated from the gas sorption measurements and the diffusion coefficient D was calculated from the sorption kinetics using similar method as in literature[7].

Table 2: Gas permeability, solubility, and diffusivity of pure Matrimid films in various casting solvents.

	N_2				**O_2**				**CO_2**			
Casting solvent	P	S	$D^{1)}$	$D^{2)}$	P	S	$D^{1)}$	$D^{2)}$	P	S	$D^{1)}$	$D^{2)}$
NMP	0.15	2.13	0.70	0.75	1.02	4.52	2.26	2.35	5.20	51.30	1.01	1.10
TCLE	0.20	2.32	0.84	0.98	1.13	4.90	2.30	2.04	5.23	51.83	1.01	1.16
$CHCl_3$	0.29	4.21	0.68	0.80	1.90	9.84	1.93	1.77	8.45	96.74	0.87	0.98

1) The diffusion coefficient D calculated from the P/S ratio.
2) The diffusion coefficient D calculated from the sorption kinetics.

Feed pressure: 3.5 bar, T = 35 °C
P = [barrer], S = 10^{-3}, cm^3 (STP)/cm^3cm Hg, D = 10^{-8}, cm^2/sec

For the Matrimid pure (in TCLE) the increase of N_2 permeability in comparison to pure Matrimid (in NMP) seems to be due to increase of D coefficient, whereas for O_2 might be attributed to slight increase of S. For CO_2, however the diffusion and solubility coefficients are comparable. For the Matrimid pure (in $CHCl_3$) the increase of N_2, O_2 and CO_2 permeability should be attributed mostly to increase of S (~ 2 times) in comparison to pure Matrimid (in NMP) and Matrimid (in TCLE). The increase of solubility coefficient S can be a result of more random structure of Matrimid polymer chain prepared in $CHCl_3$, leading to a greater free volume according with the literature[6].

I.5 Conclusions

In conclusion, the gas permeability results indicate that the permeability coefficient of Matrimid pure increases with decreasing of the boiling point of the casting solvent. The formation of more ordered and compact Matrimid polymer system depends on the time allowed for evaporation of the polymer from the solution. An increased evaporation time (e.g. high boiling point solvents), leads to higher interchain packing, and therefore to lower permeability. In contrary, fast evaporation of the polymer from the solution (e.g. low boiling point solvents) leads to more random structures, greater free volumes, and therefore greater permeability for gases.

I.6 References

[1] Chowdhury, G.; Vujosevic, R.; Matsuura, T.; Laverty, B. *Journal of Applied Polymer Science* **2000**, *77*, 1137.

[2] Khulbe, K.C.; Matsuura, T., Lamarche, G.; Kim, H.J. *Journal of Membrane Science* **1997**, *135*, 211.

[3] Hamad, F.; Khulbe, K.C.; Matsuura, T. *Journal of Membrane Science* **2002**, *204*, 27.

[4] Xiao, Y.; Chung, T.-S.; Chng, M.L. *Langmuir* **2004**, *20*, 8230.

[5] Khulbe, K.C.; Matsuura, T.; Lamarche, G.; Lamarche, A.-M. *Journal of Membrane Science* **2000**, 170, 81.

[6] Kruczek, B.; Matsuura, T. *Journal of Applied Polymer Science* **2003**, *88*, 1100.

[7] Visser, T., *Ph-D thesis*, “Mixed gas plasticization phenomena in asymmetric membranes” **2006**.

[8] Story, B.J.; Koros, W.J. *Journal of Membrane Science* **1992,** *67*, 191.

Chapter 5

Boltorn-modified poly (2, 6-dimethyl-1,4-phenylene oxide) gas separation membranes

Dana M. Sterescu, Dimitrios F. Stamatialis, Eduardo Mendes , Jan Kruse, Klaus Rätzke , Franz Faupel , Matthias Wessling

Abstract

This chapter describes the preparation, characterization and the permeation properties of poly (2, 6-dimethyl-1,4-phenylene oxide) (PPO) dense polymer films containing aliphatic hyperbranched polyesters, Boltorn (H20, H30 and H40). The Boltorn are dispersed in PPO at various concentrations.

The gas permeability results were very different between low and high concentration of Boltorn. The gas permeability of PPO with 1.0 wt % of Boltorn is 2-3 times higher than the pure polymer, while at higher concentration (9.1 wt %) of Boltorn the permeability becomes almost 50 % of the pure polymer. The gas pair selectivity, however, stays constant. The increase in permeability at low concentration of Boltorn is due to the increase of the free volume, probably due to hydrogen bonds between Boltorn and the oxygen of PPO backbone. The decreased permeability of PPO containing higher concentration of Boltorn (9.1 wt %) is due to two reasons: decrease in free volume as determined by PALS as well as phase separation. The hyperbranced polyesters form aggregates that migrate to the top surface of the membrane.

Sterescu D.M. *et al. Macromolecules* **2007**, *40*, 5400

1. Introduction

The control of gas permeability and selectivity for polymer membranes separating gases is a subject of intense research in both industry and academia[1], focusing on the relationship between the polymer structure and gas separation properties. Most of the polymers that have been investigated, however, show the general trend that highly permeable polymers possess rather low selectivity and vice versa (permeability / selectivity trade off relationship[2]).

The permeation properties of a polymer depend primarily on the packing density, the polymer chain mobility and the free volume of the polymer. Poly (2, 6-dimethyl-1,4-phenylene oxide) (PPO) is one of the very few polymers that are actually used for the industrial production of gas separation membranes[3]. Because of its high permeability and acceptable selectivity, PPO is particularly interesting for the production of nitrogen-enriched air. It is desirable to increase permeability of PPO without compromising selectivity. For this, a considerable interest has been shown in dendritic polymers. The materials are called hyperbranched polymers (HBP), to distinguish them from monodisperse dendrimers. Unique features of the dendritic architecture[4-6] result directly from the repetitive branching which occurs during their synthesis giving access to large number of reactive end-groups. Due to their availability of free volume[7], they might be attractive to control permselectivities for small molecules like gases for gas separation applications.

In fact, this chapter presents a successful increase of gas permeability based on commercially available aliphatic hyperbranched polyesters, Boltorn, mixed with PPO matrix. Small amount of Boltorn dispersed into PPO causes significant increase of membrane permeability, while at higher amounts the gas permeability decreases. A systematic analysis of PPO-Boltorn membranes is performed using Scanning Electron Microscopy (SEM), differential scanning calorimetry (DSC), Wide Angle X-ray Scattering (WAXS), positron annihilation lifetime spectroscopy (PALS), energy dispersive X-ray analysis (EDX) measurements and gas sorption experiments in order to investigate the influence of Boltorn concentration to the membrane permeation performance. It seems that at low Boltorn concentration the high gas permeability in comparison to pure PPO is due to increase polymer free volume by the Boltorn. At higher Boltorn

concentration, the free volume decreases and the Boltorn form clusters. Both phenomena cause decrease of gas permeability.

2. Experimental

2.1 Materials

For the membrane preparation the following materials were used: Poly (2,6-dimethyl-1, 4-phenylene oxide) (PPO) (Parker Filtration and Separation, MW = 150000 measured by GPC), chloroform (Merck), 1-Methyl-2-pyrrolidinone (NMP, 99 %, Acros Organics), and hyperbranched polymers commercially available as Boltorn® H20, H30, H40 (kindly supplied by Perstorp Specialty Chemicals AB, Sweden).

The hyperbranched polymers studied in this work are aliphatic polyesters using ethoxylated pentaerythritol as central cores and 2,2-bis(methylol)propionic acid (bis-MPA) as dendritic units. Boltorn H20 statistically contains two generations of bis-MPA, while Boltorn H30 and H40 have three and four generations of MPA, respectively. An example of Boltorn is shown in Figure 1. The products are all hydroxyl functional, but differ in molecular weight ($M_{w\ H20}$ = 2100 g/mole, $M_{w\ H30}$ = 3500 g/mole, $M_{w\ H40}$ = 5100 g/mole) and hydroxyl functionality. Hydroxyl number, molecular weight and polydispersity of the Boltorn polymers from the data sheet provided by Perstorp are presented elsewhere[5,8].

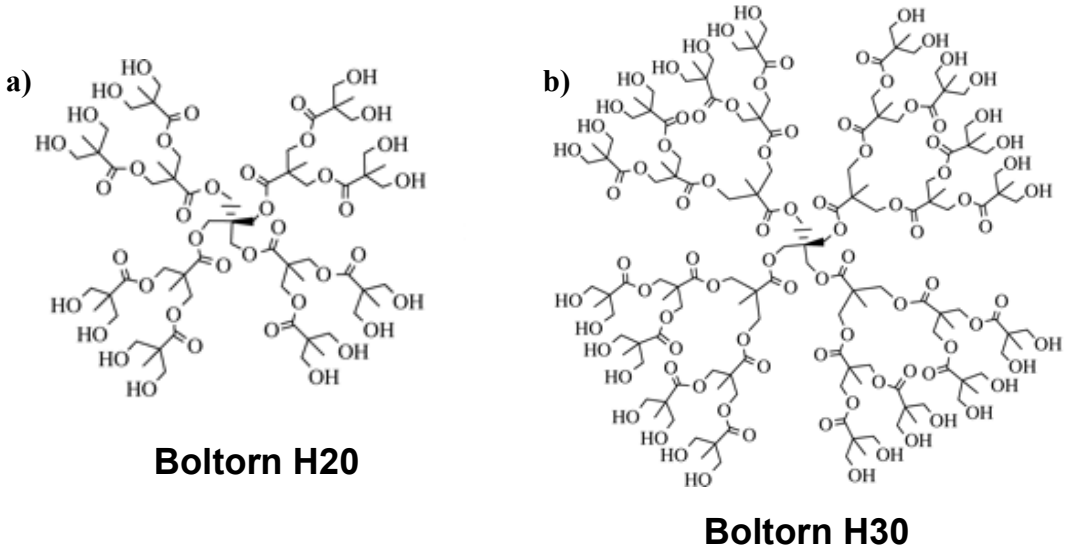

Figure 1: Schematic representation of the hyperbranched polyol molecule (a) Boltorn H20 and (b) Boltorn H30 structure.

2.2 Preparation of PPO and PPO–Boltorn membranes

For the preparation of pure PPO membranes, the PPO was dissolved in chloroform (10 wt % polymer solution). The solution was cast on a glass plate and dried first under nitrogen atmosphere at room temperature (20 -25 °C) for 3 days and then in a vacuum oven at 50 °C under nitrogen atmosphere for 2 days. Films of 40 – 70 μm thickness were prepared.

For the preparation of PPO membranes dispersed with Boltorn (three different generations: H20, H30 and H40), the PPO and Boltorn were dissolved separately: PPO in chloroform (10 wt % polymer solution) and the Boltorn in NMP (10 wt % Boltorn solution), respectively. Both solutions were stirred at room temperature until complete dissolution (for 3 – 4 hours). Then, the two solutions were mixed and stirred for 4 hours until they became homogeneous. The PPO-dispersed Boltorn solutions were cast on a glass plate and dried under nitrogen atmosphere at room temperature (20 – 25 °C) for 3 days. Then, the PPO-Boltorn films of 40 – 70 μm thickness were peeled off from the glass plate and dried in a vacuum oven at 30 °C until constant weight (for approximately 2 months). Films containing 0.5, 1.0, 2.4, 4.8, 7.0 and 9.1 wt % of Boltorn / membrane were prepared. The preparation of mechanically stable films containing more than 9.1 wt % of Boltorn was not possible. The amount of Boltorn in the membrane was calculated using the equation:

$$\%\ \text{wt (Boltorn / membrane)} = \frac{g_{\text{Boltorn}}}{g_{\text{Boltorn}} + g_{\text{PPO}}} * 100 \qquad (1)$$

For comparison, pure PPO membranes were also prepared by dissolution of the polymer in mixture of $CHCl_3$/NMP, following the procedure for the preparation of PPO-Boltorn membranes. In this case, however, without the addition of Boltorn.

2.3 Characterization of membranes

DSC measurements

The thermal properties of pure PPO and PPO-Boltorn dispersed were measured using a Perkin Elmer DSC-7 (Differential Scanning Calorimeter) in nitrogen atmosphere. The PPO-

Boltorn samples were initially heated from - 60 °C until 350 °C, cooled with liquid nitrogen, held for 5 minutes, and reheated two more times following the same steps, under nitrogen atmosphere. The heating rate was 10 °C/min and the cooling rate was 20 °C/min. The glass transition temperature, T_g, of the polymer was obtained from the third scan.

Gas permeability and Sorption

The permeation of pure nitrogen (N_2), oxygen (O_2), and carbon dioxide (CO_2) through the PPO and PPO-Boltorn dispersed was investigated at different feed pressures (1.5, 2.5 and 3.5 bar), using the set up described elsewhere[9]. Pure gas permeability coefficients were calculated from the steady state pressure increase in time in a calibrated volume at the permeate side by using the equation:

$$\frac{P}{l} = \frac{V \times 273.15 \times (p_{pt} - p_{p0})}{A \times T \times \frac{(p_{ft} + p_{f0})}{2} \times 76 \times t} \times 10^6 \qquad (2)$$

where the ideal gas law is assumed to be valid, p_{pt} , p_{ft} [bar] is the pressure at the permeate and feed side at time t, p_{p0} p_{f0} is the permeate and feed pressure at t=0, T [K] is the temperature, V [cm^3] is the calibrated permeate volume, and A [cm^2] the membrane area. The gas permeance (P/l) is expressed in GPU, i.e. 10^{-6} cm^3cm^{-2} s^{-1} $cmHg^{-1}$. Multiplying the gas permeance with the thickness of dense membrane, l [cm], gives the permeability coefficient in Barrer. All the gas permeation experiments were performed at 35 °C. Values and error bars reported in the tables and figures are based on measurements of two different membrane samples.

The gas sorption isotherms of N_2, O_2 and CO_2 in dense PPO pure (in $CHCl_3$), PPO pure (in $CHCl_3$/NMP) and PPO-Boltorn dispersed (1.0 and 9.1 wt %) films were measured at 35 °C, using a magnetic suspension balance[10] (MSB, Rubotherm). The experimental procedure was divided into five steps: a) evacuation of pressure vessel and sample for at least 24 hours; b) increase of gas pressure to desired value; c) wait until equilibrium in mass change is reached; d) record equilibrium mass, temperature and pressure; e) repeat steps b and c or if the maximum pressure is reached: evacuate sample (step a) and start measurement with new gas or new

sample. The equilibrium mass increase was corrected for buoyancy by subtracting the weight at zero sorption at a certain pressure from the vacuum weight of the sample. Using the equilibrium weight increase and the density of the polymer, the concentration (in cm^3 STP) inside the polymer (cm^3 polymer) was calculated[10].

Crank[11] showed that the sorption of a penetrant in a polymer matrix is proportional to the square root of time, assuming a constant diffusion coefficient. This behavior is called ideal Fickian sorption and the mass uptake (g) in time (M(t)) can be described with the following equation:

$$\frac{M(t)}{M_\infty} = 1 - \frac{8}{\pi^2}\sum_{m=0}^{\infty}\frac{1}{(2m+1)^2}\exp\left\{-\frac{D(2m+1)^2\pi^2 t}{L^2}\right\} \qquad (3)$$

where M_∞ is the amount of mass (g) sorbed by Fickian sorption at infinite time, D is the diffusion coefficient (m^2/s), t is the time (s), and l is the sample thickness (m). Fitting of the sorption data into this equation leads to the diffusion coefficients[12].

Scanning Electron Microscopy (SEM)

The geometrical characteristics and the morphology of the membranes were determined using a Jeol JSM-5600 LV Scanning Electron Microscope. The membrane samples were cut and sputtered with a thin layer of gold using a Balzers Union SCD 040 sputtering apparatus.

Energy Dispersive X-ray Analysis (EDX)

The local elemental composition of the PPO-Boltorn membranes was investigated by energy dispersive X-ray analysis (EDX) using a NORAN System Six (NSS) microanalysis system model C100 (Thermo Electron Corporation). This technique is used in conjunction with SEM type JSM-6480LV.

WAXS measurements

Wide Angle X-ray Scattering (WAXS) experiments were performed using a Bruker-Nonius D8-Discover equipped with 2D detector. Standard background (air and sample holder) subtraction measured at the same time and conditions were applied to all data. The sample-

detector (S-D) distance was set at 10 cm and the incident beam wavelength was 1.54 Å (Cu-Kα). Measurements were performed both perpendicular and in plane of the membrane[13]. In the first case, the sample thickness as seen by the incident beam was always less than 0.5 mm.

Positron Annihilation Lifetime Spectroscopy (PALS)

A well accepted method to determine free volume in polymers[14] is positron annihilation lifetime spectroscopy (PALS). Positrons obtained from radioactive decay annihilate with electrons in the polymer material probing the local electron density and hence atomic density. Once injected from a radioactive source, positrons form in most polymers hydrogen-like positronium (Ps) states. The pick-off lifetime of orthopositronium, ($\tau_{o\text{-}Ps}$), is well correlated to the free-volume hole size in polymers. If the spins of electron and positron add to value of one, annihilation of orthopositronium (o-Ps) is obstructed, reducing the decay rate drastically[15]. The annihilation is due to the interaction of the o-Ps with the electrons in the surrounding material because an exchange of the electrons can change the state of the orthopositronium into the fast decaying para-state. Thus, the local electron density, which is lower in larger holes, becomes a measure for the hole size. The success of PALS in polymer research is largely due to the so-called standard model developed by Tao and Eldrup[16,17]. This simple quantum mechanical model assumes the Ps to be confined to spherical holes with infinitely high walls and gives direct relationship between $\tau_{o\text{-}Ps}$ and the size of free volume holes. Since hole sizes in amorphous polymers are relatively broadly distributed, the discrete $\tau_{o\text{-}Ps}$ obtained from the fit to lifetime spectra and hence the hole radius has to be regarded as an average value[18]. On the other hand, the interpretation of the o-Ps intensity, which has often been used as a measure for the hole concentration, is questionable, as the intensity is also affected by the positronium formation probability[19]. Therefore, it will not be considered in the present paper. The average decay rate of orthopositronium in our membranes was measured and was correlated to the polymer free volume.

Positron annihilation experiments have been performed in a fast-fast coincidence setup with a home made temperature-controllable sample holder under high vacuum conditions[15].

Polymeric thin films were cut into 9x9 mm^2 pieces and stacked together with a Na-22 source (1MBq) in a sandwich like manner (total thickness ≈ 0.8 mm each) to ensure complete absorption of the positrons in the sample. The sandwich was wrapped into Aluminium-foil and put into a sample holder. Spectra were recorded with 10^7 counts within 12 h, typically. Evaluation was performed with the LT9.0 routine program using the common background subtraction and the final resolution function, which was determined as a sum of two Gaussians with FWHMs (full width at half maximum) of approx. 247 ps and 390 ps and weight of 80 % and 20 %; three life time components were assumed, where the first was kept fixed at 125 ps (lifetime of p-Ps in vacuum).

3. Results and discussion

3.1 Gas permeability

Figure 2 shows the gas permeability of PPO-H20 and PPO-H40 in comparison to pure PPO (prepared in $CHCl_3$) membranes. The permeability coefficient reaches a maximum value at 1.0 wt % and decreases with further increase of Boltorn concentration up to 9.1 wt %, where it becomes lower than PPO pure.

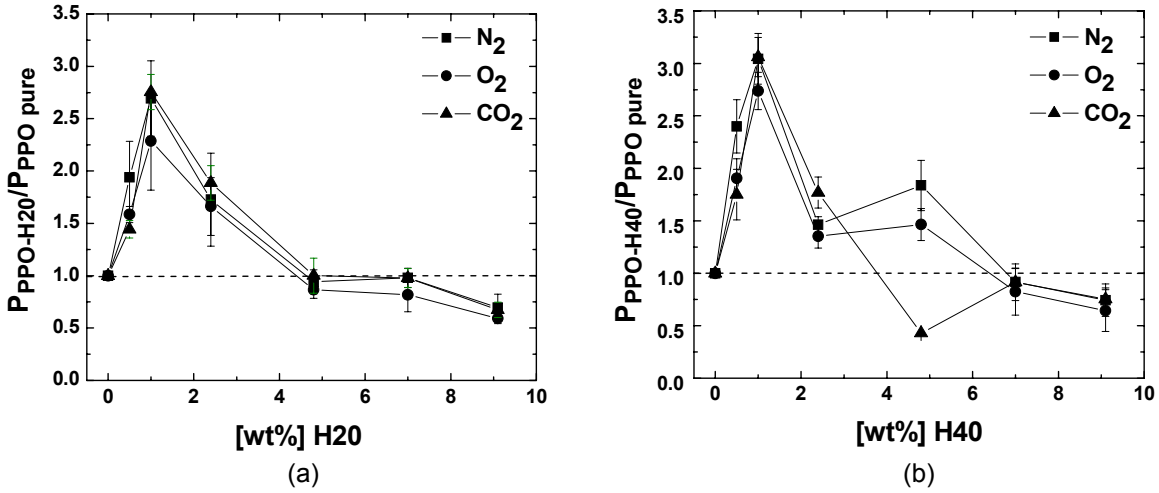

Figure 2: Permeability of (a) PPO-H20 and (b) PPO-H40 normalized with the permeability of pure PPO (in $CHCl_3$) versus the wt % Boltorn content for gases N_2 (■), O_2 (●) and CO_2 (▲) at 1.5 bar feed pressure and 35 °C.

Similar trend was found for all three gasses measured, N_2, O_2 and CO_2 and for the three generations of Boltorn (H20, H30 and H40) (see Figure 3). Besides, the gas permeability through pure PPO membranes and PPO-Boltorn is constant at different feed pressures for all three gases measured (see Figure 4 an example for O_2).

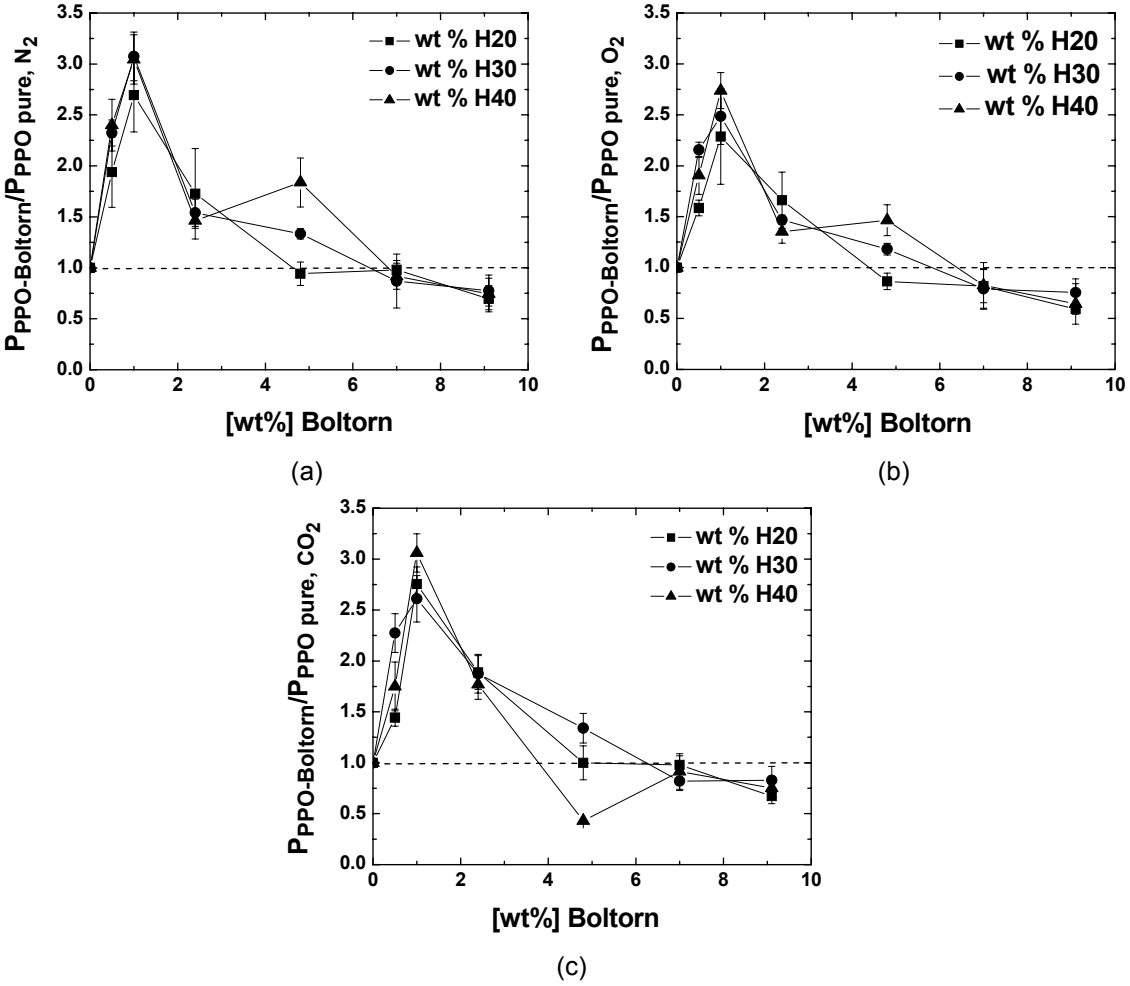

Figure 3: Permeability of PPO-Boltorn (H20 (■), H30 (●) and H40 (▲)) normalized with the permeability of pure PPO (in $CHCl_3$) versus the wt % Boltorn content for gases (a) N_2, (b) O_2 and (c) CO_2 at 1.5 bar feed pressure and 35 °C.

According with the literature[20], it is common that the casting solvent has an influence on membrane properties. To find the reason of the significant increase of gas permeability (Boltorn or/and of the casting solvent) we also compared the PPO-Boltorn membranes to pure PPO prepared in the same $CHCl_3$/NMP solvent mixture (see membrane preparation).

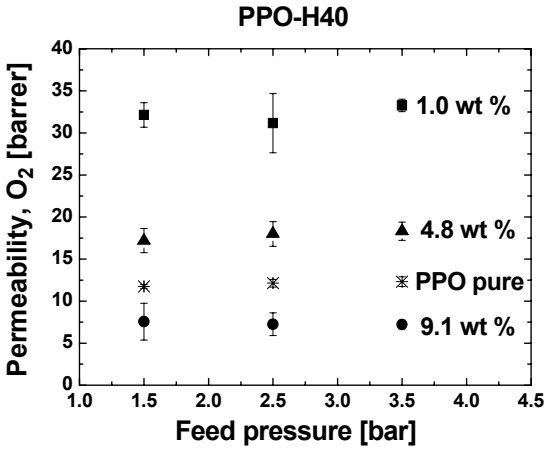

Figure 4: Oxygen permeability of PPO-H40 versus feed pressure at various H40 concentrations: 1.0 wt % (■), 4.8 wt % (▲), 9.1 wt % (●), and pure PPO (in $CHCl_3$) (✳) at 35 °C.

Table 1 shows the gas permeability of PPO pure (in $CHCl_3$), PPO-H40 1.0 wt %, PPO-H40 9.1 wt % and the pure PPO membranes prepared in the same $CHCl_3$/NMP solvent mixture. The results show indeed a difference in gas permeability between pure PPO prepared in various solvents. The nitrogen permeability coefficient of PPO-H40 1.0 wt % increases 89 % in comparison to PPO pure in the same $CHCl_3$/NMP mixture and 207 % in comparison to PPO pure (in $CHCl_3$). Similar behavior was found also for O_2 and CO_2 gases. For PPO-H40 9.1 wt % the nitrogen permeability coefficient decreases 43 % in comparison to PPO pure prepared in the same $CHCl_3$/NMP mixture, instead of 26 % in comparison to PPO pure (in $CHCl_3$). These results demonstrate that both the Boltorn and the casting solvent have an influence on the gas membrane permeability.

Table 1: Permeability results of PPO and PPO-H40 films (Feed pressure: 1.5 bar, T = 35 °C)

	Permeability [barrer]		
Membranes	**N_2**	**O_2**	**CO_2**
PPO pure ($CHCl_3$)	2.7 ± 0.1	11.7 ± 0.2	50.7 ± 2.6
PPO pure ($CHCl_3$/NMP)	4.4 ± 0.2	16.2 ± 0.5	63.9 ± 1.6
PPO-H40 1.0 wt % H40	8.3 ± 0.6	32.1 ± 1.5	155.1 ± 1.4
PPO pure ($CHCl_3$/NMP)	3.5 ± 0.1	16.1 ± 0.3	65.7 ± 1.2
PPO-H40 9.1 wt % H40	2.0 ± 0.4	7.6 ± 2.2	38.1 ± 3.5

Table 2 presents the ideal gas selectivity of PPO-H40 and pure PPO (in $CHCl_3$) at a feed pressure of 1.5 bar corresponding to the average of two different membrane samples. Similar results were found also for pure PPO (in $CHCl_3$/NMP). The selectivity generally stays constant (if one takes into account the standard deviation). Some exceptions are observed for the films with 0.5, and 4.8 wt % Boltorn. Their CO_2/N_2 selectivity decreases approximately 22 - 27 % than the pure PPO, while it increases for PPO-Boltorn 2.4 wt %. Similar values of the ideal gas selectivity were found also for PPO-H20 and PPO-H30 membranes.

Table 2: Ideal gas selectivities of PPO and PPO-H40 films (Feed pressure: 1.5 bar, T = 35 °C)

	Ideal Selectivity		
Membranes	P_{O2}/P_{N2}	P_{CO2}/P_{N2}	P_{CO2}/P_{O2}
PPO pure ($CHCl_3$)	4.3 ± 0.1	18.7 ± 1.1	4.3 ± 0.3
PPO-H_{40} 0.5 wt.%	3.4 ± 0.6	13.6 ± 2.5	4.0 ± 0.7
PPO-H_{40} 1.0 wt.%	3.9 ± 0.5	18.8 ± 1.5	4.8 ± 0.3
PPO-H_{40} 2.4 wt.%	4.0 ± 0.4	22.6 ± 1.7	5.6 ± 0.5
PPO-H_{40} 4.8 wt.%	3.5 ± 0.7	14.5 ± 1.9	4.2 ± 0.4
PPO-H_{40} 7.0 wt.%	3.9 ± 1.5	18.6 ± 5.1	4.8 ± 1.9
PPO-H_{40} 9.1 wt.%	3.8 ± 1.8	18.9 ± 5.5	5.0 ± 1.9

3.2 Scanning Electron Microscopy (SEM)

Scanning Electron Microscopy (SEM) was used to investigate the distribution of Boltorn in the PPO structure. Figure 5 shows some typical results for our membranes. The micrographs were obtained using a Jeol JSM-5600 LV Scanning Electron Microscope with magnification of 950x and 5000x.

The SEM micrographs of pure PPO (in $CHCl_3$) and pure PPO (in $CHCl_3$/NMP) show similar dense and compact structure (see Figure 5a). At higher Boltorn concentration in PPO however, phase separation occurs resulting in a dispersed particulate structure (see Figure 5), in agreement with Boogh et al.[21]. The PPO-H40 1.0 wt% membrane (Figure 5b) has a dense and

compact structure comparable with the pure polymer. The formation of the particulate structure is mostly visible at higher Boltorn concentration (Figure 5c). The PPO-H40 9.1 wt% membrane seems to be different at both sides, one dense homogeneous layer at the glass side and one more heterogeneous layer at the air side (Figure 5c).

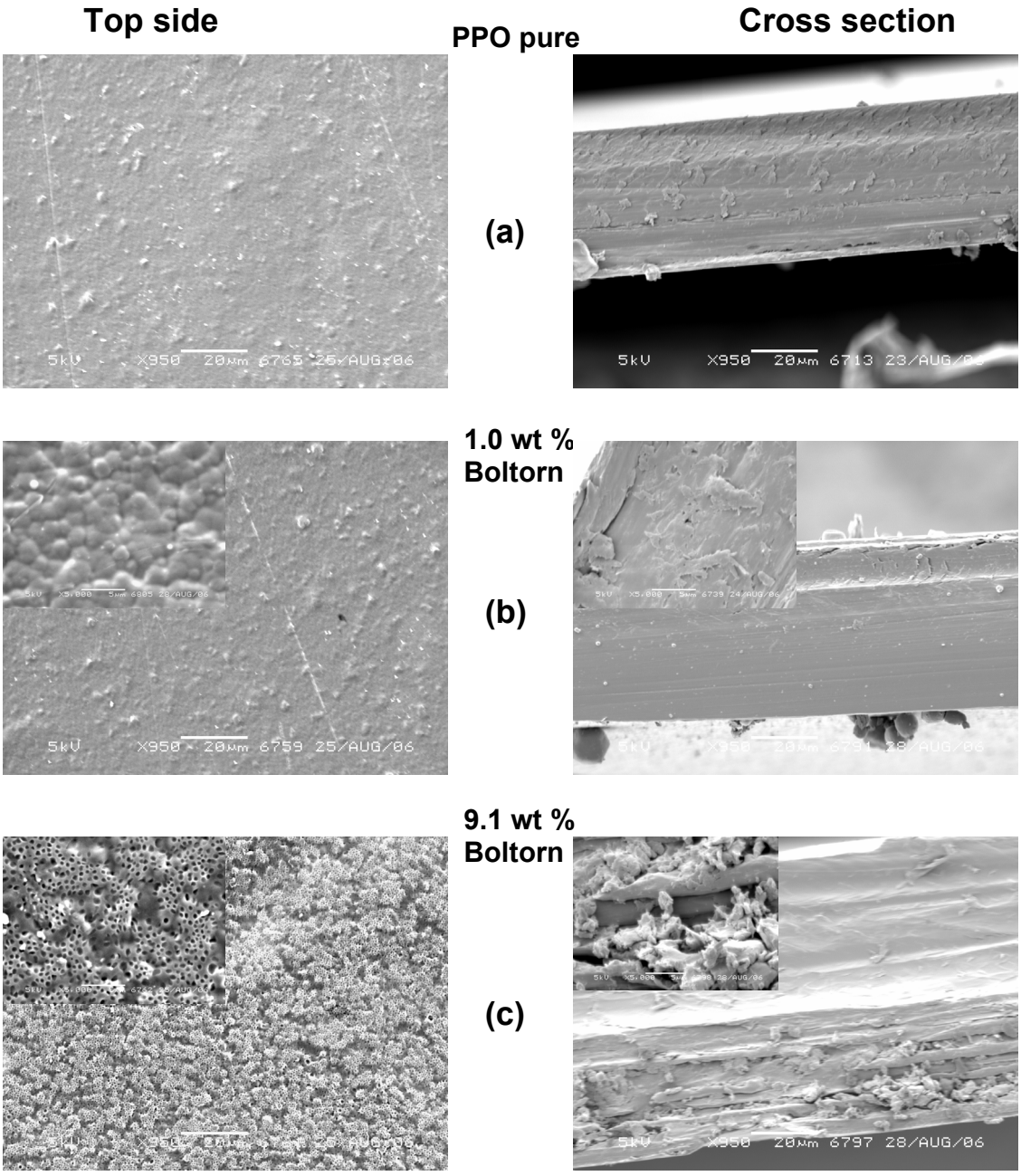

Figure 5: SEM micrographs of PPO and PPO-H40 membranes containing various Boltorn H40 concentrations (insets are zoom at magnification 5000x).

The absence of phase separation at low concentration of H40 (1.0 wt %) in PPO is probably due to the network formation linking the hyperbranched molecules to PPO chain by the hydrogen bonds[21]. An indication of this is given by the unchanged surface structure after washing of the membrane with NMP solvent. For this, we kept the PPO-Boltorn membranes four days in NMP (known as good solvent for Boltorn, but not for PPO). The membranes were dried afterwords in N_2 box for 2 days and vacuum oven at 80 °C for 2 days and analyzed again by SEM. The SEM micrographs of PPO-H40 1.0 wt% after "washing" with NMP look similar with the pure PPO suggesting that no Boltorn was washed out from the membrane surfaces. In contrary, PPO-H40 9.1 wt% washed in NMP has "holes" at the top surface, instead of the dispersed particulate structure seen before (see Figure 6).

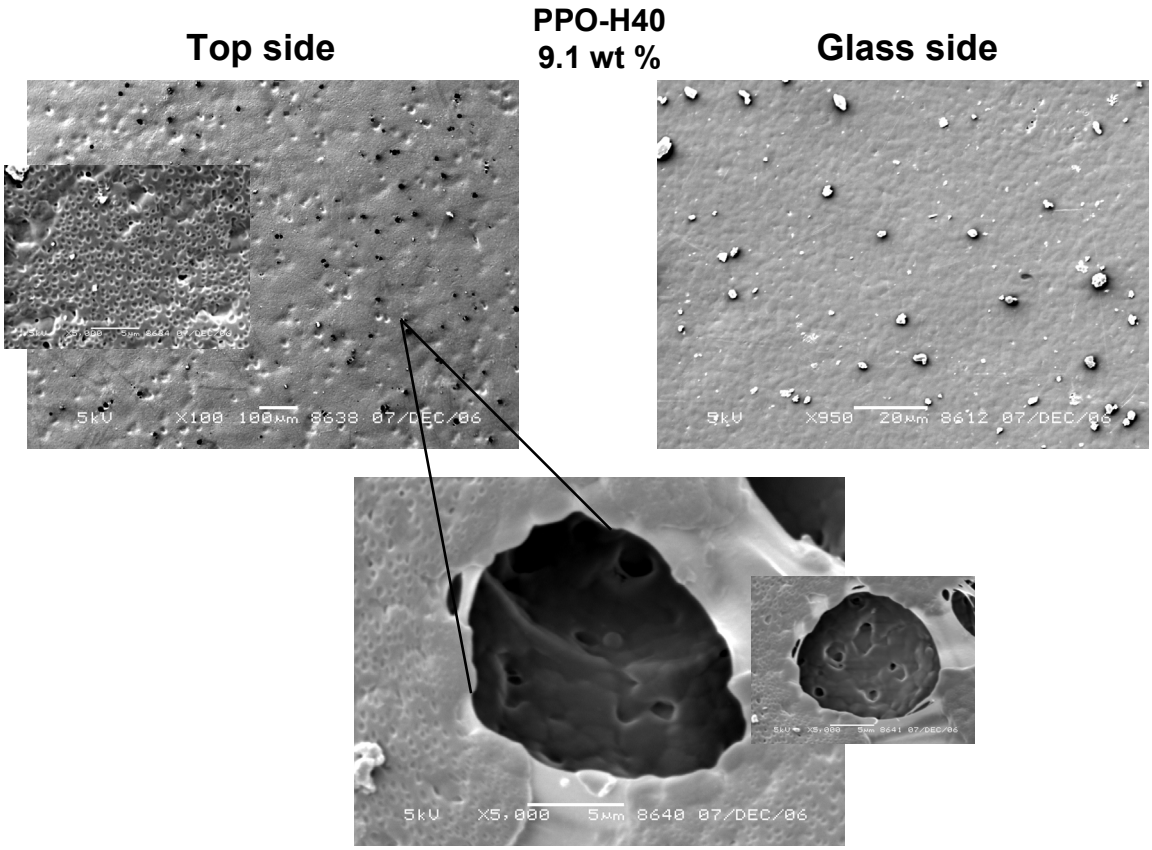

Figure 6: SEM micrographs of PPO-H40 9.1 wt % (that includes a zoom of the top surface, 5000x).

The “holes” were probably created after dissolution of Boltorn by NMP, while the glass side keeps its dense structure similar to the pure PPO. This test suggests that at low Boltorn concentrations (1.0 wt %), Boltorn is well mixed into the polymer structure, while for higher concentrations (9.1 wt %) the Boltorn migrates to the air surface and forms agglomerates. Due to the formation of such composite structure higher concentrations of Boltorn lead to a loss in mechanical strength. Therefore, mechanically stable membranes containing higher concentrations of Boltorn than 9.1 wt % could not be prepared.

3.3 Energy Dispersive X-ray Analysis (EDX)

The surface compositions of 6 different samples were analyzed by EDX. The carbon (C) and oxygen (O) content of the pure Boltorn (H40), pure PPO (in $CHCl_3$), pure PPO (in $CHCl_3$/NMP), and PPO-H40 samples were measured. The results of pure PPO (in $CHCl_3$) and pure PPO (in $CHCl_3$/NMP) are similar, therefore we compared the PPO-H40 to pure PPO (in $CHCl_3$) (see Table 3).

Table 3: Elemental composition of the H40 pure, PPO pure (in $CHCl_3$) and PPO-Boltorn membranes obtained by EDX.

Sample	C, [wt%]	O, [wt%]
H40 (powder)	75	25
H40 (pellet)	75	25
PPO pure (in $CHCl_3$)	96	4
PPO-H40 1.0 wt %	95	5
PPO-H40 9.1 wt %	93	7

The average C/O ratio of pure PPO is 8/1 instead of 5/3 for pure Boltorn (H40).The PPO-H40 1 wt % and PPO-pure membrane show almost the same C and O content, whereas the PPO-H40 9.1 wt % shows slightly lower carbon content at air side surface than the PPO-pure sample. This difference is small, because the average composition of the surface is compared. If the carbon content is measured locally the differences become more significant. Figure 7 shows the EDX-

SEM micrograph and the corresponding carbon content of the PPO-H40 9.1 wt % versus the position at the membrane surface. The agglomerates visible on the PPO-H40 air side contain significantly lower amount of carbon than the rest of the surface and are probably H40.

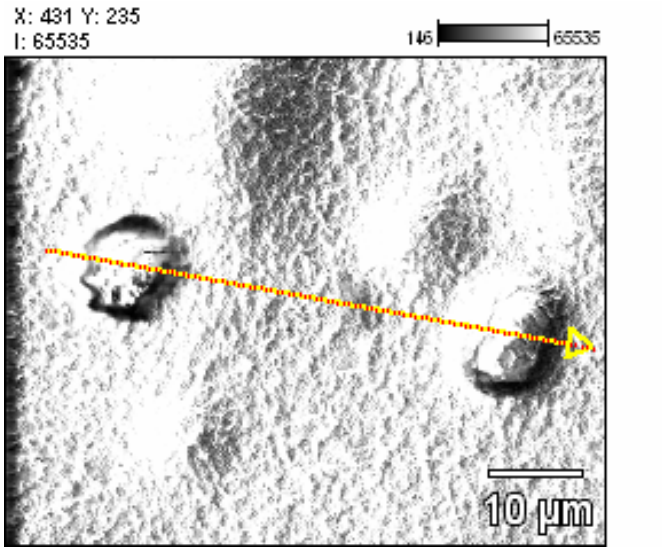

(a)

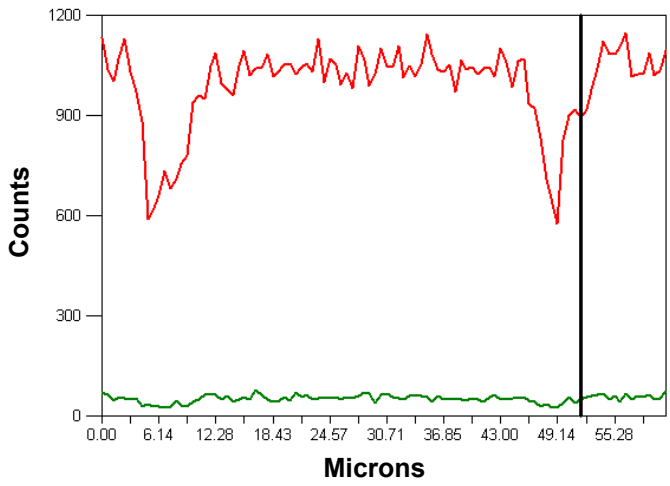

(b)

Figure 7: (a) SEM micrograph of PPO-H40 9.1 wt % membrane (top surface), (b) EDX spectra of PPO-H40 9.1 wt % membrane. (Accelerating Voltage: 10.0 kV, Magnification: 1000)

3.4 DSC measurements

DSC results show similar T_g for PPO film prepared in $CHCl_3$ and $CHCl_3$/NMP, respectively. Therefore we compared the PPO-H40 to pure PPO in $CHCl_3$. Table 4 shows that the T_g of PPO-H40 1 wt % decreases to 209 °C in comparison with the pure PPO (T_g = 214 °C). The T_g of PPO-H40 9.1 wt % is however comparable with the pure PPO. Boltorn H40 has T_g at 42 °C and melting point at 63 °C. PPO-H40 1 wt % has one T_m at 241 °C, which is close to the T_m of pure PPO (251 °C). However, PPO-H40 9.1 wt % has two melting peaks at 215 °C and 239 °C probably corresponding to the two phases visualized by SEM. The presence of two distinct T_m confirms the phase separation at 9.1 wt % Boltorn.

Table 4: DSC results of PPO, H40 and PPO-H40 samples.

Samples	T_g, [°C]	T_m, [°C]
PPO	214	251
H40	42	63
PPO-H_{40} 1.0 wt%	209	241
PPO-H_{40} 9.1 wt%	212	215 239

3.5 Positron Annihilation Lifetime Spectroscopy (PALS)

The free volume in PPO-H40 1 wt% and 9.1 wt % was determined by PALS and compared with the pure PPO sample. The PALS results of pure PPO prepared in $CHCl_3$ and those prepared in $CHCl_3$/NMP are very similar with each other; therefore here we use for comparison only pure PPO in $CHCl_3$. Figure 8a shows the original lifetime spectra of the samples. In the evaluation of our results the term “dispersion“ will be frequently used in the context of o-Ps lifetime. In older evaluation methods, the lifetime of o-Ps was accepted to reflect a mean hole size. Newer evaluation software, as the one used in this work, assumes a distribution of lifetimes. We believe this is more suitable assumption, as holes in a non-crystalline polymer are supposed to be distributed in size as well. This distribution is assumed to be log-normal, and the dispersion (or σ) given is the standard deviation of the log-normal lifetime distribution. The

increase in orthopositronium lifetime reflects an increase of the average free volume size (indicator for average volume is the o-Ps lifetime, indicator for width is the dispersion, σ). The data are evaluated with respect to a single o-positronium lifetime, distribution and intensity (Figure 8b - the dotted lines are used to guide the eye and do not correspond to experimental data). It was found[7] using PALS measurements that H40 has a free volume of 0.0635 nm^3. This will be taken into account in a more detailed data evaluation.

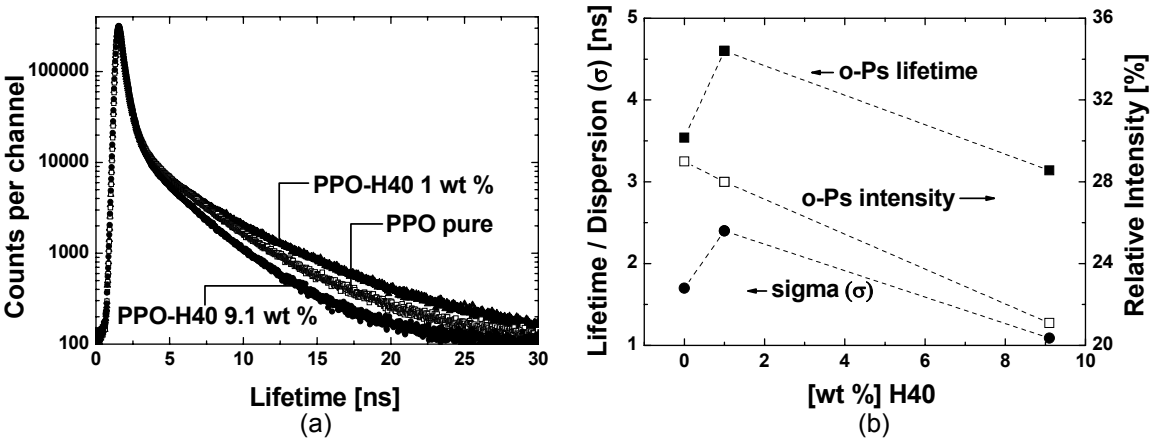

Figure 8: (a) PALS spectra of pure PPO (in $CHCl_3$) reference sample and PPO with different concentrations of Boltorn (1.0 and 9.1 wt %), (b) orthopositronium-lifetime, -dispersion (σ) and –relative intensity, of pure PPO (in $CHCl_3$) and PPO-Boltorn.

For the PPO-H40 1 wt % the o-Ps lifetime, as a measure of the average free volume and the dispersion is higher than pure PPO (see Figure 8b). The intensity decreases only slightly. This shows that the average free volume (increase of o-Ps lifetime) and the total free volume (increase of of o-Ps lifetime and σ) increases compared to the pure PPO. For the PPO-H40 9.1 wt %, o-Ps lifetime, dispersion and intensity decrease, indicating decreased free volume compared to pure PPO. At first glance, one would expect a further increase in free volume with increased concentration. However, if already 1 wt % of Boltorn increases the free volume and creates stress within the polymer structure, a further increase in concentration might shift the overall distribution of free volume to very high values. Therefore, it is possible that the largest holes are filled by Boltorn. Other holes, smaller then the critical size are contracted and also filled with Boltorn. Hence, the largest holes are filled, the larger part of the distribution of free volume is cut off, therefore average value and width of distribution decrease consequently the gas

permeability decreases (see section 3.1). This hypothesis seems consistent with EDX measurement, which shows agglomerates of H40 for the PPO-H40 9.1 wt % membrane and the permeability measurements.

The PALS results suggest that the increased permeability of PPO containing low concentration of Boltorn (1.0 wt %) is due to increase of the average and total free volume of the PPO-H40 1.0 wt % sample in comparison to pure PPO. The interaction between the hydroxyl end groups of Boltorn with the electron pair of the oxygen atom of the PPO backbone may induce hydrogen bonds formation[7,22]. In such a way the 1.0 wt % of Boltorn molecules are retained in the PPO membrane phase by the hydrogen bonds introducing an extra interstitial chain space. This leads to an increased free volume and therefore to an increased permeability (Table 1). The decreased permeability of PPO containing higher concentration of Boltorn (9.1 wt %) is due to the decrease of polymer free volume. In this case the hyperbranced polyesters form aggregates (shown by EDX and SEM) in the large holes created, which can be stabilized by hydrogen bonding of terminal groups[6]. Two different models of crystallization can occur (proposed by Malmström[7]): intermolecular crystallization, without mixing of end-groups and intra-molecular crystallization. Most probably, during the drying process segregation of Boltorn occurs, preferentially at the air side of the film (as shown by SEM, section 3.2). Because the largest holes are filled, the larger part of the distribution of free volume is cut off and therefore the average and total free volume decreases leading to a decreased permeability, in agreement with the literature[23].

3.6 WAXS analysis

Figure 9a displays spectra of PPO powder (pw) and H40 powder (pw) as received, of PPO-H40 1.0 wt % and pure PPO (in $CHCl_3$/NMP) film. The results are displayed when the incident beam is perpendicular to the film (front view) and parallel to the film (side view), respectively. Main scattering peaks are numbered. Comparison of the scattering of pure PPO powder with pure PPO (in $CHCl_3$/NMP) (Figure 9a,b) clearly indicates strong similarity: peak positions and relative intensities are very similar.

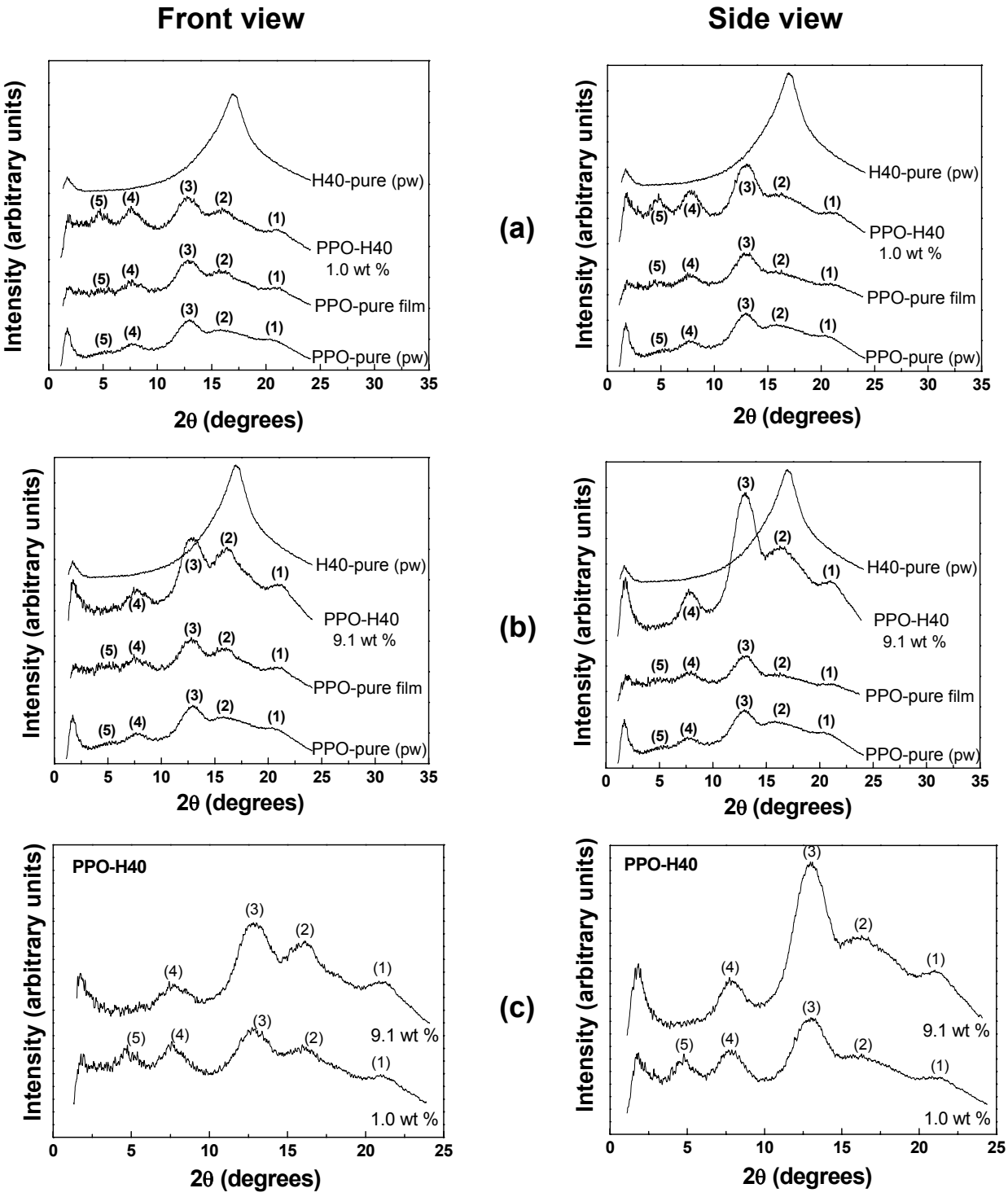

Figure 9: Scattering intensity as function of the scattering angle of: (a) pure H40 powder, pure PPO powder, PPO-H40 1.0 wt % and pure PPO (in $CHCl_3$/NMP), (b) pure H40 powder, pure PPO powder, PPO-H40 9.1 wt % and pure PPO (in $CHCl_3$/NMP), (c) PPO-H40 1.0 wt % and 9.1 wt % H40. For (c) - the scattering pattern of pure H40 multiplied by the volume fraction has been subtracted from PPO-H40.

The scattering of the PPO-H40 1.0 wt % is similar to pure PPO (Figure 9a, front view). The main difference in this spectrum is the enhancement of a low intensity maximum in sample PPO-H40 (1.0 wt %) - peak (5) - by the addition of a small amount of Boltorn to the PPO film. This peak seems also to be present in the PPO powder[24,25] although also with extreme low intensity. The same situation is also observed in the side view (Figure 9a) whereas the same peaks are slightly brighter. This is probably due to the anisotropy of the sample that favors the formation of crystal planes in the plane of the film.

Further increase of the Boltorn concentration to 9.1 wt %, leads to similar results (see Figure 9b, front and side view). The scattering intensities are stronger in the side view situation than in the front view. Furthermore, the strong and very broad pure Boltorn (H40) scattering peak placed almost at the same position of polymer peak number (2) ($2\theta \sim 16^{\circ}$) strongly enhances most of the polymer peaks. Peak (5) ($2\theta \sim 5^{\circ}$), is almost not visible in the PPO-H40 9.1 wt % and this may be related to the fact that at that position, the contribution of the Boltorn scattering is the lowest in the whole scattering window. Peak number (5) appears as the less enhanced of the polymer peaks.

For better understanding of change in degree of crystallinity the scattering pattern of PPO-H40 1.0 wt % and PPO-H40 9.1 wt % H40 was plotted as a function of the scattering angle, where the scattering pattern of pure H40 multiplied by the volume fraction present in the sample has been subtracted from the films containing Boltorn (see Figure 9c). In this very qualitative analysis that also assumes that the Boltorn peak remains unchanged in the polymer matrix, it is very clear that enhancement of crystallinity occurs practically only in the plane of the film. Also, Figure 9a indicates the enhancement of peak 5 in the presence of low amounts of H40 while the other peaks seem to be enhanced with the increase of H40 amount (Figure 9b). Since the SEM micrographs show a phase separation in two rather distinct layers, it is reasonable to associate these WAXS results with this phenomenon.

Similar results are obtained for the scattering of mixtures of PPO and H20. Figure 10a displays results for PPO-H20 with incident beam perpendicular to the polymer film, and H20 concentrations of 1.0 and 9.1 wt %. A similar situation as for H40 is obtained and it is remarkable

that the scattering curves are very similar, including the observations for peak (5) (2θ ~5º) that become almost absent for higher Boltorn concentrations. Using the same arguments as above, these curves suggest that the presence of H20 does not introduce significant changes in PPO crystallinity in that direction in any of the studied concentrations. This is also the case for PPO-H30 mixtures (Figure 10b) where scattering of samples containing 1.0 and 9.1 wt % are displayed. The curves are very similar as before. The "anomalous" scattering relating to peak 5 that is only present at lower Boltorn concentrations may have different origins. Nevertheless, it seems that it cannot be associated to the preparation conditions and solvent in the pure polymer film. The spectra of pure PPO (in $CHCl_3$/NMP) prepared with various NMP concentrations (Figure 9a,b) are extremely similar.

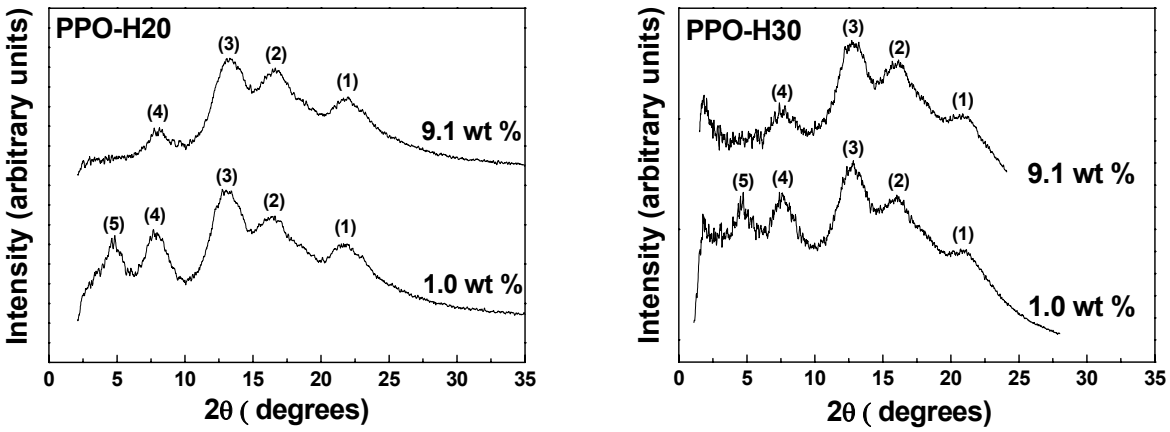

Figure 10: Scattering intensity (front view) as function of the scattering angle of: (a) PPO-H20 with 1.0 wt % and 9.1 wt % H20, (b) PPO-H30 with 1.0 wt % and 9.1 wt % H30.

In conclusion, qualitatively, variation on the degree of crystallinity due to the presence of H40 is at maximum very small in the direction perpendicular to the film. It seems however, enhanced in the direction of the film plane. The presence (or not) of the scattering peak (5) at 5º cannot be associated to the solvent composition used to prepare the films and its enhancement due to small amounts of Boltorn may be explained as follows. When small amounts of H40 are diluted in the PPO matrix they produce inclusions of large curvature, while, larger amounts aggregate, producing inclusions with much smaller curvature in the polymer matrix. Therefore,

small amounts of H40 create higher stresses in the polymer matrix, leading to larger influence on the crystalline peaks of the matrix. In any case, a definitive explanation of this effect would require a more detailed systematic investigation, beyond the scope of the present work.

3.7 Gas sorption

Figure 11 presents the sorption isotherms of CO_2, N_2 and O_2 through PPO-H40 1.0 wt %, and PPO-H40 9.1 wt % in comparison to pure PPO (in $CHCl_3$/NMP) at 35 °C. (The sorption isotherms for pure PPO prepared in various $CHCl_3$/NMP mixtures are similar.) The sorption isotherms are fitted by the dual mode sorption model[26].

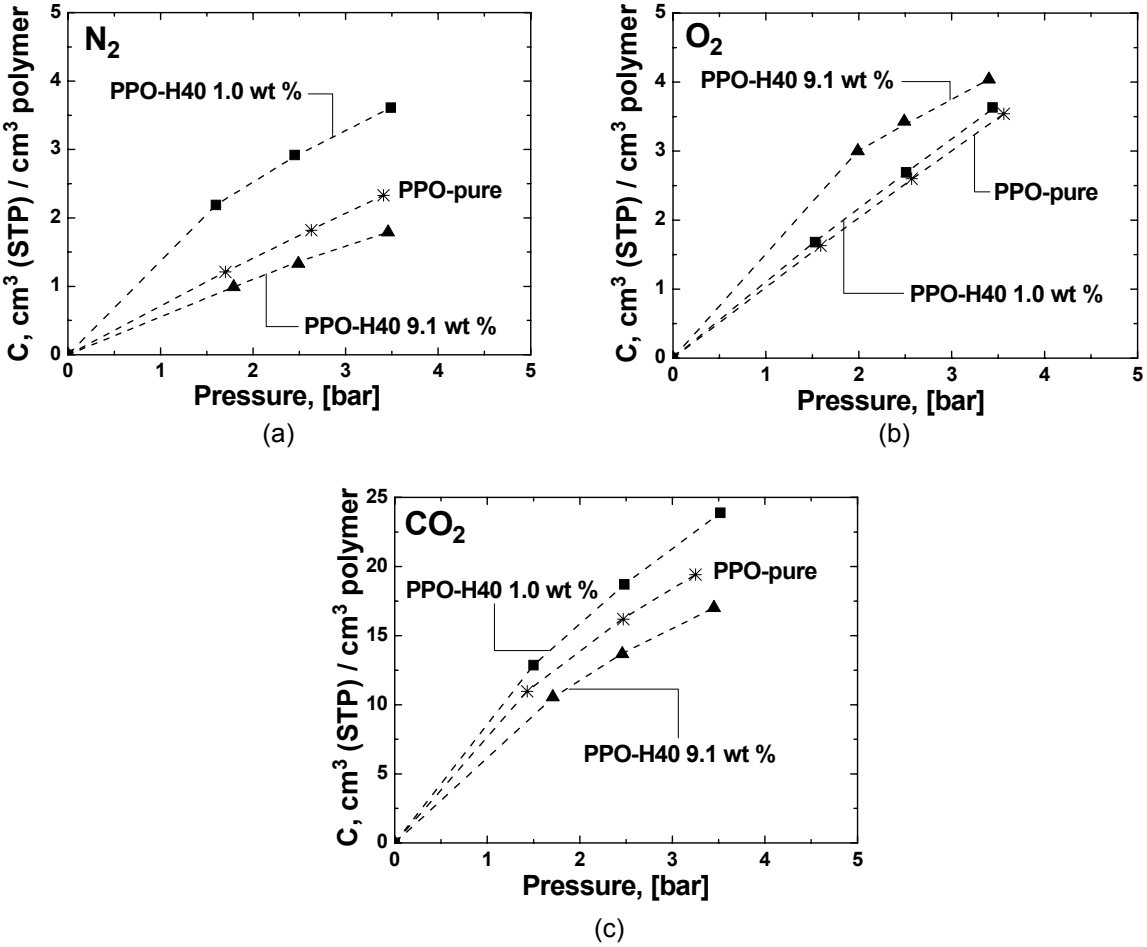

Figure 11: Sorption isotherms for (a) N_2, (b) O_2, and (c) CO_2 of PPO-H40 1.0 wt % H40 (■) and PPO-H40 with 9.1 wt % H40 (▲) in comparison to pure PPO (in $CHCl_3$/NMP) (✳). The dotted lines are model lines, which are fitted according to the dual mode sorption model. T = 35 °C.

For O_2 the difference in sorption between the PPO-H40 1.0 wt % and pure PPO is not significant. However, for PPO-H40 9.1 wt % the sorption is higher than the pure PPO. The segregated layer of H40 aggregates perhaps acts as an oxygen barrier material[7]. However, for N_2 and CO_2 the sorption is higher for PPO-H40 1.0 wt % due to the increase of free volume.

The sorption isotherms are necessary to de-convolute the permeability into its solubility and diffusivity contributions. Table 5 reports the permeability, solubility and diffusivity coefficients of N_2, O_2 and CO_2 gases of PPO-H40 1.0 wt %, PPO-H40 9.1 wt % and PPO pure (in $CHCl_3$/NMP) at 35 °C and 1.5 bar feed pressure. Since some difference in gas permeability between the pure PPO prepared in $CHCl_3$ and $CHCl_3$/NMP, respectively were found (see Table 1) the results for pure PPO (in $CHCl_3$) are also presented. The solubility coefficient S was estimated from the gas sorption measurements and the diffusion coefficient D was calculated from the P/S ratio. To confirm the validity of this calculation, the diffusion coefficient D for all three gases was also calculated from the sorption kinetics using similar method as in literature[12]. The values of D found by both methods are generally in good agreement (see Table 5).

Table 5: Gas permeability, solubility, and diffusivity of PPO and PPO-H40 films.

	N_2				**O_2**				**CO_2**			
Membrane	P	S	$D^{1)}$	$D^{2)}$	P	S	$D^{1)}$	$D^{2)}$	P	S	$D^{1)}$	$D^{2)}$
PPO pure ($CHCl_3$)	2.7	8.4	3.2	3.1	11.7	11.0	10.7	9.9	50.7	78.3	6.5	5.3
PPO pure ($CHCl_3$/NMP)	4.4	9.5	4.6	4.1	16.2	13.7	11.8	11.9	63.9	101.0	6.3	5.9
PPO-H40 1.0 wt %	8.3	18.5	4.5	3.9	32.2	14.6	22.0	23.4	155.1	114.1	13.6	10.8
PPO pure ($CHCl_3$/NMP)	3.5	10.8	3.3	3.2	16.1	13.8	11.6	12.2	65.7	104.9	6.3	6.1
PPO-H40 9.1 wt %	2.0	7.4	2.7	2.4	7.6	22.2	3.4	3.8	38.1	84.8	4.5	4.9

1) The diffusion coefficient D calculated from the P/S ratio.
2) The diffusion coefficient D calculated from the sorption kinetics.
Feed pressure: 1.5 bar, T = 35 °C
P = [barrer], S = 10^{-3}, cm^3 (STP)/cm^3cm Hg, D = 10^{-8}, cm^2/sec

The N_2 diffusivity coefficients are about the same for PPO-H40 1.0 wt % and the PPO pure (in $CHCl_3$/NMP) membrane. Then, the increase of N_2 permeability for the PPO-H40 1.0 wt %

membrane should be attributed to increase of S. For O_2 and CO_2 however, the increase of permeability through the PPO-H40 1.0 wt % in comparison to PPO pure can mostly be attributed to increase of D, while the solubility coefficients are rather comparable. This fits well with the results obtained by PALS (section 3.5) suggesting that the PPO-H40 1.0 wt % membrane has higher free volume. The free volume created in the polymer matrix is less accessible to fast diffusion of the big N_2 (with the highest gas molecule diameter from all three gases measured), although its solubility into membrane increases.

For the PPO-H40 9.1 wt % the decrease of N_2 and CO_2 permeability in comparison to pure PPO seems to be due to the decrease of both S and D. For O_2 the decrease of permeability could be attributed to decrease of D. The decrease of diffusion coefficient D can be a result of phase separation (Boltorn clustering) leading to a lower free volume (as seen by PALS, section 3.5). Interestingly, the solubility of O_2 to the PPO-H40 9.1 wt % dispersed membranes increases in comparison to pure PPO, probably due to an increase O_2 affinity induced by the higher Boltorn content.

4. Conclusions

The gas permeability of PPO-Boltorn 1.0 wt % increases more than two times than the pure polymer (prepared in the same solvent mixture), while at higher concentration of Boltorn (9.1 wt %) the permeability becomes lower than pure PPO. The increase in permeability at low concentration of Boltorn in PPO is due to increase of the polymer free volume. The interaction between the hydroxyl end groups of Boltorn with the electron pair of the oxygen atom of the PPO backbone may induce hydrogen bonds formation creating a more open structure.

The decreased permeability of PPO containing higher concentration of Boltorn (9.1 wt %) is due to the Boltorn aggregation, and reduced free volume. Due to a large number of peripheral hydroxyl groups the Boltorn may have stronger intermolecular interaction. Therefore, at higher Boltorn concentrations in PPO, they form aggregates that migrate to the membrane surface. This phenomenon leads to phase separation and loss of the free volume and therefore to a decrease in gas permeability.

Acknowledgement

The authors wish to thank Dr. Mircea Manea for the Boltorn supply, and Dr. Arie Zwijnenburg for the EDX measurements.

5. References

[1] Wang, Y.-C.; Huang, S.-H.; Hu, C.-C.; Li, C.-L.; Lee, K.-R.; Liaw, D.-J.; Lai, J.-Y. *Journal Membrane Science* **2004**, *248*, 15-25.

[2] Freeman, B.D. *Macromolecules* **1999**, *32*, 375.

[3] Albers, J.H.M.; Smid, J.; Kusters, A.P.M. *US Patent 5.129.920*, "Gas separation apparatus and also method for separating gases by means of such an apparatus", **1992**.

[4] Mulkern, T.J.; Beck Tan, N.C. *Polymer* **2000**, *41*, 3193-3203.

[5] Hsieh, T.-T.; Tiu, C.; Simon, G.P. *Polymer* **2001**, *42*, 1931-1939.

[6] Rogunova, M.; Lynch, T.-Y. S.; Pretzer, W.; Kulzick, M.; Hiltner, A.; Baer' E. *Journal of Applied Polymer Science* **2000**, *77*, 1207-1217.

[7] Rittinge, R. *Bachelor thesis*, "Free Volume Characterization of Hyperbranched Polymers", Lunds University, Sweden, **2002**.

[8] Pettersson, B. Properties and Applications of Dendritic polymers, Sweden, **2001**.

[9] Barsema, J.N.; Kapantaidakis, G.C.; van der Vegt, N.F.A.; Koops, G.H.; Wessling, M. *Journal of Membrane Science* **2003**, *216*, 195.

[10] Visser, T.; Koops, G.H.; Wessling, M. *Journal of Membrane Science* **2005**, *252*, 265-277.

[11] Crank, J., The mathematics of diffusion, 2nd ed., Oxford: Clarendon Press **1975**.

[12] Visser, T., *Ph-D thesis*, "Mixed gas plasticization phenomena in asymmetric membranes" **2006**.

[13] Sterescu, D.M.; Stamatialis, D.F.; Mendes, E.; Wübbenhorst, M.; Wessling, M. *Macromolecules* **2006**, *39*, 9234-9242.

[14] Kruse, J.; Kanzow, J.; Rätzke, K.; Faupel, F.; Heuchel, M.; Frahn, J.; Hofmann, D. *Membrane News* **2004**, *66*, 51-54.

[15] Kruse, J.; Kanzow, J.; Rätzke, K.; Faupel, F.; Heuchel, M.; Frahn, J.; Hofmann, D. *Macromolecules* **2005**, *38*, 9638-9643.

[16] Eldrup, M.; Lightbody, D.; Sherwood, J.N. *J. Chem. Phys.* **1981,** *63*, 51.

[17] Tao, S.J. *J. Chem. Phys.* **1972,** *56*, 5499.

[18] Nagel, C.; Schmidtke, E.; Günther-Schade, K.; Hofmann, D.; Fritsch, D.; Strunskus, T.; Faupel, F. *Macromolecules* **2000**, *33*, 2242-2248.

[19] Jean, Y.C. Principles and applications of positron & positronium chemistry, World Scientific, **2003**.

[20] Xiao, Y.; Chung, T.-S.; Chng, M.L. *Langmuir* **2004**, *20*, 8230-8238.

[21] Boogh, L.; Pettersson, B.; Månson, J.-A. E. *Polymer* **1999**, *40*, 2249-2261.

[22] Polotskaya, G.A.; Gladchenko, S.V.; Pen'kova, A.V.; Kuznetsov, V.M.; Toikka, A.M. *Russian Journal of Applied Chemistry* **2005**, *78*, 1468-1473.

[23] Aoki, T.; Kaneko, T. *Polymer Journal* **2005**, *37*(10), 717.

[24] Chowdhury, G.; Kruczek, B.; Matsuura, T., Polyphenylene Oxide and Modified Polyphenylene Oxide Membranes Gas, Vapor and Liquid Separation, Kluwer Academic Publishers, USA, **2001**.

[25] Khulbe, K.C.; Matsuura, T.; Lamarche, G.; Lamarche, A.-M. *Journal of Membrane Science* **2000**, 170, 81-89.

[26] Kanehashi, S.; Nagai, K. *Journal of Membrane Science* **2005**, *253 (1-2),* 117-138.

Chapter 6

Boltorn-modified Matrimid and P84 gas separation membranes

Dana M. Sterescu, Dimitrios F. Stamatialis, Matthias Wessling

Abstract

This chapter describes the preparation, characterization and the permeation properties of polyimide BTDA-AAPTMI (Matrimid 5218) and co-polyimide BTDA-TDI/MDI (P84) dense polymer films containing aliphatic hyperbranched polyesters, Boltorn (H40). The Boltorn are dispersed in Matrimid and P84, respectively at various concentrations. For Matrimid-Boltorn 1.0 wt % membrane the nitrogen permeability increases but with significant loss in selectivity, while at higher concentrations (5.0 and 10.0 wt %) of Boltorn the permeability becomes lower than of the pure polymer and the selectivity generally stays constant. The dispersion of various concentration of Boltorn (1.0, 5.0 and 10.0 wt %) in P84 decreases the permeability for all concentrations used in comparison to P84 pure, while the selectivity generally stays constant.

Sterescu D.M. *et al. Polymer, submitted for publication August 2007*

1. Introduction

Over the last decades, polymeric membranes have proven to operate successfully in industrial gas separations[1]. Special attention has been concentrated on the relationship between the polymer structure and gas separation properties. Most of the polymers that have been investigated, however, show the general trend that highly permeable polymers possess rather low selectivity. This often referred to as the permeability / selectivity trade off relationship[2]. In the last two decades, various engineering glassy polymers have been developed on experimental and also commercial level[3]. These materials combine high selectivities with acceptable permeability coefficients, and therefore, are suitable for the preparation of gas separation membranes. Polyimides, like BTDA-AAPTMI (Matrimid 5218) or BTDA-TDI/MDI (P84), show excellent intrinsic gas separation properties and robust mechanical properties to withstand high-pressure gas feeds[4].

A considerable interest has been shown in dendritic polymers as the hyperbranched polymers (HBP). The exceptional features of the dendritic architecture[5-7] result directly from the repetitive branching giving access to large number of reactive end-groups. Due to their availability of free volume[8], they are attractive to control permselectivities for small molecules like gases for gas separation applications, as shown in Chapter 5.

Compared to poly (2, 6-dimethyl-1,4-phenylene oxide) (PPO), which was modified in Chapter 5, the polyimides show high selectivities for gas separation processes. However, the gas permeability of polyimides is rather low compared to PPO. Therefore, the increase of permeability of polyimides would lead to membranes showing high selectivities combined with good gas permeabilities.

This paper presents the gas permeability properties of Matrimid 5218 and co-polyimide P84 membranes containing aliphatic hyperbranched polyesters, Boltorn. Small amount of Boltorn dispersed into Matrimid increases membrane N_2 and O_2 permeability in comparison to pure Matrimid, while at higher amounts of Boltorn the gas permeability decreases. For P84-Boltorn the gas permeability is always lower than pure P84. A systematic analysis of Matrimid and P84 dispersed with Boltorn membranes is performed using Scanning Electron Microscopy (SEM),

differential scanning calorimetry (DSC), Wide Angle X-ray Scattering (WAXS), contact angle measurements and gas sorption experiments in order to investigate the influence of Boltorn concentration to the membrane permeation performance.

2. Experimental

2.1 Materials

For the membrane preparation the following materials were used: BTDA-AAPTMI polyimide (known as Matrimid 5218, from Ciba Specialty Chemicals Corp.) and co-polyimide BTDA-TDI/MDI (known as P84, from Lenzing). Their chemical structure is shown in Figure 1.

(a) Matrimid 5218

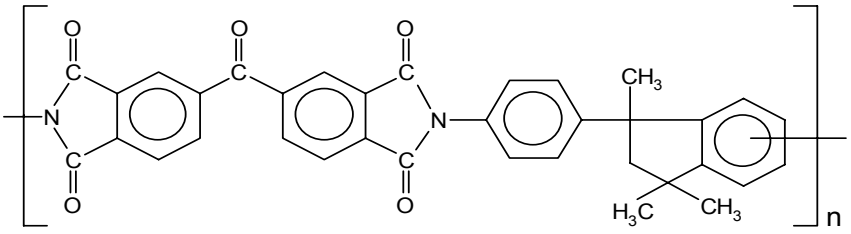

(b) P84

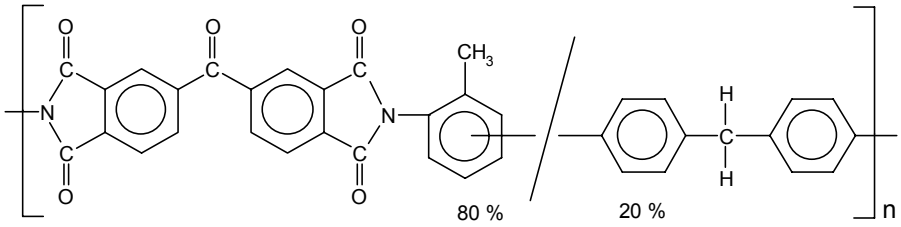

Figure 1: Chemical structure of: (a) Matrimid 5218 polyimide and (b) BTDA – TDI/MDI (P84) co-polyimide.

Other chemicals used: 1-Methyl-2-pyrrolidinone (NMP, 99 %, Acros Organics), and hyperbranched polymers commercially available as Boltorn® H40 (kindly supplied by Perstorp Specialty Chemicals AB, Sweden). They are aliphatic polyesters using ethoxylated pentaerythritol as central cores and 2,2-bis(methylol)propionic acid (bis-MPA) as dendritic units (Figure 2). The

products are all hydroxyl functional. Hydroxyl number, molecular weight and polydispersity of the Boltorn polymers from the data sheet provided by Perstorp are presented elsewhere[6,9].

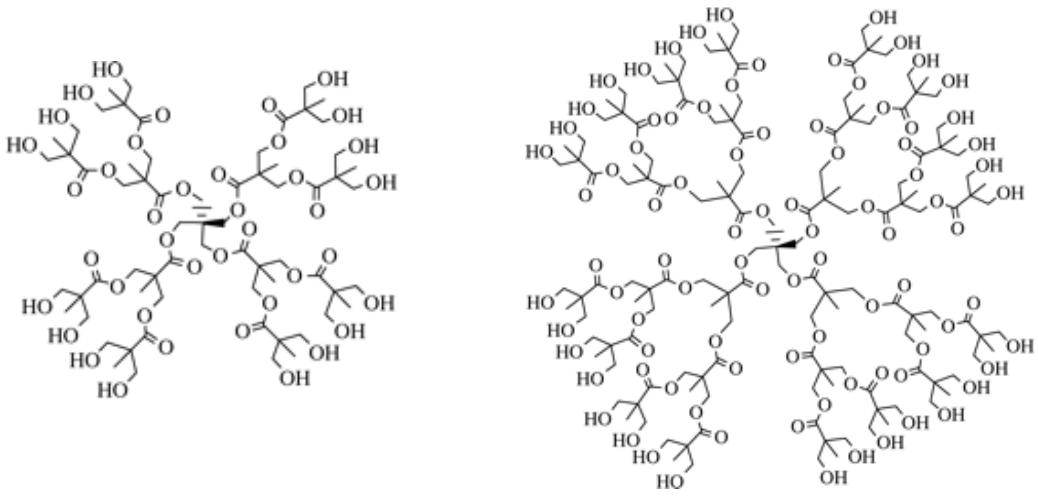

(a) H20

(b) H30

Figure 2: Schematic representation of the hyperbranched polyol molecule (a) Boltorn H20 and (b) Boltorn H30 structure.

2.2 Preparation of the membranes

For the preparation of pure Matrimid membranes, the polymer was dissolved in NMP solvent (10 wt % polymer solution). The solution was cast on a glass plate and dried first under nitrogen atmosphere at room temperature (20 -25 °C) for 7 days, then in a vacuum oven at 80 °C for 7 days, and then in a vacuum oven at 100 °C for 7 days. Finally, dry films with a thickness of 40 – 50 μm were obtained.

For the preparation of Matrimid membranes dispersed with Boltorn (H40), the Matrimid and the Boltorn were dissolved in NMP (10 wt % polymer solution). The solution was stirred at room temperature until complete dissolution (for 3 – 4 hours). The Matrimid-dispersed Boltorn membranes were cast and dried using the same method as for the pure Matrimid. Dry films with a thickness of 40 – 50 μm were obtained. Films containing 1.0, 5.0 and 10.0 wt % of Boltorn / membrane were prepared. All membranes were kept in vacuum oven at 30 °C until constant weight (for approximately 2 months).

The pure P84 and P84-Boltorn (H40) membranes were prepared in NMP solvent following similar procedure as for the pure Matrimid and Matrimid-Boltorn (H40) membranes.

2.3 Characterization of membranes

Density measurements

The density measurements of all membranes were performed using an AccuPyc 1330 Pycnometer with a 0.1 cm^3 sample insert. The pressures observed upon filling the sample chamber with the gas and then discharging it into a second empty chamber allows computation of the density of the sample.

DSC measurements

The thermal properties of pure Matrimid, pure P84, Matrimid-Boltorn and P84-Boltorn were measured using a Perkin Elmer DSC-7 (Differential Scanning Calorimeter) in nitrogen atmosphere. The samples were initially heated from - 50 °C until 380 °C, cooled with liquid nitrogen, held for 5 minutes, and reheated two more times following the same steps. The heating rate was 10 °C/min and the cooling rate was 20 °C/min. The glass transition temperature, T_g, of the polymer was obtained from the third scan.

Scanning Electron Microscopy (SEM)

The morphology of the developed Matrimid and P84 dispersed with Boltorn membranes were determined by using a Jeol JSM-5600 LV Scanning Electron Microscope. The membrane samples were freeze fractured using liquid nitrogen and sputtered with a thin layer of gold using a Balzers Union SCD 040 sputtering apparatus.

Contact angle measurements

Static liquid-air contact angles were measured with a goniometer (OCA 15, Data Physics). Drops of one microliter Milli-Q water were formed at the needle tip and contact angles were measured 10 seconds after placing the drop on the substrate. The equilibrium contact angle

(θ) of a liquid with a solid substrate is determined by the interfacial tensions $\gamma_{liquid/vapor}$ (γ_{LV}) - which is the surface tension of that liquid -, $\gamma_{solid/vapor}$ (γ_{SV}) and $\gamma_{solid/liquid}$ (γ_{SL}) acting at the three phase contact point. The relationship between these three interfacial tensions is given by Youngs equation (Eq. 1).

$$\cos\theta = \frac{\gamma_{SV} - \gamma_{SL}}{\gamma_{LV}} \qquad (1)$$

Gas permeability and Sorption

The permeation of pure nitrogen (N_2), oxygen (O_2), and carbon dioxide (CO_2) through the Matrimid, P84, Matrimid-Boltorn and P84-Boltorn was investigated at 3.5 bar feed pressure, using the set up described elsewhere[10]. Pure gas permeability coefficients were calculated from the steady state pressure increase in time in a calibrated volume at the permeate side by using the equation:

$$\frac{P}{l} = \frac{V \times 273.15 \times (p_{pt} - p_{p0})}{A \times T \times \frac{(p_{ft} + p_{f0})}{2} \times 76 \times t} \times 10^6 \qquad (2)$$

where the ideal gas law is assumed to be valid, p_{pt} , p_{ft} [bar] is the pressure at the permeate and feed side at time t, p_{p0} p_{f0} is the permeate and feed pressure at t=0, T [K] is the temperature, V [cm^3] is the calibrated permeate volume, and A [cm^2] the membrane area. The gas permeance (P/l) is expressed in GPU, i.e. 10^{-6} cm^3cm^{-2} s^{-1} $cmHg^{-1}$. Multiplying the gas permeance with the thickness of dense membrane, l [cm], gives the permeability coefficient in Barrer. All the gas permeation experiments were performed at 35 °C. Values and error bars reported in the tables and figures are based on measurements of two different membrane samples.

The gas sorption isotherms of N_2, O_2 and CO_2 in dense Matrimid pure and P84 pure, Matrimid and P84 dispersed with Boltorn (1.0 and 10.0 wt %) films were measured at 35 °C, using a magnetic suspension balance[11] (MSB, Rubotherm). The experimental procedure was described elsewhere[12]. The equilibrium mass increase was corrected for buoyancy by subtracting the weight at zero sorption at a certain pressure from the vacuum weight of the sample. Using the

equilibrium weight increase and the density of the polymer, the concentration (in cm^3 STP) inside the polymer (cm^3 polymer) was calculated[11].

Crank[13] shows that the sorption of a penetrant in a polymer matrix is proportional to the square root of time, assuming a constant diffusion coefficient. This behavior is called ideal Fickian sorption and the mass uptake (g) in time (M(t)) can be described with the following equation:

$$\frac{M(t)}{M_\infty} = 1 - \frac{8}{\pi^2}\sum_{m=0}^{\infty}\frac{1}{(2m+1)^2}\exp\left\{-\frac{D(2m+1)^2\pi^2 t}{L^2}\right\} \qquad (3)$$

where M_∞ is the amount of mass (g) sorbed by Fickian sorption at infinite time, D is the diffusion coefficient (m^2/s), t is the time (s), and l is the sample thickness (m). Fitting of the sorption data into this equation leads to the diffusion coefficients[14].

WAXS measurements

Wide Angle X-ray Scattering (WAXS) experiments were performed using a Bruker-Nonius D8-Discover equipped with 2D detector. Standard background (air and sample holder) subtraction measured at the same time and conditions were applied to all data. The sample-detector (S-D) distance was set at 10 cm and the incident beam wavelength was 1.54 Å (Cu-Kα). Measurements were performed both perpendicular and in the plane of the membrane[12]. In the first case, the sample thickness as seen by the incident beam was always less than 0.5 mm.

3. Results and discussion

3.1 Scanning Electron Microscopy (SEM)

Scanning Electron Microscopy (SEM) was used to investigate the distribution of Boltorn in the Matrimid and P84 structures. Figures 3 - 5 show some typical results for our membranes. The micrographs were obtained using a Jeol JSM-5600 LV Scanning Electron Microscope with magnification of 1000x and 5000x. Morphology studies using SEM showed that a two-phase morphology was characteristic of all Boltorn dispersed in Matrimid and also P84 samples, with more or less spherical droplets of the minor phase (Boltorn) dispersed in a continuous matrix phase, comparable with Mulkern T.J. et al.[5] findings for polystyrene mixed with Boltorn.

The SEM micrographs of both pure Matrimid and pure P84 show similar dense and compact structure (surface and cross-section). It seems that at various Boltorn concentrations (1.0 and 10.0 wt %) in Matrimid, phase separation occurs resulting in a dispersed particulate structure (see Figure 3).

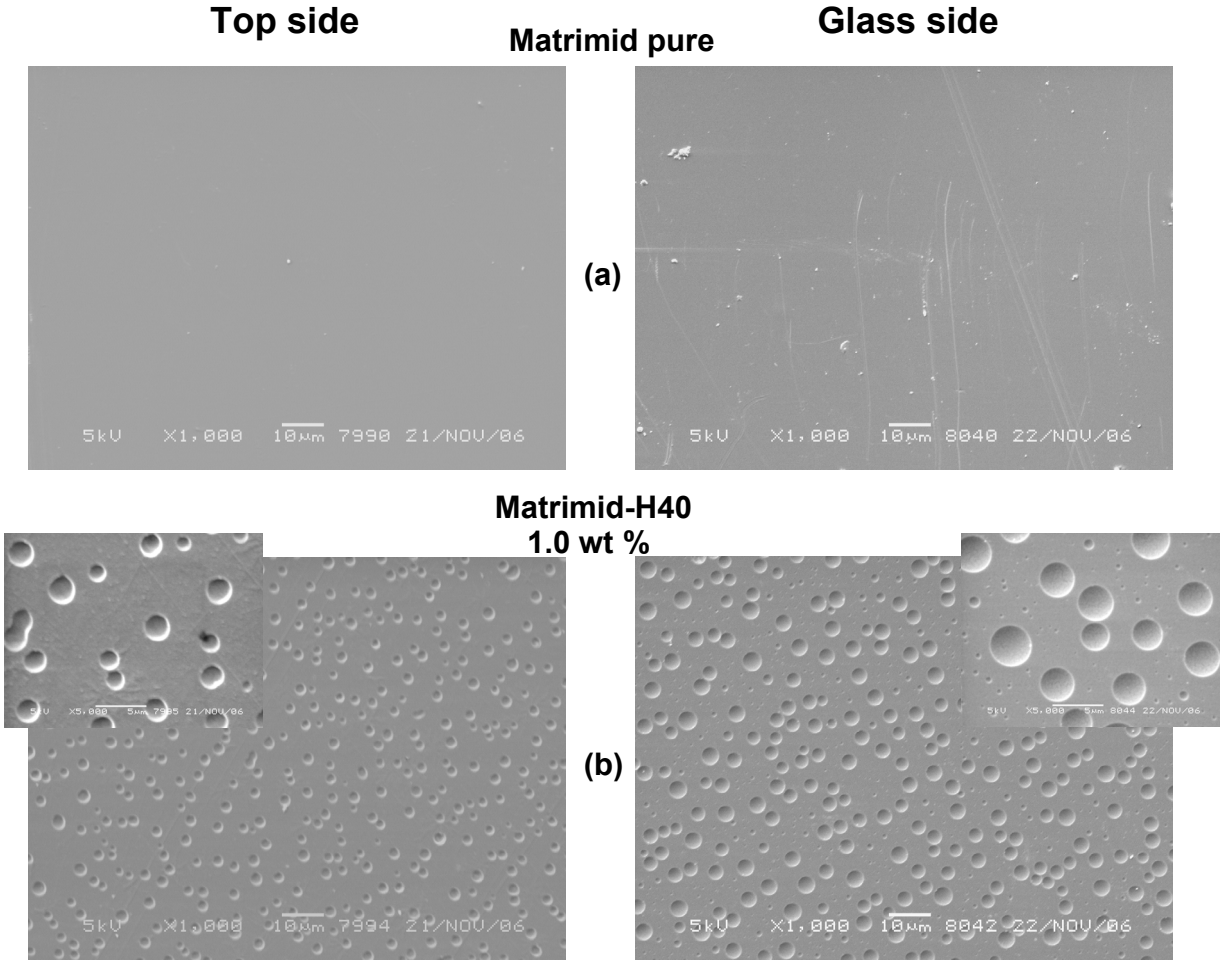

Figure 3: SEM micrographs of (a) Matrimid-pure, and (b) Matrimid-H40 1.0 wt % membranes (insets are zoom at magnification 5000x).

Similar results were also found by Boogh L. et al.[15] for modified DGEBF epoxy resin with Boltorn. Furthermore, at the top side of P84-Boltorn 1.0 and 10.0 wt % membranes the dispersed particulate structure consists in big circles surrounded by smaller ones, while at the glass side SEM micrographs show the formation of dispersed “holes” structure (Figure 4).

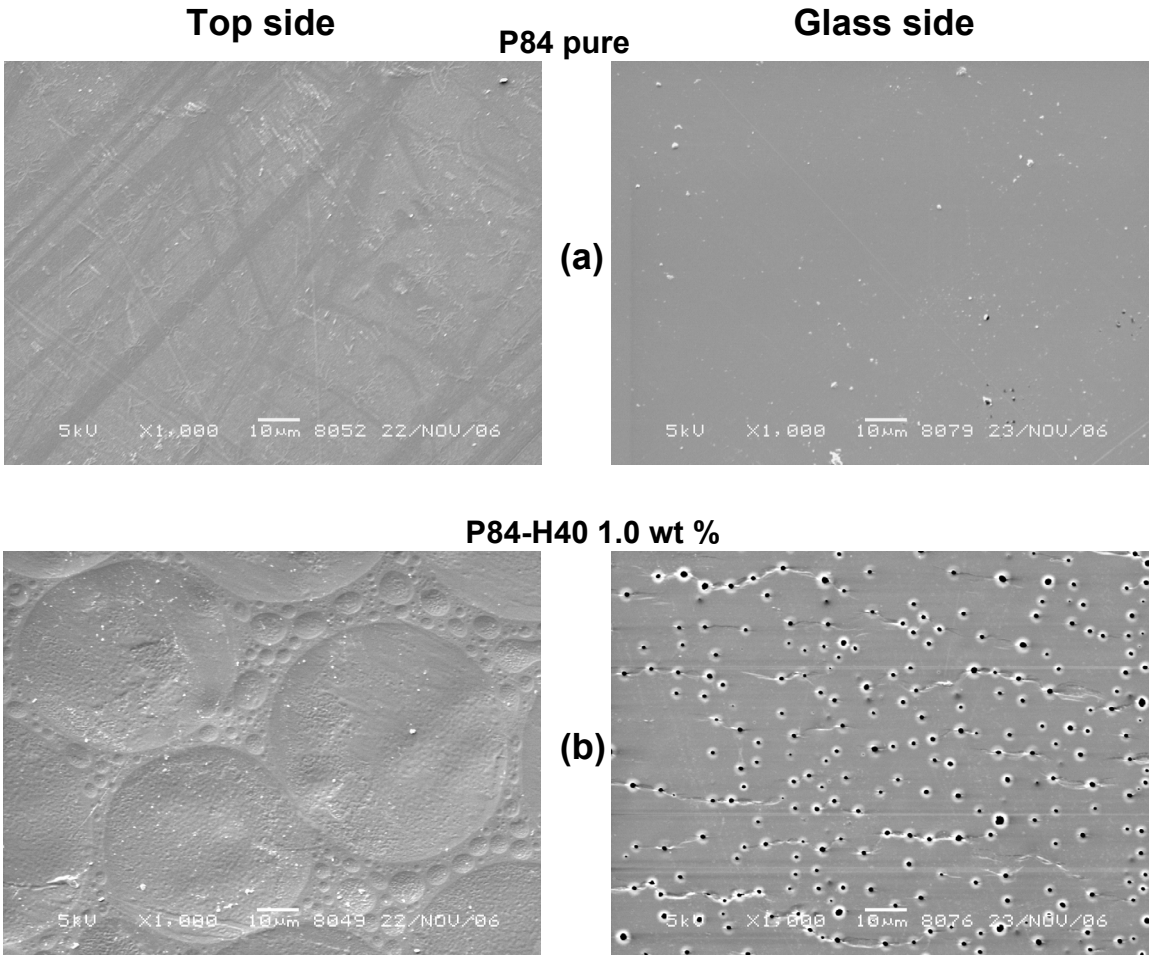

Figure 4: SEM micrographs of (a) P84-pure, and (b) P84-H40 1.0 wt % membranes.

In contrast to PPO-Boltorn (see chapter 5), the dispersed particulate structure seems to be present at both sides - top and glass side - of the Matrimid-Boltorn and P84-Boltorn membranes. Moreover, the SEM micrographs of both - Matrimid and P84 dispersed with Boltorn - at 1.0 and 10.0 wt % show the presence of “holes” in the cross-section (see Figures 5). This might be due to the “washing” out the Boltorn agglomerates during the sample preparation for SEM analysis.

In order to investigate further the film structure, we kept the Matrimid-Boltorn and P84-Boltorn membranes four days in water (known as solvent for Boltorn, but not for the polymers). The membranes were dried afterwords in N_2 box for 2 days and vacuum oven at 50 °C for 2 days. The SEM micrographs of Matrimid-H40 (1.0 and 10.0 wt %) after “washing” with H_2O look similar with the original sample before “washing” (Figure 6). In contrary, the SEM micrographs of P84-

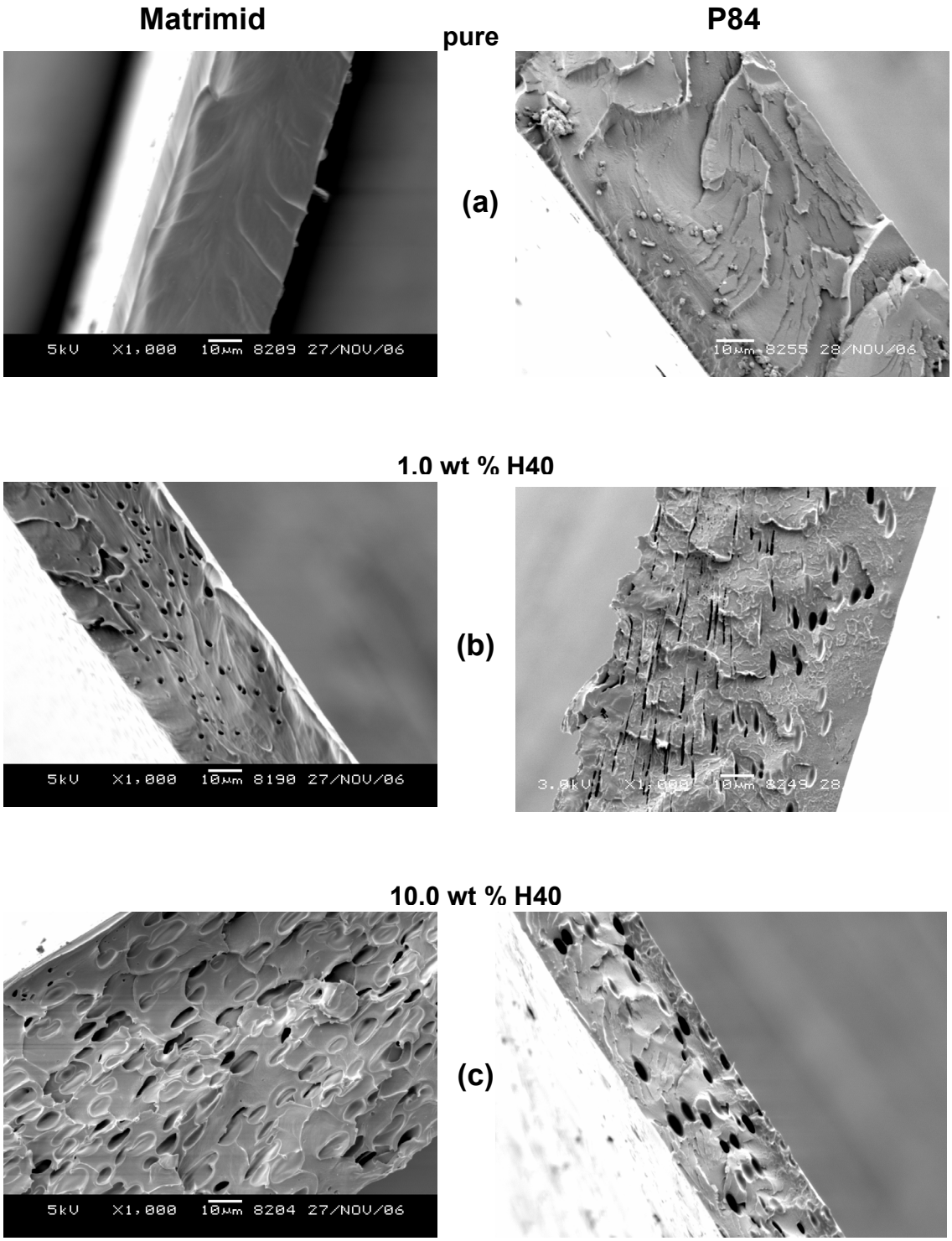

Figure 5: SEM micrographs of Matrimid and P84: (a) pure polymer, (b) 1.0 wt % H40 and (c) 10.0 wt % H40 membrane cross-section.

H40 (1.0 and 10.0 wt %) washed in H_2O show bigger "holes" at the glass surface, instead of the dispersed particulate structure seen before. These results are similar with the results found also for PPO (see chapter 5), except that the holes are visible at the glass side for P84-H40 instead of top side for PPO-H40. The "holes" were probably created after dissolution of Boltorn by H_2O, while the top side keeps its particulate structure similar to the original sample (Figure 6).

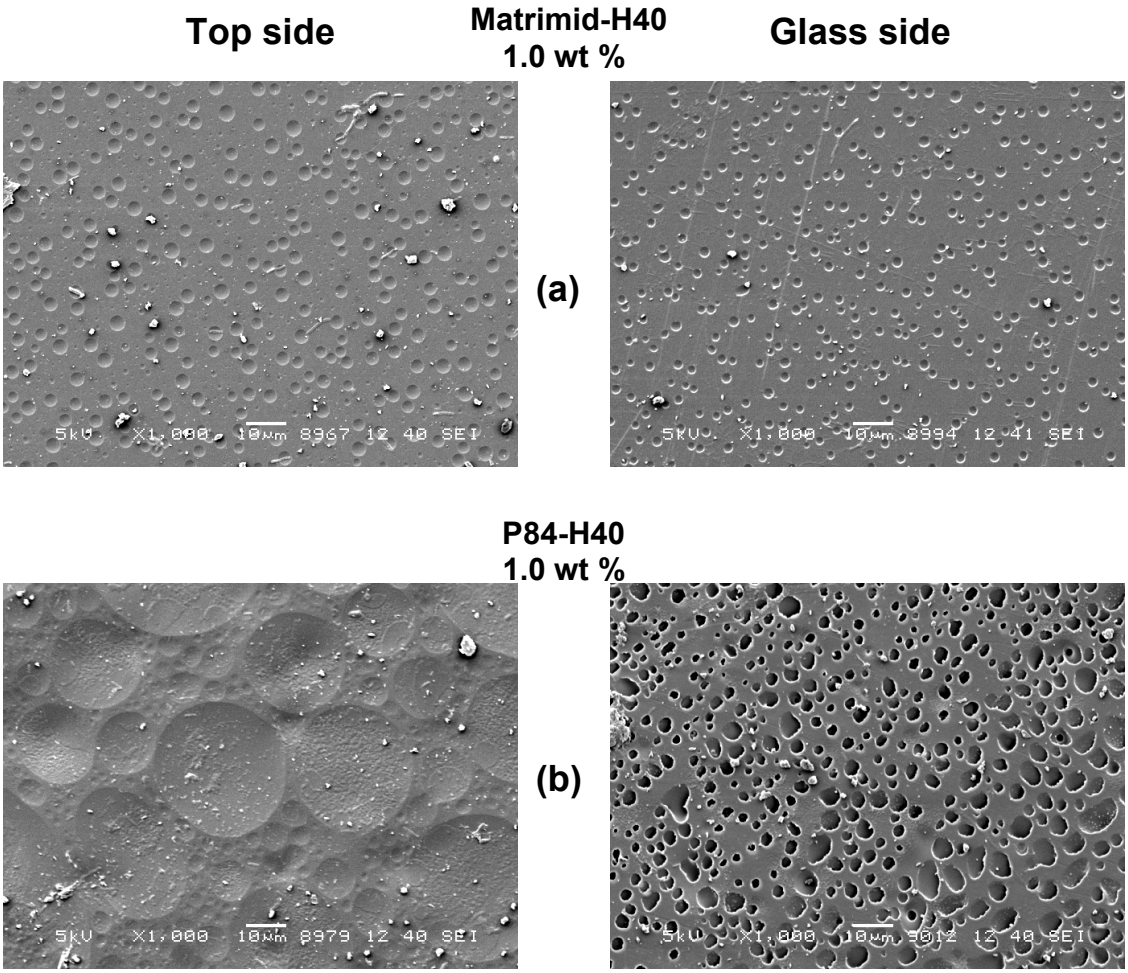

Figure 6: SEM micrographs of (a) Matrimid-H40 1.0 wt %, and (b) P84-H40 1.0 wt % membranes after "washing" with H_2O.

This test suggests that for P84-H40, Boltorn migrates to both surfaces, preferentially to the glass side, and forms agglomerates. However, for Matrimid differences between the original samples and after "washing" (with H_2O) could not be visualized by SEM as for P84 and PPO.

This fact suggests that probably a large part of Boltorn is retained inside the polymer matrix perhaps due to hydrogen bonds formation, similar to PPO.

The Boltorn migration to the membrane surfaces is supported by the contact angle measurements of both surfaces of the Matrimid and P84 membranes (pure and containing Boltorn) shown in Table 1. The contact angle of Matrimid as well as of P84 containing Boltorn decreases for both surfaces in comparison to the pure polymer. For Matrimid-H40 1.0 wt % the contact angle is similar for both surfaces, whereas for P84-H40 1.0 wt % the contact angle of the glass side is lower than of the top side, indicating a preferred migration of the Boltorn to the glass side of the membrane. However, with increasing Boltorn content (10.0 wt %) the contact angle of top side becomes similar with the glass side, for both polymers dispersed with Boltorn, with values below the pure polymer membrane.

Table 1: Contact angle results of Matrimid-H40 and P84-H40 films.

Sample	Contact angle, [°]			
	Matrimid- H40		P84- H40	
wt % H40	air side	glass side	air side	glass side
0	92.00	90.25	80.00	78.50
1.0	59.00	57.15	60.55	49.10
10.0	56.85	57.95	51.75	54.40

3.2 DSC measurements

Table 2 shows that the T_g of Matrimid-H40 1.0 wt % increases to 345 °C in comparison to pure Matrimid (T_g = 333 °C). This indicates that the Matrimid polymer chain with 1.0 wt % H40 becomes slightly more stiffened and probably there is suppressed inter-chain packing as well as some possible conformational changes in the backbone. Perhaps, as a consequence an extra interstitial chain space is created and the free volume of the membrane might increase, too. Additionally, the density of Matrimid-H40 1.0 wt % dispersed decreases to 1.23 g/cm^3 in comparison to pure polymer (ρ = 1.32 g/cm^3) , suggesting more open structure. For the Matrimid-H40 10.0 wt % (T_g = 330 °C) no significant change in T_g was found in comparison to pure Matrimid (T_g = 333 °C). Matrimid-H40 10.0 wt % has two T_g at 43 °C and 330 °C, each of which is associated with an individual dispersion component, Boltorn and Matrimid, respectively. Boltorn

H40 has T_g at 42 °C. Besides, the density of Matrimid-H40 10.0 wt % dispersed increases to 1.41 g/cm^3 in comparison to pure polymer (ρ = 1.32 g/cm^3) , suggesting a more compact structure.

Table 2: DSC and density results of Matrimid and P84 with various Boltorn concentrations.

Polymer	wt % H40	Density, [g/cm^3]	T_g, [°C]
Matrimid	0	1.32	333
	1.0	1.23	345
	10.0	1.41	43 330
P84	0	1.39	316
	1.0	1.45	289
	10.0	1.54	49 277

Table 2 shows that the T_g of P84-H40 1.0 and 10.0 wt % decreases to 289 °C and 277°C, respectively in comparison to pure P84 (T_g = 316 °C). P84-H40 10.0 wt % has two T_g at 49 °C and 277 °C, each of which is associated with an individual dispersion component, Boltorn and P84, respectively. Additionally, the density of P84-H40 1.0 and 10.0 wt % increases to 1.45 and 1.54 g/cm^3, respectively in comparison to pure polymer (ρ = 1.39 g/cm^3) , indicating more compact structure. The presence of the two distinct T_g (at 10.0 wt % of Boltorn) confirms the immiscibility between the Boltorn and the two polymers (Matrimid and P84) matrix, in agreement with Mulkern T.J. et al.[5].

3.3 WAXS analysis

Figure 7 displays spectra of pure Matrimid, P84 and H40, as well as of Matrimid-H40 and P84-H40 (1.0 and 10.0 wt %) films when the incident beam is perpendicular to the film (– Figure 7a and 7c - (front view) and parallel to the film – Figure 7b and 7d - (side view), respectively). Figure 7a and 7b clearly indicate strong similarity: peak position and relative intensity are very similar in all three Matrimid containing samples. It seems that the presence of H40 does not

cause significant changes in Matrimid amorphous structure. Similar results are obtained for the scattering of mixtures of P84 and H40 (Figure 7c and 7d). It is remarkable that the scattering

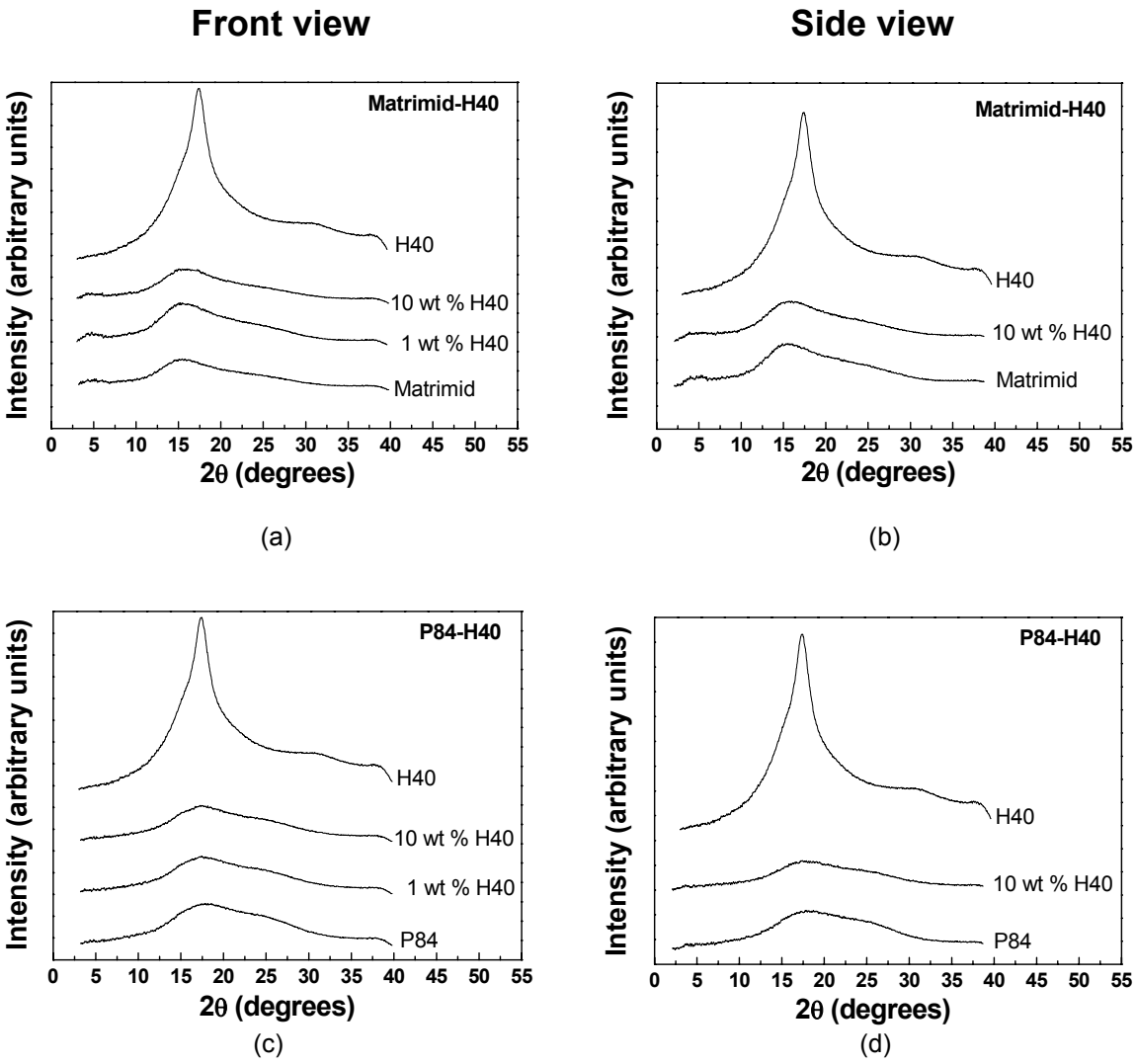

Figure 7: Scattering intensity as a function of the scattering angle for: (a) pure H40, Matrimid-H40 with 1.0 and 10.0 wt % H40 - from front, (b) pure H40, Matrimid-H40 with 10.0 wt % H40 - from side, (c) pure H40, P84-H40 with 1.0 and 10.0 wt % H40 - from front, and (d) pure H40, P84-H40 with 10.0 wt % H40 - from side.

curves are very similar - from front and side view. The presence of H40 does not seem to introduce significant changes in P84 amorphous structure at any of the studied concentrations.

In conclusion, the WAXS results indicate a strong similarity of H40 dispersed in Matrimid and P84 to pure polymer membranes, suggesting that no relevant changes in both polymers amorphous structure was induced at any of the studied concentrations of Boltorn (H40).

3.4 Gas permeability and gas sorption

Figure 8 shows the gas permeability of Matrimid-H40 and P84-H40 in comparison to the pure polymer membranes measured at 35 °C and 3.5 bar feed pressure. The permeability values for N_2, O_2 and CO_2 of pure Matrimid are in agreement with the literature[14]. The N_2 permeability through Matrimid-H40 1.0 wt % increases considerably (more than 4 times) compared to the permeability of the pure Matrimid (Figure 8a), whereas the permeability increases slightly for O_2 (28 %) and stays more or less constant for CO_2 (see also Table 3).

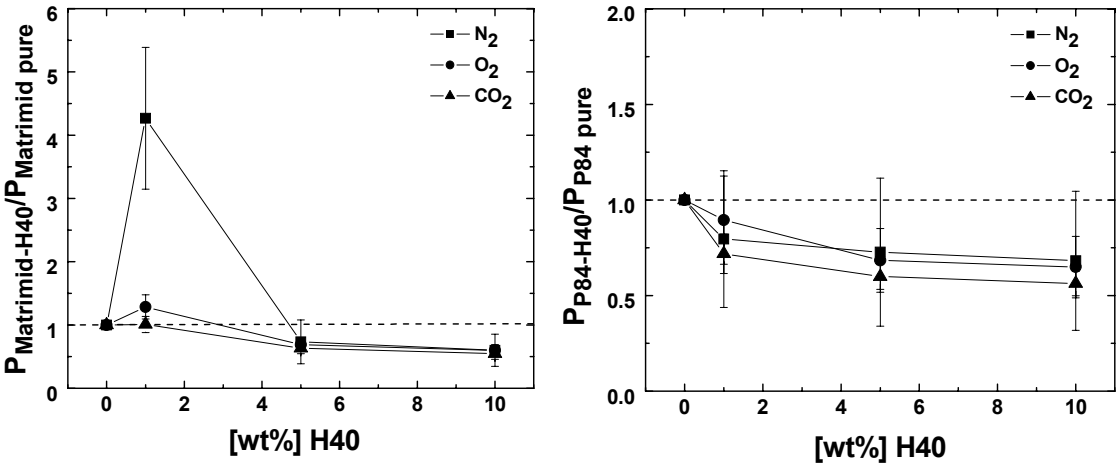

(a) (b)

Figure 8: Permeability of (a) Matrimid-H40 and (b) P84-H40 for N_2 (■), O_2 (●) and CO_2 (▲) normalized with the permeability of pure polymer versus the wt % H40 content at 3.5 bar feed pressure and 35 °C.

With increasing Boltorn content (5.0 and 10.0 wt %) the permeability of Matrimid-H40 decreases and becomes lower than pure Matrimid. Table 3 presents the ideal gas selectivity at 3.5 bar feed pressure corresponding to the average of two different membrane samples. The ideal gas selectivity of Matrimid-H40 1.0 wt % decreases significantly in comparison to pure Matrimid due to increase of N_2 permeability, whereas the selectivity of Matrimid-H40 5.0 and 10.0 wt % stay almost constant within the experimental error of our measurements.

The permeability coefficient of P84 for all gasses (N_2, O_2 and CO_2) decreases with increasing Boltorn content compared to the pure polymer (Figure 8b and Table 4). The ideal gas selectivity of P84-H40 generally stays constant with increasing concentration of Boltorn and is

comparable with P84 pure. Due to the low permeability of N_2 the experimental error leads to a wide range of selectivity values. Therefore, the ideal gas selectivities of P84 are not presented here.

Table 3: Permeability results and ideal gas selectivities of pure Matrimid and Matrimid-H40 films. (Feed pressure: 3.5 bar, T = 35 °C)

	Permeability, [barrer]			Ideal Selectivity		
wt % H40 in Matrimid	**N_2**	**O_2**	**CO_2**	**P_{O2}/P_{N2}**	**P_{CO2}/P_{N2}**	**P_{CO2}/P_{O2}**
0	0.15 ± 0.03	1.02 ± 0.09	5.20 ± 0.40	6.8 ± 2.0	34.7 ± 9.6	5.1 ± 0.8
1.0	0.64 ± 0.04	1.31 ± 0.08	5.25 ± 0.62	2.0 ± 0.3	8.2 ± 1.5	4.0 ± 0.7
5.0	0.11 ± 0.03	0.70 ± 0.04	3.29 ± 0.20	6.4 ± 2.1	29.9 ± 10.0	4.7 ± 0.6
10.0	0.09 ± 0.02	0.61 ± 0.04	2.85 ± 0.25	6.8 ± 1.9	31.7 ± 9.8	4.7 ± 0.7

The DSC, density and SEM results give an insight into the thermal and morphological parameters. Perhaps, the introduction of 1.0 wt % H40 to the Matrimid enhances the free volume (as shown for PPO) and the mobility of N_2 and O_2 gas molecules increases. The permeability of N_2 (the biggest gas molecule in diameter) increases a lot, this might indicate that the free volume introduced in the polymer is rather big and therefore leads to a substantial loss in selectivity. The lower density of the Matrimid-H40 seems to support this hypothesis. For Matrimid-H40 10.0 wt % phase separation occurs and probably decrease in free volume, indicated by the higher density and lower glass transition temperature in comparison to pure polymer, therefore the permeability for all three gas molecules decreases, as found also for P84-H40.

Table 4: Permeability results of pure P84 and P84 -H40 films. (Feed pressure: 3.5 bar, T = 35 °C)

	Permeability, [barrer]		
wt % H40 in P84	**N_2**	**O_2**	**CO_2**
0	0.05 ± 0.01	0.57 ± 0.08	1.67 ± 0.10
1.0	0.04 ± 0.01	0.51 ± 0.06	1.20 ± 0.10
5.0	0.03 ± 0.01	0.39 ± 0.04	1.00 ± 0.05
10.0	0.03 ± 0.01	0.37 ± 0.04	0.94 ± 0.05

These results are similar to the findings in Chapter 5. A comparison of the addition of Boltorn to Matrimid and to PPO shows the same trend. The permeability increases to a maximum at 1 wt % of Boltorn and decreases at higher Boltorn concentrations. The main difference is situated in the gas selectivities. Whereas the selectivities for the modified PPO membranes kept constant with increasing of gas permeability, the selectivity of modified Matrimid decreases significantly which indicates the presence of unselective free volume, as explained already in Chapter 4.

The decrease of gas permeability values for Matrimid containing higher concentration of Boltorn (5.0 and 10.0 wt %) can probably be attributed to the increased intersegmental mobility of the polymer chain, clustering of Boltorn, and the reduced free volume due to the space filling effect by Boltorn, comparable with the findings for PAMAM in 6FDA[17]. Due to a large number of peripheral hydroxyl groups the Boltorn may have stronger intermolecular interaction.

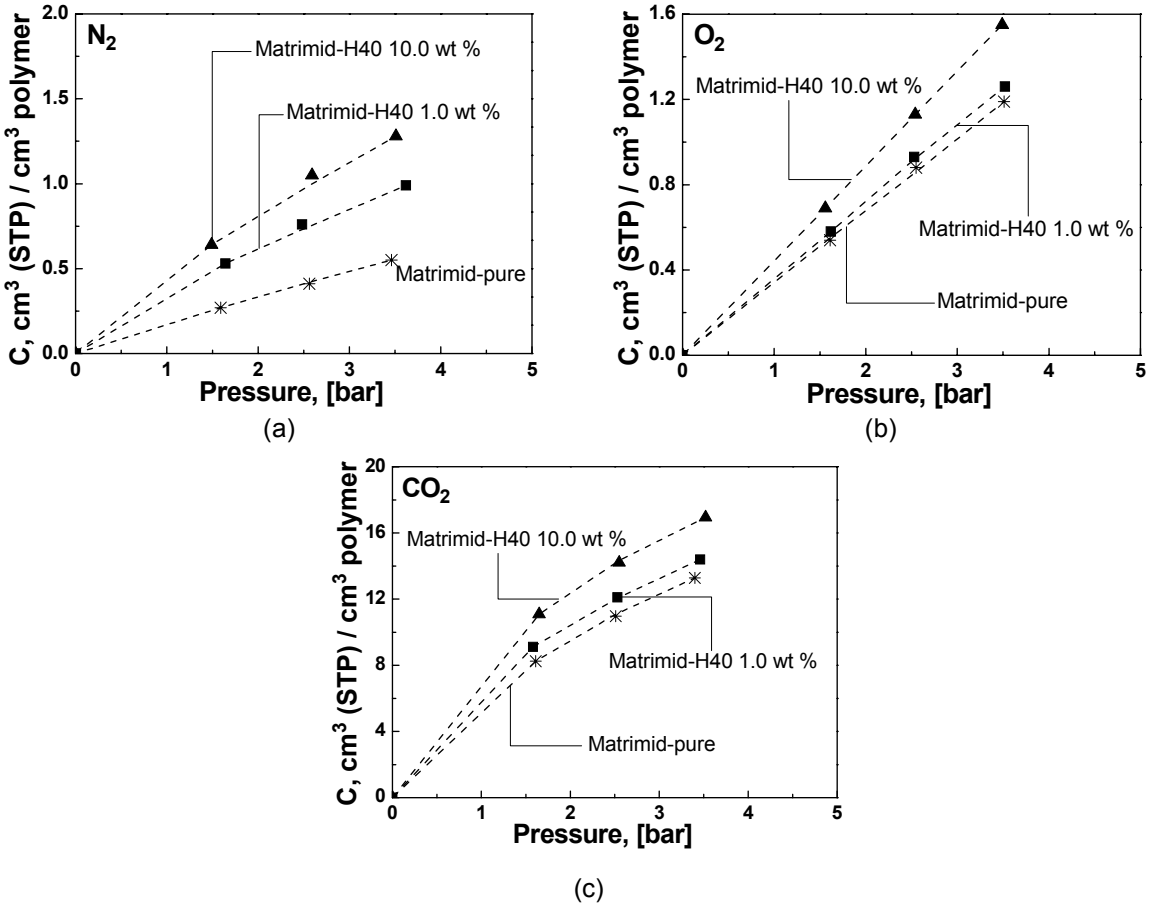

Figure 9: Sorption isotherms for (a) N_2, (b) O_2, and (c) CO_2 of Matrimid-H40 with 1.0 wt % H40 (■) and 10.0 wt % H40 (▲) in comparison to pure Matrimid (✳). The dotted lines are model lines, which are fitted according to the dual mode sorption model. T = 35 °C.

Therefore, at higher Boltorn concentrations in Matrimid, they form aggregates that partly migrate to the membrane surface. This phenomenon leads to phase separation and loss of the free volume and therefore to a decrease in gas permeability. However, the ideal selectivity generally stays constant. Similar effect was found also for P84-H40 at all Boltorn concentrations used (1.0, 5.0 and 10.0 wt %).

Figures 9 and 10 present the sorption isotherms of CO_2, N_2 and O_2 through Matrimid-H40 and P84-H40 in comparison to the pure polymers at 35 °C. The sorption isotherms are fitted by the dual mode sorption model[16]. For O_2 and CO_2 the difference in sorption between the Matrimid-H40 1.0 and 10.0 wt % is not significant, and they are both slightly higher than the pure Matrimid. However, for N_2 the sorption is somewhat higher for Matrimid-H40 10.0 wt % (Figure 9a).

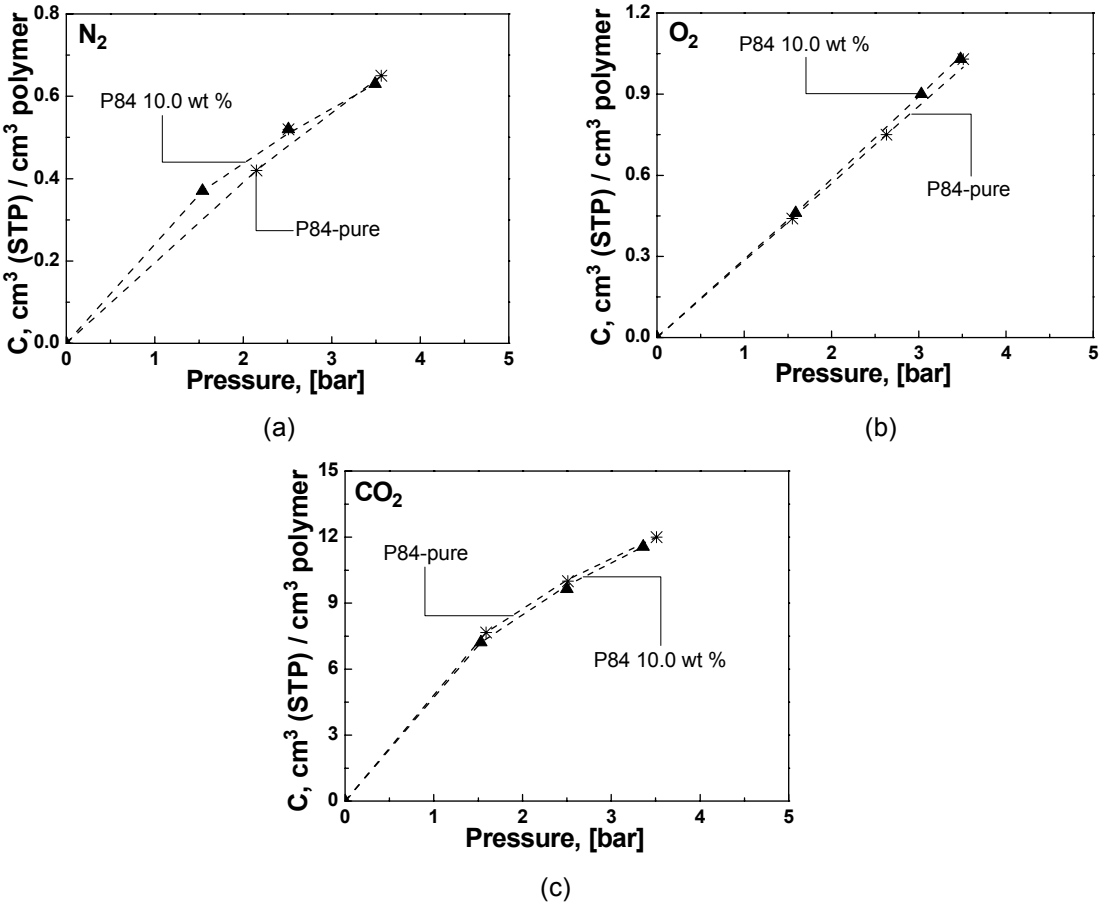

Figure 10: Sorption isotherms for (a) N_2, (b) O_2, and (c) CO_2 of P84-H40 with 10.0 wt % H40 (▲) in comparison to pure P84 (✳). The dotted lines are model lines, which are fitted according to the dual mode sorption model. T = 35 °C.

The sorption of CO_2, N_2 and O_2 of P84-H40 10.0 wt % are very similar to the pure P84 as shown in Figure 10. The sorption isotherms are necessary to deconvolute the permeability into its solubility and diffusivity contributions. Tables 5 and 6 report the permeability, solubility and diffusivity coefficients of N_2, O_2 and CO_2 gases in Matrimid-H40 and P84-H40, respectively in comparison to the pure polymers at 35 °C and 3.5 bar feed pressure. The solubility coefficient S was estimated from the gas sorption measurements and the diffusion coefficient D was calculated from the P/S ratio. To confirm the validity of this calculation the diffusion coefficient D, for all three gases, was also calculated from the sorption kinetics using similar method as in literature[14]. The values of D found by both methods are generally in good agreement (see Table 5 and 6).

Table 5: Gas permeability, solubility, and diffusivity of pure Matrimid and Matrimid-H40 films.

	N_2				**O_2**				**CO_2**			
wt % H40 in Matrimid	P	S	$D^{1)}$	$D^{2)}$	P	S	$D^{1)}$	$D^{2)}$	P	S	$D^{1)}$	$D^{2)}$
0	0.15	2.13	0.70	0.75	1.02	4.52	2.26	2.35	5.20	51.30	1.01	1.10
1.0	0.64	3.65	1.75	1.86	1.31	4.81	2.72	2.84	5.25	53.80	0.97	1.05
10.0	0.09	3.98	0.23	0.29	0.61	5.89	1.03	1.09	2.85	64.18	0.44	0.51

1) The diffusion coefficient D calculated from the P/S ratio.
2) The diffusion coefficient D calculated from the sorption kinetics.

Feed pressure: 3.5 bar, T = 35 °C
P = [barrer], S = 10^{-3}, cm^3 (STP)/cm^3cm Hg, D = 10^{-8}, cm^2/sec

For the Matrimid-H40 1.0 wt % the increase of N_2 and O_2 permeability in comparison to pure Matrimid seems to be due to the increase of both S and D. However, for N_2 the diffusion coefficient D increases the most (~ 150 %), whereas for O_2 the diffusion coefficient increases less (~ 20 %). The increase of diffusion coefficient D can be a result of suppressed inter-chain packing (see DSC) associated with a lower polymer density leading probably to higher free volume. For CO_2 however, the diffusion and solubility coefficients are rather comparable, therefore the permeability stays constant. The low increase of D for O_2 and CO_2 is probably due to their smaller gas molecule diameter in comparison to N_2. These results are similar to the findings in Chapter 4 (formation of unselective free volume). The increase of the free volume of a polymer to such

extent leads to the strongest increase of the diffusivity coefficient. Therefore also the permeability of the gas molecules with the biggest diameter show the strongest increase compared to the smaller gas molecules, but therefore they show a strong loss in selectivity.

For the Matrimid-H40 10.0 wt % the solubility for N_2, O_2 and CO_2 slightly increases in comparison to pure Matrimid, but the decrease of permeability should be attributed to the decrease of D (Table 5).

Table 6: Gas permeability, solubility, and diffusivity of pure P84 and P84-H40 films.

	N_2				O_2				CO_2			
wt % H40 in P84	P	S	$D^{1)}$	$D^{2)}$	P	S	$D^{1)}$	$D^{2)}$	P	S	$D^{1)}$	$D^{2)}$
0	0.05	2.43	0.20	0.24	0.57	3.80	1.50	1.49	1.67	45.52	0.37	0.34
10.0	0.03	2.39	0.13	0.15	0.37	3.95	0.94	0.90	0.94	44.87	0.21	0.18

1) The diffusion coefficient D calculated from the P/S ratio.
2) The diffusion coefficient D calculated from the sorption kinetics.

Feed pressure: 3.5 bar, T = 35 °C
P = [barrer], S = 10^{-3}, cm^3 (STP)/cm^3cm Hg, D = 10^{-8}, cm^2/sec

The N_2, O_2 and CO_2 solubility coefficients are about equal for P84-H40 10.0 wt % and P84 pure membranes (see Table 6). Then, the decrease of N_2, O_2 and CO_2 permeability for the 10.0 wt % H40 membrane should be mostly attributed to decrease of D. The decrease of diffusivity coefficient D, for Matrimid and P84 with 10.0 wt % H40, can be a result of phase separation occurring (Boltorn clustering), inducing a more compact structure (as seen by DSC and density measurements) leading probably to a lower free volume, similar to Matrimid-H40 10.0 wt %.

4. Conclusions

Morphology studies using SEM showed that a two-phase morphology was characteristic of all Boltorn dispersed in Matrimid and P84 samples.

The N_2 and O_2 gas permeability of Matrimid-Boltorn 1.0 wt % increases compared to the pure polymer, while it stays more or less constant for CO_2. The ideal gas selectivity decreases

significantly. The significant increase in N_2 permeability at low concentration of Boltorn in Matrimid is probably due to the free volume arising from the characteristic hyperbranched structure of Boltorn and also created by the stiffening of the polymer chain by the introduction of H40 into Matrimid matrix, comparable with the findings for hyperbranched polymers in 6FDA[17]. This effect has less influence for O_2 and CO_2 gases, probably due to their smaller gas molecule diameter in comparison to N_2. These results are similar to the findings in Chapter 4 (formation of unselective free volume). A comparison of the addition of Boltorn to Matrimid and to PPO shows the same trend. The permeability increases to a maximum at 1 wt % of Boltorn and decreases at higher Boltorn concentrations. The main difference is situated in the gas selectivities. Whereas the selectivities for the modified PPO membranes kept constant with increasing of gas permeability, the selectivity of modified Matrimid decreases significantly which indicates the presence of unselective free volume, as explained already in Chapter 4. The increase of the free volume of a polymer to such extent leads to the strongest increase of the diffusivity coefficient. Therefore also the permeability of the gas molecules with the biggest diameter show the strongest increase compared to the smaller gas molecules, but therefore they show a strong loss in selectivity. In contrary, this phenomenon seems to be absent in P84-H40 1.0 wt % where the permeability for all three gases decreases in comparison to pure P84, while the selectivity stays constant.

The decrease of gas permeability values for Matrimid containing higher concentration of Boltorn (5.0 and 10.0 wt %) can probably be attributed to the increased intersegmental mobility of the polymer chain, clustering of Boltorn, and the reduced free volume due to the space filling effect by Boltorn, comparable with the findings for PAMAM in 6FDA[17]. Due to a large number of peripheral hydroxyl groups the Boltorn may have stronger intermolecular interaction. Therefore, at higher Boltorn concentrations in Matrimid, they form aggregates that partly migrate to the membrane surface. This phenomenon leads to phase separation and loss of the free volume and therefore to a decrease in gas permeability. However, the ideal selectivity generally stays constant. Similar effect was found also for P84-H40 at all Boltorn concentrations used (1.0, 5.0 and 10.0 wt %).

Acknowledgment

The authors wish to thank Dr. Eduardo Mendes for the WAXS analysis.

5. References

[1] Baker, R.W. *Ind. Eng. Chem. Res.* **2002**, *41*, 1393.

[2] Freeman, B.D. *Macromolecules* **1999**, *32*, 375.

[3] Koros, W.J.; Fleming, G.K. *J. Membrane Science* **1993**, *83*, 1.

[4] Wind, J.D.; Paul, D.R.; Koros, W.J. *J. Membrane Science* **2004**, *228*, 227.

[5] Mulkern, T.J.; Beck Tan, N.C. *Polymer* **2000**, *41*, 3193.

[6] Hsieh, T.-T.; Tiu, C.; Simon, G.P. *Polymer* **2001**, *42*, 1931.

[7] Rogunova, M.; Lynch, T.-Y. S.; Pretzer, W.; Kulzick, M.; Hiltner, A.; Baer' E. *Journal of Applied Polymer Science* **2000**, *77*, 1207.

[8] Rittinge, R. *Bachelor thesis*, "Free Volume Characterization of Hyperbranched Polymers", Lunds University, Sweden, **2002**.

[9] Pettersson, B. Properties and Applications of Dendritic polymers, Sweden, **2001**.

[10] Barsema, J.N.; Kapantaidakis, G.C.; van der Vegt, N.F.A.; Koops, G.H.; Wessling, M. *Journal of Membrane Science* **2003**, *216*, 195.

[11] Visser, T.; Koops, G.H.; Wessling, M. *Journal of Membrane Science* **2005**, *252*, 265.

[12] Sterescu, D.M.; Stamatialis, D.F.; Mendes, E.; Wübbenhorst, M.; Wessling, M. *Macromolecules* **2006**, *39*, 9234.

[13] Crank, J., The mathematics of diffusion, 2nd ed., Oxford: Clarendon Press **1975**.

[14] Visser, T. *Ph-D thesis,* "Mixed gas plasticization phenomena in asymmetric membranes" **2006.**

[15] Boogh, L.; Pettersson, B.; Månson, J.-A. E. *Polymer* **1999**, *40*, 2249.

[16] Kanehashi, S.; Nagai, K. *Journal of Membrane Science* **2005**, *253 (1-2),* 117.

[17] Aoki, T.; Kaneko, T. *Polymer Journal* **2005**, *37*(10), 717.

Summary

This thesis describes the development of new materials for membrane based gas separation processes. Long-term stable, loosely packed (high free volume) amorphous polymer films were prepared by introduction of super-molecular pendant groups, which possess hard-sphere properties to avoid dense molecular scale packing of adjacent polymer chains during membrane preparation.

The first part of this thesis (Chapter 2 to 4) focuses on Fullerene - based polymer modification concepts to develop high free volume polymer films. In **Chapter 2, "Novel gas separation membranes containing covalently bonded fullerenes"** the preparation of novel membranes by covalent coupling of fullerenes (C_{60}) to poly (2, 6-dimethyl-1,4-phenylene oxide) (PPO) is presented. The PPO-C_{60} bonded membranes exhibited significantly higher gas permeability (up to 80 %) in comparison to pure PPO without change in ideal gas selectivity, while dispersing the bucky-balls into the polymer reduced the gas permeability. PPO-C_{60} bonded membranes stored at 30 °C showed the same high permeation properties as the freshly prepared ones. However, membranes stored at 100 °C showed 30 to 40 % lower gas permeability than the fresh samples due to polymer aging. These results represent a first step in analyzing the relationship between the C_{60} bonded on the polymer chain and the gas transport properties.

In **Chapter 3, "Fullerene-modified poly (2, 6-dimethyl-1,4-phenylene oxide) gas separation membranes: Why binding is better than dispersing"**, a systematic analysis of the membrane structures using H-NMR, DSC, PALS - free volume and gas sorption measurements are performed to identify the reason behind the significant increase of the gas permeability through the PPO-C_{60} bonded membranes. The permeability of PPO-C_{60} bonded membranes increases with increasing C_{60} concentration, probably due to the stiffening of the polymer chain by the introduction of C_{60} resulting in increase of polymer free volume. The permeability of PPO-C_{60} dispersed membranes decreases with increasing C_{60} concentration. This is probably due to the clustering of the dispersed fullerene and the higher crystalline gas impermeable fraction (due to

the clustering) than in pure PPO or PPO-C_{60} bonded. The clusters seemed to form lamellas oriented parallel to the membrane plane.

In **Chapter 4, "Fullerene-modified Matrimid gas separation membranes"**, the commercial polyimide BTDA-AAPTMI (Matrimid 5218) is modified to improve its membrane-transport properties as a gas-separation material. Fullerenes were covalently coupled or dispersed in the polymer. The dispersion of fullerenes (0.25 and 1.0 wt %) and the covalent bonding of 0.25 wt % fullerenes to Matrimid did not affect the permeability and selectivity compared to the pure polymer. It seems that there are no significant changes in the polymer structure induced by the dispersion of C_{60}, supported by DSC, WAXS and SEM, therefore the permeability and selectivity stayed constant. The covalent coupling of 1.0 wt % of fullerenes resulted in a tremendous increase in permeability but significant loss in selectivity. Matrimid is an amorphous polymer with more rigid polymer chain in comparison to PPO, which is known to be a semi-crystalline polymer. Therefore a good packing of the polymer chains around the C_{60} coupled to Matrimid is not possible. Due to the suppression of interchain packing by the introduction of bulky C_{60} group to very rigid Matrimid polymer chain, as well as some possible conformational changes in the backbone the intrachain motion around the flexible hinge points might be inhibited creating so called "defects" in the polymer packing. That might lead to a higher increase of free volume compared to the increase created by bonding of C_{60} to PPO. Therefore the permeability increased but the ideal gas selectivity decreased in comparison to pure Matrimid. However, this phenomenon seems to be suppressed for Matrimid-C_{60} 0.25 wt % probably due to the low amount of C_{60} used, leading to a similar permeability and selectivity as for pure Matrimid.

The second part of this thesis (Chapter 5 and 6) focuses on hyperbranched polymer - based polymer modification concepts to develop high free volume polymer films. In **Chapter 5, "Boltorn-modified poly (2, 6-dimethyl-1,4-phenylene oxide) gas separation membranes",** dense PPO polymer films containing aliphatic hyperbranched polyesters, Boltorn (H20, H30 and H40) are prepared and investigated. The gas permeability of PPO-Boltorn 1.0 wt % increased more than two times in comparison to the pure polymer (prepared in the same solvent mixture), while at higher concentration of Boltorn (9.1 wt %) the permeability became lower than of the pure

PPO. The increase in permeability at low concentration of Boltorn in PPO is due to an increase of the free volume of the polymer. The interaction between the hydroxyl end groups of Boltorn with the electron pair of the oxygen atom of the PPO backbone may induce hydrogen bonds formation creating a more open structure. PPO containing higher concentration of Boltorn (9.1 wt %) showed a decreased permeability. Due to a large number of peripheral hydroxyl groups the Boltorn may have stronger intermolecular interaction leading to aggregation and reduced free volume. At higher Boltorn concentrations in PPO, the Boltorn formed aggregates that migrate to the membrane surface leading to phase separation and loss of the free volume and therefore to a decrease in gas permeability.

Chapter 6, **"Boltorn-modified Matrimid and P84 gas separation membranes",** describes the preparation, characterization and the permeation properties of polyimide BTDA-AAPTMI (Matrimid 5218) and co-polyimide BTDA-TDI/MDI (P84) dense polymer films containing aliphatic hyperbranched polyesters, Boltorn (H40) at various concentrations. A two-phase morphology was characteristic for all Matrimid and P84 samples containing Boltorn. For Matrimid-Boltorn 1.0 wt % the N_2 permeability increased but with significant loss in selectivity, while at higher concentrations (5.0 and 10.0 wt %) of Boltorn the permeability became lower than of the pure polymer and the selectivity generally stayed constant. The significant increase in N_2 permeability at low concentration of Boltorn in Matrimid is probably due to the free volume arising from the characteristic hyperbranched structure of Boltorn and also created by the stiffening of the polymer chain by the introduction of H40 into Matrimid matrix, comparable with the findings for hyperbranched polymers in 6FDA. This effect has less influence for O_2 and CO_2 gases, probably due to their smaller gas molecule diameter in comparison to N_2. These results are similar to the findings in Chapter 4 (formation of unselective free volume). A comparison of the addition of Boltorn to Matrimid and to PPO showed the same trend. The permeability increased to a maximum at 1 wt % of Boltorn and decreased at higher Boltorn concentrations due to aggregation. The main difference can be found in the gas selectivities, which kept constant for the modified PPO membranes with increasing gas permeability, whereas the selectivity of modified Matrimid decreased significantly. This loss in selectivity indicates the presence of unselective free

volume. The increase of the free volume of a polymer leads to strong increase of gas diffusivity: in fact, the permeability of the gas molecules with the biggest diameter shows the strongest increase compared to the smaller gas molecules, and therefore the selectivity decreases. The decrease of gas permeability values for Matrimid containing higher concentration of Boltorn (5.0 and 10.0 wt %) can probably be attributed to the increased intersegmental mobility of the polymer chain, clustering of Boltorn, and the reduced free volume due to the space filling effect by Boltorn, comparable with the findings for PAMAM in 6FDA. Due to a large number of peripheral hydroxyl groups the Boltorn may have stronger intermolecular interaction. Therefore, at higher Boltorn concentrations in Matrimid, they form aggregates that partly migrate to the membrane surface. This phenomenon leads to phase separation and loss of free volume and therefore to a decrease in gas permeability. However, the ideal selectivity generally stays constant. Similar results were found for P84-H40. The dispersion of various concentration of Boltorn (1.0, 5.0 and 10.0 wt %) in P84 decreases the gas permeability in comparison to P84 pure, while the selectivity generally stays constant.

Reflections and Outlook

This thesis dealt with the development of new membrane materials for gas separation processes. Polymer films were prepared by introducing super-molecular pendant groups, possessing hard-sphere properties to avoid dense molecular scale packing of adjacent polymer chains during membrane preparation resulting in high free volume.

The first part of this thesis focused on Fullerene-based polymer modification concepts to develop a new branch of polymers for high performance membrane separations. The second part of this thesis focused on hyperbranched polymers (HPB) – based polymer modification concepts to develop high free volume polymer films.

This thesis clearly shows that binding of the nano-additives such as fullerenes is advantageous compared to dispersing. Binding leads to a good distribution of the fullerenes inside the polymeric material and therefore to an increase in free volume and therefore in permeability with increasing content of the additive. Dispersing fullerenes shows a different trend, leading to a decreased permeability with increasing fullerene content due to the formation of fullerene clusters. The use of dendrimers as additive shows a similar effect. At low concentrations dendrimer is well distributed inside the polymer causing strong increase in free volume and in gas permeability. At higher concentrations the dendrimers form agglomerates inside the polymer leading to phase separation and a reduced permeability. The maximum of gas permeability at low dendrimer concentration, (chapter 5) indicates the existence of a balance between increase of free volume and densification due to clustering and phase separation. Similar results have been reported for the addition of carbon nanotubes[1] and silica nanoparticles[2] in membranes Nierengarten[3] proposed the decoration of fullerenes with dendrimers as an efficient strategy to prevent the irreversible aggregation resulting from the strong fullerene-fullerene interactions.

The increase of free volume by addition of nano-additives can also affect the selectivity of the prepared polymeric membrane. Whereas the increase of the free volume in the semi-crystalline PPO only increased the permeability of all gases in the same way (creation of selective free volume), the modification of the amorphous polyimide Matrimid resulted in drastic increase in

permeability of the biggest gas, nitrogen and in rather low increase of the permeabilities of the smaller gases (creation of unselective free volume). For matrimid, in contrast to PPO, a dense packing of the polymer chain around the additive is not possible. In this case defects are probably created inside the polymer structure leading to increase of diffusivity. Permeation tests with smaller gas molecules would perhaps confirm this hypothesis.

The results presented in this thesis give a good indication in which direction the development of nano-composite gas separation membranes should go in the future. The polymer which is chosen to be modified should not contain a rigid structure like polyimides. A small increase in the free volume of Matrimid for example results already in a loss of selectivity[4]. Semi-crystalline polymers such as PPO give a good basis for the addition of nano-additives to increase the polymeric free volume without compromising selectivity. Boltorn dendrimers have shown the highest effectivity in increasing the free volume of the polymer. In order to add a higher amount of dendrimers into the polymer, the decorated fullerenes should then be dispersed or even bound in or onto the polymer. By this method agglomeration of the dendrimers could be avoided.

Another way of improving the gas separation performance of polymers is the preparation of novel polymeric solubility-selective gas separation membrane materials. Recent work of Freeman and coworkers has focused on materials in which CO_2 is highly soluble and can therefore be used to remove CO_2 from natural gas[5]. By adding dendrimers containing amine or azide groups[6] into polymers, CO_2 solubility-selective gas separation membrane materials could be created. A combination of these kinds of dendrimers with the decoration method of fullerenes mentioned before would lead to the development of polymeric gas separation membranes with an increased free volume and increased CO_2 solubility.

References

[1] Cong, H.; Zhang, J.; Radosz, M.; Shen, Y. *J. Mem. Sci.* **2007**, *294*, 178.

[2] Cong, H.; Hu, X.; Radosz, M.; Shen, Y. *Ind. Eng. Chem. Res.* **2007**, *46*, 2567.

[3] Nierengarten, J.-F. *New J. Chem.* **2004**, *28*, 1177.

[4] Guiver, M.D.; Robertson, G.P.; Dai, Y.; Bilodeau, F.; Kang, Y.S.; Lee, K.J.; Jho, J.Y.; Won, J. *J. Polymer Science, Part A: Polymer Chemistry* **2002**, *40*, 4193.

[5] Freemantle, M. *Chem. Eng. News*, **2005**, *83*, 49.

[6] Kovvali, A.S.; Chen, H.; Sirkar, K.K. *J. Am. Chem. Soc.* **2000**, *122*, 7594.

Samenvatting

Dit proefschrift beschrijft de ontwikkeling van nieuwe materialen voor membraangebaseerde gasscheidingsprocessen. Stabiele, losgepakte (hoog vrij volume) amorfe polymeerfilms zijn gesynthetiseerd door het aanbrengen van super-moleculaire zijgroepen. Deze fungeren als harde bollen en voorkomen hiermee de dichte pakking van polymeerketens op moleculaire schaal tijdens de membraanbereiding.

Het eerste gedeelte van dit proefschrift (hoofdstuk 2 t/m 4) is toegespitst op polymeermodificatie met fullerenen om hoog vrij volume polymeerfilms te creeren. In **Hoofdstuk 2, "Novel gas separation membranes containing covalently bonded fullerenes"** wordt de synthese van nieuwe membranen door middel van covalente binding van fullerenen (C_{60}) aan poly(2,6-dimethyl-1,4-phenyleenoxide) (PPO) beschreven. De PPO-C_{60} gebonden membranen laten een significante toename in de gaspermeabiliteit (tot 80 %) zien in vergelijking met ongemodificeerd PPO zonder verlies van selectiviteit, terwijl het dispergeren van deze bucky-balls in het polymeer een afname in de gaspermeabiliteit veroorzaakt. PPO-C_{60} gebonden membranen welke zijn bewaard bij 30 °C vertonen dezelfde hoog permeabele eigenschappen als direct na bereiding. Echter, membranen bewaard bij 100 °C vertonen een daling van 30 tot 40 % in de gaspermeabiliteit veroorzaakt door veroudering. Deze resultaten zijn een eerste stap in de analyse van de relatie tussen polymeerketens met gebonden C_{60} en de gastransporteigenschappen.

In **Hoofdstuk 3, Fullerene-modified poly(2,6-dimethyl-1,4-phenylene oxide) gas separation membranes: Why binding is better than dispersing"**, wordt een systematische analyse van de membraanstructuur met behulp van ^{1}H-NMR, DSC, PALS – vrij volume en gassorptiemetingen beschreven om de reden van deze significante toename van de gaspermeabiliteit in PPO-C_{60} gebonden membranen te onderzoeken. De permeabiliteit van PPO-C_{60} gebonden membranen nam toe met toenemende concentratie C_{60}. Dit wordt waarschijnlijk veroorzaakt door de verstijving van de polymeerketens met toevoeging van C_{60} en dientengevolge een toename van het vrije volume. De permeabiliteit van PPO met gedispergeerd

C_{60} nam af met toenemende concentratie C_{60}. Deze afname wordt waarschijnlijk veroorzaakt door clustering van het gedispergeerde fullereen met als gevolg een hogere impermeabele kristallijne fase in vergelijking met puur PPO en gebonden PPO-C_{60}. Deze clusters lijken lamellen te vormen met een oriëntatie loodrecht op het membraanoppervlak.

In **Hoofdstuk 4, "Fullerene-modified Matrimid gas separation membranes"**, wordt het commercieel verkrijgbare polyimide BTDA-AAPTMI (Matrimid 5218) gemodificeerd om de membraantransporteigenschappen gericht op het gebruik als gasscheidingsmateriaal te verbeteren. Fullerenen zijn covalent gebonden aan of gedispergeerd in het polymeer. Het dispergeren van fullereen (0.25 en 1.0 wt %) en het covalent binden van 0.25 wt % fullereen aan Matrimid heeft geen invloed op de permeabiliteit en selectiviteit in vergelijking met het pure polymeer. Het lijkt alsof er geen significante veranderingen optreden in de structuur van het polymeer door het dispergeren van C_{60}, ondersteund door DSC, WAXS en SEM, en hierdoor permeabiliteit en selectiviteit constant blijven. Het covalent binden van 1.0 wt % fullereen had een enorme stijging van de permeabiliteit tot gevolg, echter de selectiviteit daalde significant. Matrimid is een amorf polymeer met een stijvere keten in vergelijking met het semi-kristallijne PPO. Dit heeft als gevolg dat een goede pakking van de polymeerketens rond het gebonden C_{60} aan Matrimid niet mogelijk is. Door de afname van de intermoleculaire pakking door binding van het volumineuze C_{60} aan de zeer stijve Matrimid polymeerketens alsmede mogelijke veranderingen in de polymeerconformatie, kan de beweging rond flexible scharnierpunten in de keten geremd worden, wat kan leiden tot zogeheten defecten in de polymeerpakking. Deze defecten leiden mogelijk tot een grotere toename van het vrij volume in vergelijking met de toename van het vrij volume in gebonden PPO-C_{60}. Hierdoor neemt de permeabiliteit toe, maar daalt de ideale gasselectiviteit in vergelijking met puur Matrimid. Echter, dit effect lijkt te worden geminimaliseerd voor Matrimid-C60 0.25 wt % vanwege de kleine hoeveelheid toegevoegd C_{60}, waardoor permeabiliteit en selectiviteit vergelijkbaar zijn met puur Matrimid.

Het tweede gedeelde van dit proefschrift (Hoofdstuk 5 en 6) is gericht op het gebruik van sterk vertakte polymeren voor polymeermodificatie om hoog vrij volume polymeerfilms te ontwikkelen. In **Hoofdstuk 5, "Boltorn-modified poly(2,6-dimethyl-1,4-phenylene oxide) gas separation membranes"**, worden dichte PPO films gemodificeerd met alifatische sterk vertakte polyesters, Boltorn (H20, H30 en H40), geprepareerd en onderzocht. De gas permeabiliteit van PPO-Boltorn 1.0 wt % nam meer dan 200% toe in vergelijking met puur PPO (bereiding in hetzelfde oplosmiddel), terwijl bij hogere concentraties Boltorn (9.1 wt %) de permeabiliteit afnam tot onder de waarde voor puur PPO. De toename in permeabiliteit bij lage concentraties Boltorn in PPO wordt veroorzaakt door een toename van het vrije volume van het polymeer. De interactie tussen de hydroxyl eindgroepen van Boltorn met het electronenpaar van het zuurstofatoom in de PPO hoofdketen kan leiden tot waterstofbrug vorming waardoor een opener structuur ontstaat. PPO met hogere concentratie Boltorn (9.1 wt %) liet een afname in permeabiliteit zien. Door een hoog aantal aan de buitenzijde gelegen hydroxylgroepen kan het Boltorn sterke intermoleculaire interacties vertonen, welke leiden tot aggregatie en een afname in het vrij volume. Verdere toename in concentratie leidt tot de vorming van Boltorn aggregaten, welke migreren naar het membraanoppervlak, met als gevolg fasescheiding, verlies van vrij volume en hieraan gekoppeld gaspermeabiliteit.

Hoofdstuk 6, **"Boltorn-modified Matrimid and P84 gas separation membranes"**, beschrijft de bereiding, karakterisatie en de permeatie eigenschappen van polyimide BTDA-AAPTMI (Matrimid 5218) and co-polyimide BTDA-TDI/MDI (P84) dichte polymeerfilms met alifatische sterk vertakte polyesters Boltorn (H40) bij verschillende concentraties. Matrimid en P84 met Boltorn vertonen beide een twee-fase morfologie. Voor Matrimid-Boltorn 1.0 wt % neemt de N_2 permeabiliteit toe, echter met een significante afname in selectiviteit, terwijl bij hogere concentraties (5.0 en 10.0 wt %) Boltorn de permeabiliteit lager is dan het pure polymeer met nagenoeg gelijkblijvende selectiviteit. Deze sterke toename van N_2 permeabiliteit bij lage concentraties Boltorn in Matrimid wordt waarschijnlijk veroorzaakt door de toename van vrij volume door de karakteristieke sterk vertakte structuur van Boltorn en het verstijvende effect op de polymeerketen vergelijkbaar met de resultaten van deze sterk vertakte polymeren in 6FDA. Dit

effect beinvloedt O_2 en CO_2 in mindere mate, waarschijnlijk door hun kleinere molecuul diameter in vergelijking met N_2. Deze resultaten zijn vergelijkbaar met Hoofdstuk 4 (vorming van niet selectief vrij volume). Een vergelijking van de toevoeging van Boltorn aan Matrimid en PPO laat dezelfde trends zien. De permeabiliteit stijgt tot een maximum bij toevoeging van 1 wt % Boltorn en neemt vervolgens af voor hogere concentraties door aggregatie. Een groot verschil treedt op in de gasselectiviteit, welke gelijk blijft voor gemodificeerde PPO membranen, terwijl de selectiviteit voor gemodificeerde Matrimid membranen sterk daalt. Dit verlies in selectiviteit duidt op de aanwezigheid van niet selectief vrij volume. De toename van het vrij volume van een polymeer in dergelijke mate leidt tot een sterke toename van de diffusiecoefficient. Dit heeft als gevolg dat de permeabiliteit van de gasmoleculen met de grootste diameter de sterkste toename zal vertonen in vergelijking met de kleinere gasmoleculen en zo een sterke afname in selectiviteit laten zien. De afname van de gaspermeabiliteit voor Matrimid met hogere concentraties Boltorn (5.0 en 10.0 wt %) kan waarschijnlijk worden toegewezen aan de toegenomen intersegmentele beweeglijkheid van de polymeerketen, clustering van Boltorn en het afgenomen vrij volume door het opvullende effect van Boltorn, vergelijkbaar met de resultaten van PAMAM in 6FDA. Door een hoog aantal aan de buitenzijde gelegen hydroxylgroepen van Boltorn kan het sterke intermoleculaire interacties aangaan. Hierdoor vormt Boltorn bij hogere concentraties aggregaten die naar het Matrimid membraanoppervlak migreren. Dit verschijnsel leidt tot faseschеiding en verlies van vrij volume tot gevolg, resulterend in een afname van de gaspermeabiliteit. Echter, de ideale gasselectiviteit blijft over het algemeen gelijk. Een vergelijkbaar effect treedt op voor P84-H40. Het dispergeren van verschillende concentraties Boltorn (1.0, 5.0 en 10.0 wt %) in P84 leidt tot een afname van de permeabiliteit voor alle concentraties in vergelijking met puur P84, terwijl de selectiviteit gelijk blijft.

Acknowledgement

If –

If you can keep your head when all about you
Are losing theirs and blaming it on you;
If you can trust yourself when all men doubt you,
But make allowance for their doubting too;
If you can wait and not be tired by waiting,
Or being lied about, don't deal in lies,
Or being hated, don't give way to hating,
And yet don't look too good, nor talk too wise;

If you can dream - and not make dreams your master;
If you can think - and not make thoughts your aim,
If you can meet with Triumph and Disaster
And treat those two impostors just the same;
If you can bear to hear the truth you've spoken
Twisted by knaves to make a trap for fools,
Or watch the things you gave your life to, broken,
And stoop and build 'em up with worn-out tools;

If you can make one heap of all your winnings
And risk it on one turn of pitch-and-toss,
And lose, and start again at your beginnings
And never breathe a word about your loss;
If you can force your heart and nerve and sinew
To serve your turn long after they are gone,
And so hold on when there is nothing in you
Except the Will which says to them: 'Hold on!'

If you can talk with crowds and keep your virtue,
Or walk with Kings - nor lose the common touch,
If neither foes nor loving friends can hurt you,
If all men count with you, but none too much;
If you can fill the unforgiving minute
With sixty seconds' worth of distance run,
Yours is the Earth and everything that's in it,
And - which is more - you'll be a Man, my son!

by Joseph Rudyard Kipling

Herewith I would like to thank a great number of people without whose help, advice and never ending support this thesis would not have been possible:

Matthias, Dimitris, Nico, Rob, Klaus, Jan, Eduardo, Arie, Clemens, Jens, Joao, Maik, Tymen, Sander, Harmen, Bas Kluijtmans, Antoine, Greet, Susanne, John, Herman, Erik, Lydia, Yvette, Thomas, Lothar, Sybrand, Jonathan, Mircea Manea, Mircea Teodorescu, Marius, Gina, Carmen, Mariana, Magda, Maria, Nela, Wim, Valer, Vincent, Patricia, Heddy, Adrian, d-na Ileana Voicu, Andrei.

Thank you all Membrane Technology Group for the nice time being there.

And last but not least I would like to thank to my family from Germany and from Romania. Mama, tata, Giani, Madalin si Cristian va multumesc din suflet pentru toata dragostea pe care mi-ati daruit-o. Bei meiner Familie in Deutschland möchte ich mich herzlich bedanken für die Unterstützung und die Liebe die mir entgegengebracht wurde.

And of course the most wonderful person I have ever met, and without whose patience, endurance and endless love this thesis would not have been finished: Jörg. My love, thank you so much for your incredible support and resilience during all this period of time. I love you!